PHYTOPLANKTON PATCHINESS AROUND THE GÖKSU RIVER ESTUARY

(NORTH-EASTERN MEDITERRANEAN)

A THESIS SUBMITTED TO

GRADUATE SCHOOL OF MARINE SCIENCES

OF

MIDDLE EAST TECHNICAL UNIVERSITY

BY

BEGÜM ECE TOHUMCU

IN PARTIAL FULFILLMENT OF THE REQUIREMENTS

FOR THE DEGREE OF

MASTER OF SCIENCE

IN THE DEPARTMENT OF MARINE BIOLOGY AND FISHERIES

JANUARY 2020

Approval of the thesis

PHYTOPLANKTON PATCHINESS AROUND THE GÖKSU RIVER ESTUARY

(NORTH-EASTERN MEDITERRANEAN)

Submitted by **Begüm Ece Tohumcu** in partial fulfillment of the requirements for the degree of **Master of Science in the Department of Marine Biology and Fisheries, Middle East Technical University** by,

Assoc. Prof. Dr. Barış Salihoğlu
Director _____

Prof. Dr. Zahit Uysal
Head of Department _____

Prof. Dr. Zahit Uysal
Supervisor _____

Examining Committee Members:

Prof. Dr. Sevim Polat
Çukurova University,
The Faculty of Fısheries _____

Assoc. Prof. Dr. Mustafa Koçak
METU-IMS _____

Prof. Dr. Zahit Uysal
METU-IMS _____

Date:

I hereby declare that all information in this document has been obtained and presented in accordance with academic rules and ethical conduct. I also declare that, as required by these rules and conduct, I have fully cited and referenced all material and results that are not original to this work.

Name, Last name: Begüm Ece Tohumcu

Signature:

ABSTRACT

PHYTOPLANKTON PATCHINESS AROUND THE GÖKSU RIVER ESTUARY (NORTH-EASTERN MEDITERRANEAN)

Begüm Ece Tohumcu

MSc., Department of Marine Biology and Fisheries

Supervisor: Prof. Dr. Zahit Uysal

January 2020, 112 pages

Seasonal phytoplankton samplings were made onboard R/V *Bilim-2* of the Institute of Marine Sciences of Middle East Technical University around the Göksu River estuary to reveal a possible patchy distribution of phytoplankton due to presence of contrasting water masses with varying trophicity. To achieve this, biological, physical and chemical parameters were collected from 51 stations representing nutrient-rich Göksu River estuary, productive coastal, mesotrophic shelf and oligotrophic offshore waters. Over the year, the total number of 246 phytoplankton species belonging to Bacillariophyceae (79), Pyrrophyceae (146), Prymnesiophyceae (16), Cryptophyceae, Chrysophyceae, Euglenophyceae, Ebriophyceae and Chlorophyceae (with single species each) were identified. The community was found most diverse during spring followed by winter, summer and fall. Based on seasonal surface mean cell abundances, summer population abundances (2.3×10^5 cells/l) were exceeded much the winter (1.2×10^5 cells/l), spring (1.1×10^5 cells/l) and lastly fall (2.6×10^4 cells/l) population densities. Diatoms were

observed dominant over dinoflagellates and remaining other groups in all seasons. The population has always found most species diverse and abundant in shallow coastal areas fed by nutrient-rich Göksu River and Lamas creek waters. Taşucu Bay surface waters have retained maximal population densities in all seasons due to direct freshwater inputs from the nearby Göksu River.

Based on the Spearman Rank Correlation analysis, highly significant positive correlation between surface phytoplankton abundance and ambient temperature ($r = 0.675$, $P < 0.01$) and negative correlation with surface salinity ($r = -0.398$, $P < 0.01$) whereas almost no correlation with any of nutrient species were observed in fall. In contrast, highly significant positive correlations were only present with nutrients (nitrate, nitrite, silicate) in winter. Despite a highly significant negative correlation with salinity ($r = -0.806$, $P < 0.01$), highly significant positive correlations with phosphate, nitrate, nitrite were observed in spring. Lastly, in summer, a highly significant negative correlation between phytoplankton abundance and salinity & temperature and a significant positive relationship with phosphate ($r = 0.283$, $P < 0.01$) were observed.

Similar to Pielous' index values, Shannon diversity index values were found maximal during spring followed in decreasing order by fall, winter and summer. Multivariate analyses have shown the formation of several distinct phytoplankton assemblages in each season. The number of patches observed in fall (10) and in winter (8) have exceeded greatly those observed in spring (2) and summer (3). Despite the very complex affinities observed within various minor patches observed in fall and winter, surface flora has split into two major, namely coastal - offshore, and east - west subpopulations in spring and summer.

Key Words: Phytoplankton, Abundance, Diversity, Patchiness, Nutrient Salts, Göksu River, Northeastern Mediterranean

ÖZ

GÖKSU NEHRİ ETKİ ALANINDA FİTOPLANKTON YAMALARI (KUZEYDOĞU AKDENİZ)

Begüm Ece Tohumcu

Yüksek Lisans, Deniz Biyolojisi ve Balıkçılık Bölümü

Tez Yöneticisi: Prof. Dr. Zahit Uysal

Ocak 2020, 112 sayfa

Değişken trofik özelliklere sahip su kütlelerinin varlığından kaynaklı fitoplanktonun olası düzensiz dağılımını ortaya çıkarmak için Orta Doğu Teknik Üniversitesi Deniz Bilimleri Enstitüsü'ne ait R / V Bilim-2 araştırma gemisi ile Göksu Nehri ağızında mevsimsel fitoplankton örneklemeleri yapılmıştır. Çalışma kapsamında besin tuzları açısından zengin Göksu Nehri ağzı, ötrofik kıyı, mezotrofik sahanlık ve oligotrofik açık deniz sularını temsilen 51 istasyondan biyolojik, fiziksel ve kimyasal parametreler toplanmıştır. Yıl boyunca, Bacillariophyceae (79), Pyrrophyceae (146), Prymnesiophyceae (16), Cryptophyceae, Chrysophyceae, Euglenophyceae, Ebriophyceae and Chlorophyceae (her biri tek türle mevcut) sınıflarına ait olmak üzere toplam 246 fitoplankton türü tanımlanmıştır. En yüksek fitoplankton çeşitliliği ilkbaharda saptanırken, sırasıyla kış, yaz ve sonbahar mevsimleri bunu takip etmiştir. Mevsimsel yüzey ortalama hücre bollukları göz önüne alındığında, en yüksek düzeydeki yaz mevsimine ait fitoplankton populasyon bolluğunu (2.3×10^5 hücre / l) sırası ile kış (1.2×10^5 hücre / l), ilkbahar (1.1×10^5 hücre / l) ve sonbahar (2.6×10^4 hücre) izlemiştir.

Diyatomların, tüm mevsimlerde dinoflagellatlardan ve diğer gruplardan daha baskın olduğu gözlenmiştir. Besin tuzları açısından zengin Göksu Nehri ve Lamas dere suları ile beslenen sığ kıyı bölgelerinde fitoplankton türce zengin ve bol miktarda bulmuştur. Taşucu Körfezi yüzey suları, yakındaki Göksu Nehrinden doğrudan gelen tatlı su girdileri nedeniyle her mevsimde maksimum hücre yoğunluğuna sahip olmuştur.

Spearman-Rank Korelasyon analiz sonuçları, sonbahar mevsiminde yüzey fitoplankton bolluğu ve ortam sıcaklığı ($r = 0.675$, $P < 0.01$) arasında yüksek düzeyde pozitif korelasyonu ve yüzey tuzluluğu ile negatif korelasyonu ($r = -0.398$, $P < 0.01$) bunların yanısıra besin tuzları arasında hiçbir korelasyonun mevcut olmadığını göstermiştir. Buna karşılık, kışın sadece besin tuzlarıyla (nitrat, nitrit, silikat) ile oldukça belirgin pozitif ilişkiler saptanmıştır. İlkbaharda ise yüzey tuzluluğu ile yüksek oranda belirgin ters yönlü ilişki ($r = -0.806$, $P < 0.01$) gösterirken, fosfat, nitrat, nitrit ile oldukça belirgin pozitif ilişkiler göstermiştir. Son olarak, yaz aylarında, fitoplankton bolluğu ile tuzluluk ve sıcaklık arasında oldukça belirgin bir ters ilişki gözlenirken fosfat ile belirgin bir pozitif ilişki ($r = 0.283$, $P < 0.01$) gözlenmiştir.

Pielou'nun endeks değerlerine benzer şekilde Shannon çeşitlilik endeks değerleri ilkbaharda en yüksek olarak bulunmuş olup bunu sırası ile azalarak sonbahar, kış ve yaz mevsimleri izlemiştir. Yapılan çok değişkenli analizler sonucunda, her mevsimde birkaç farklı fitoplankton yama oluşumu saptanmıştır. Sonbahar (10) ve kış aylarında (8) gözlemlenen yama sayısının, ilkbahar (2) ve yaz aylarında (3) gözlemlenenlerden sayıca çok fazla olduğu saptanmıştır. Sonbahar ve kış aylarında gözlemlenen sayıca çok ve karmaşık yapıdaki küçük yama oluşumlarına karşın ilkbahar ve yaz aylarında, yüzey florası, kıyı - açık deniz ve doğu - batı alt popülasyonları olmak üzere iki ana bölüme ayrılmıştır.

Anahtar Kelimeler: Fitoplankton, Biyoçeşitlilik, Bolluk, Fitoplankton Yamaları, Besin Tuzları, Göksu Nehri, Kuzeydoğu Akdeniz

To my family,
For their unconditional love and support

ACKNOWLEDGEMENTS

Firstly, I would like to express my genuine gratitude to my advisor Prof. Dr. Zahit Uysal, for providing me with the essential skills and his constant guidance throughout my study. I would also like to express my sincere appreciations to members of the examining committee, Prof. Dr. Sevim Polat and Assoc. Prof. Dr. Mustafa Koçak for their helpful suggestions and corrections on the thesis. I wish to extend my special thanks to Dr. Yeşim Örek, Assist. Prof. Dr. Nebil Yücel and Dr. Meltem Ok for their academic and moral supports.

I would like to thank setüstü people for creating the most supportive, fun and warm environment in this institute. Also, I want to thank my friends; Saba Başkır, Batıkan Bilir, Nilan Cansu, Bulut Çağdaş, Selin Deliceırmak, Fatıma Nur Oğul and Cem Serimözü for their support and love in this process. They forced me to sit down and write or forced me to take a break when I got stuck. I am grateful for their help, advice and English corrections. I would also like to thank the whole RV/Bilim 2 crew for their support and for the excellent time and food we shared on the night shifts during surveys.

I want to express my greatest gratitude to my family. In the process, they were there for me when I was stressed out; they found a way to calm me down. They gave me strength and the energy to write this thesis.

Lastly, I would like to express my sincere thanks to The Scientific and Technological Research Council of Turkey. This thesis has been supported by TUBITAK-2210-C National Scholarship Programme for MSc Students for priority subjects and TUBITAK-1001 project (116Y125). The data collected and used for this study was obtained from the project titled “Impact assessment of Hydrolectric Power Plants (HEPP) to marine ecosystems”, funded by TUBITAK (116Y125).

TABLE OF CONTENTS

LIST OF FIGURES

LIST OF TABLES

1. INTRODUCTION

Oceans offer several of ecosystem services, including food resources that are crucial to humanity (Lawton, 1998). Human populations are concentrated on the coast, making coastal ecosystems one of the most affected and changed regions worldwide. Anthropogenic pressures directly affect marine biodiversity through exploitation, pollution and habitat destruction. Also, it indirectly impairs diversity by changing climate and ocean biogeochemistry (Parsons *et al.,* 2014). Therefore, it is important to investigate the ecosystem sensitivities that may arise due to anthropogenic pressures in these regions (Adger *et al.,* 2005).

To fully assess the natural and anthropogenic factors influencing the marine ecosystem, it is essential to determine the contribution of the riverine and atmospheric input to the system (Koçak, 2016). It is particularly necessary for semi-enclosed seas, such as the Mediterranean Sea, under significant environmental stress and deterioration (Martin *et al.,* 1989). Rivers are substantial sources of freshwater and nutrients that contribute to the production of the Mediterranean. Studies are emphasizing that the river discharges and nutrients transferred by the rivers to the Mediterranean have changed significantly in the last decades. It is underlined that river dam construction, and water extraction processes for irrigation and other purposes (Margat and Treyer, 2004) have been developing rapidly since the 1950s, and have profoundly changed the natural functioning of the Mediterranean rivers. This situation is expected to cause long-term changes in the marine ecosystem (Ludwig *et al*., 2009).

The Göksu River flows from the provinces of Antalya, Konya, Karaman and Mersin. It discharges from the Silifke into the northeastern Mediterranean. The length of the river is 260 km, and the basin area is 10000 km^2 (T.C.Orman ve Su İşleri Bakanlığı, 2013). The average flow rate of the Göksu River is 130 m^3/s, where it reaches the highest value during May (Demirel, 2010). Being one of the major perennial rivers draining to the

Çukurova Basin, Göksu River contributes significantly to the nutrient budget and productivity of the northeastern Mediterranean shelf waters.

For marine ecosystems, phytoplankton communities play an essential role by creating a bottom-up effect on the food web (Pomati *et al.*, 2011). Moreover, the spatial heterogeneity of these organisms significantly affects the balance, diversity, dynamics and regional productivity of the ecosystem; to fully understand the marine ecosystem, it is important to comprehend phytoplankton community structures and patchiness (Hillmer *et al.*, 2008). The species in the phytoplankton communities show functional diversity due to having different requirements such as light intensity or diet. Although the main taxonomic groups (e.g., diatoms, dinoflagellates, cyanobacteria) have a certain physiological and morphological plasticity within groups, they differ in their mean functional features (Corcoran & Boeing, 2012a). It is mentioned that communities with representative species from various taxonomic groups may be more productive or stable than communities with fewer species (Corcoran & Boeing, 2012b).

The main aim of this study is to detect the possible effects of contrasting water masses including Göksu River estuary, productive coastal, mesotrophic shelf and oligotrophic offshore waters on phytoplankton abundance and composition. It is also aimed to explore the phytoplankton species diversity and phytoplankton patch formation in this area in order to understand the current state of the ecosystem and create a database for further researches.

Since this study was conducted in the northern Levantine Basin (NLB) in the Eastern Mediterranean and focuses on the impact of the river on sea surface waters, the main focus will be on the surface waters in this part of the Mediterranean.

1.1 The Mediterranean

The Mediterranean is a semi-enclosed sea located in the mid-latitudes. Its coverage is 2.5 million square kilometres, and its volume is nearly 4 million cubic kilometres. The Mediterranean is connected to the Atlantic Ocean via Strait of Gibraltar and the Black Sea via Turkish Straits. It is known that the Mediterranean consists of two almost equal sizes of basins, the western Mediterranean and the eastern Mediterranean (Robinson *et al*., 1992). The Strait of Sicily connects these two basins. The western basin contains the Alboran Sea, the Balearic Sea, the Ligurian Sea and the Tyrrhenian Sea, while the eastern basin contains the Adriatic Sea, the Ionian Sea, the Aegean Sea and the Levantine basin (Figure 1).

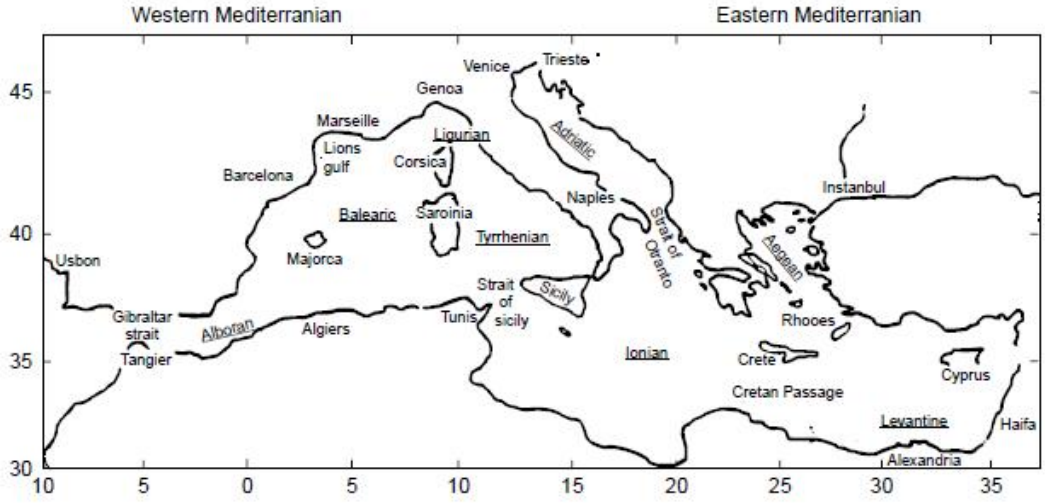

Figure 1 Geographic Features of the Mediterranean Sea. (Robinson *et al*., 1992)

1.2 Physical Properties

The water circulation in the Mediterranean acts as an ocean system by having complicated and dynamic circulation patterns shaped by the various spatial and temporal scales as basin, sub-basin and mesoscale (Fernández *et al.*, 2005). Also, the Mediterranean contributes indirectly to the global thermohaline cycle by exchanging water and supplementary properties with the North Atlantic Ocean.

Hyper-saline Levantine Intermediate Water (LIW) formed in the easternmost Mediterranean and enters into North Atlantic Sea from the Mediterranean through the Strait of Gibraltar (Malanotte-Rizzoli, 2001). As can be seen from Figure 2, this high-salinity intermediate water body passes the basin at the counter direction of the surface flow from the Strait of Gibraltar to the Atlantic Ocean (Özsoy *et al*., 1989).

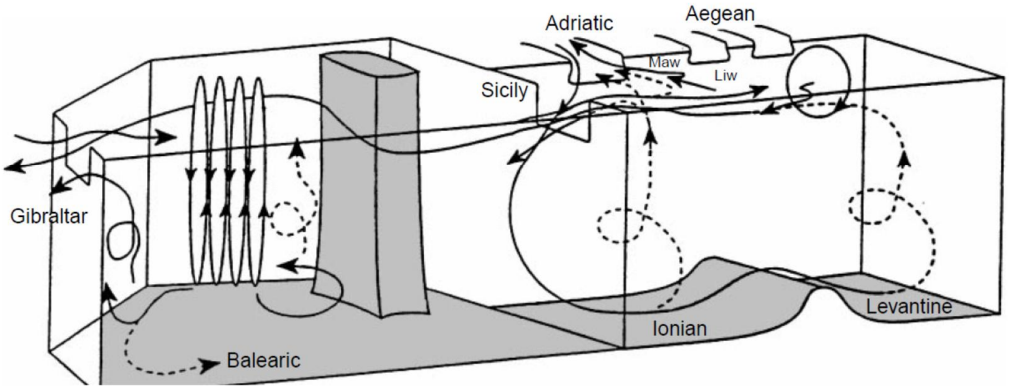

Figure 2 Path of Levantine Intermediate Water (LIW) in the entire Mediterranean (Robinson *et al*., 1992).

In the eastern Mediterranean, the upper thermocline circulation is associated with various sub-basin scales and mesoscale circulations. The Atlantic water moves to the Mediterranean through the Strait of Gibraltar. Atlantic-Ionian Stream is thought to feed the Mid-Mediterranean-Jet, which divided into two as a northward flow feeding the Asia Minor Current and a southward flow (Figure 3).

In this current system; Rhodes gyre, Shikmona gyre and Asia Minor Current are significant components of the circulation in the NBL and its ecosystem (Malanotte-Rizzoli *et al*., 2014).

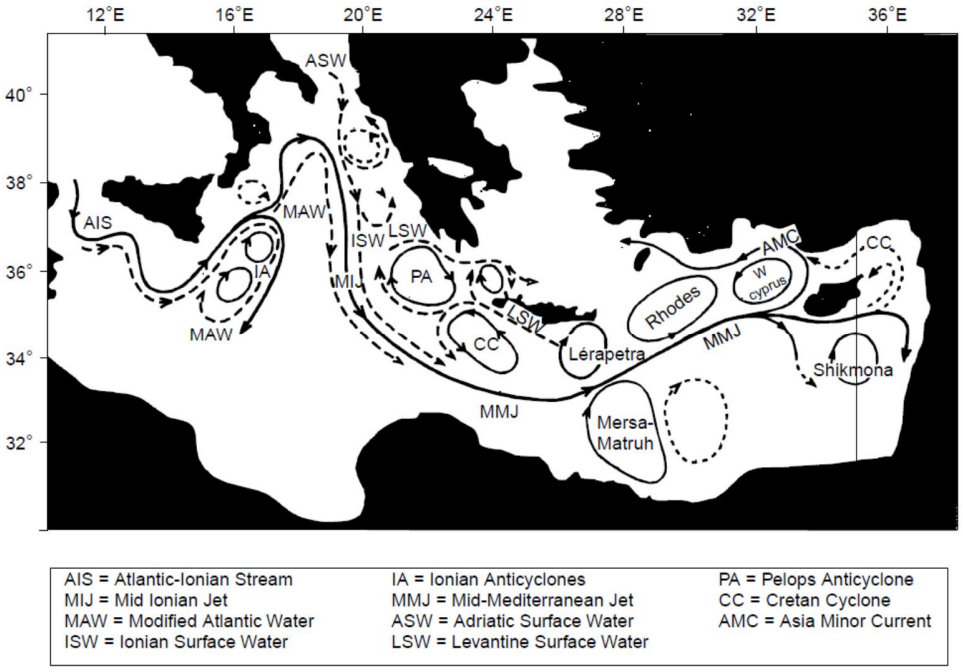

Figure 3 The upper thermocline circulation in the Eastern Mediterranean Sea (Robinson *et al*., 1992).

It is stated that one of the reasons why the Mediterranean is an attractive study area for many researchers is its role in the global thermohaline circulation. Another reason is that the Mediterranean can be considered as a small-scale model of the ocean systems due to having similar processes with the world's oceans (Lacombe *et al.*, 1981, Bergamasco & Malanotte-Rizzoli, 2010).

The Mediterranean is a basin where evaporation exceeds precipitation and freshwater input. At the Strait of Gibraltar, the temperature of the Atlantic water mass (along the way to the eastern basin it becomes a Modified Atlantic Water (MAW)) is 15□ at the surface layer, and salinity of the Atlantic water is 36.2 psu (Bergamasco & Malanotte-Rizzoli, 2010).

According to data from the Mediterranean surface water for 30 years (1986-2015) obtained from Copernicus Marine service, the temperature increases from west to east. The distribution of sea surface temperature (SST) data indicates that the SST was the highest in the southeast and that the southern and southeastern Mediterranean are approximately 3-5 □ warmer than other parts. The northern parts of the Sea SST values are lower. Surface water temperatures are between 14.1-24.3□ according to the average values calculated according to months (Figure 4). It has been found that since 1986, the annual average of SST has increased linearly by 0.4 □ over the entire Mediterranean. (Sakalli & Başusta, 2018).

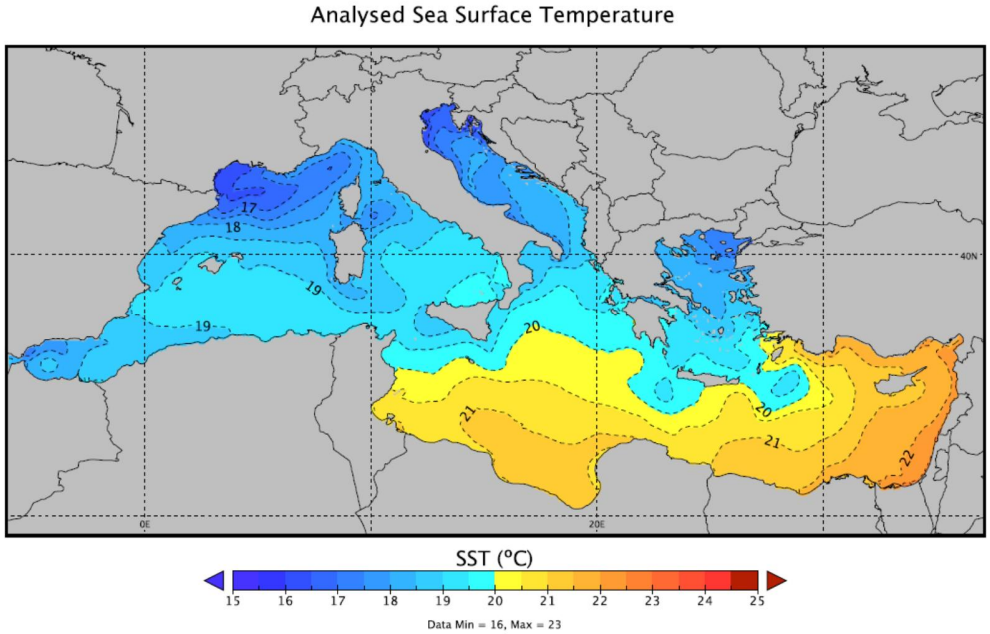

Figure 4 Spatial distribution of high resolution (4x4 km) mean sea surface temperature in the Mediterranean for 30 years (1986-2015) (Sakalli & Başusta, 2018).

The spatial distribution of average annual surface salinity in the Mediterranean basin is shown in Figure 5. This data is presented for 26 years (1987-2013) by using the re-analysis of the Mediterranean Forecasting System. Salinity values of the Mediterranean surface layer ranged from 36.2 psu near the Strait of Gibraltar to 38.6 psu in the Levantine Basin (Soukissian *et al*., 2017).

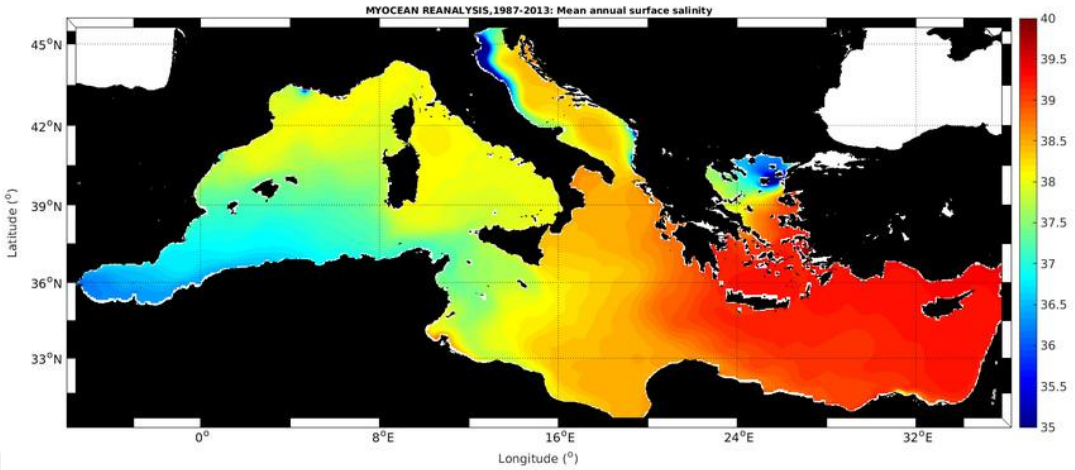

Figure 5 Mean annual surface salinity in the entire Mediterranean Sea. Data obtained from Mediterranean Forecasting System reanalysis (Soukissian *et al*., 2017)

1.3 Chemical Properties

In the Mediterranean, nutrient concentrations are low, and these values decrease from west to east in the basin. In Figure 6, inorganic phosphate, nitrate and silicate values of all Mediterranean basins are given as a function of depth together with the values those observed for Eastern Atlantic to make comparisons (McGill, 1965). As it is understood from the figure, the lowest values for these three nutrient salts are obtained from surface waters. In addition, the Eastern Atlantic water has higher values in terms of these three nutrient salts than all the Mediterranean basins. This is caused by the formation of LIW, sinking water mass due to its high salinity in the Mediterranean Sea. The sinking process creates anti-cyclonic eddies which cause the surface waters to become nutrient-poor (Salihoğlu *et al*., 1990).

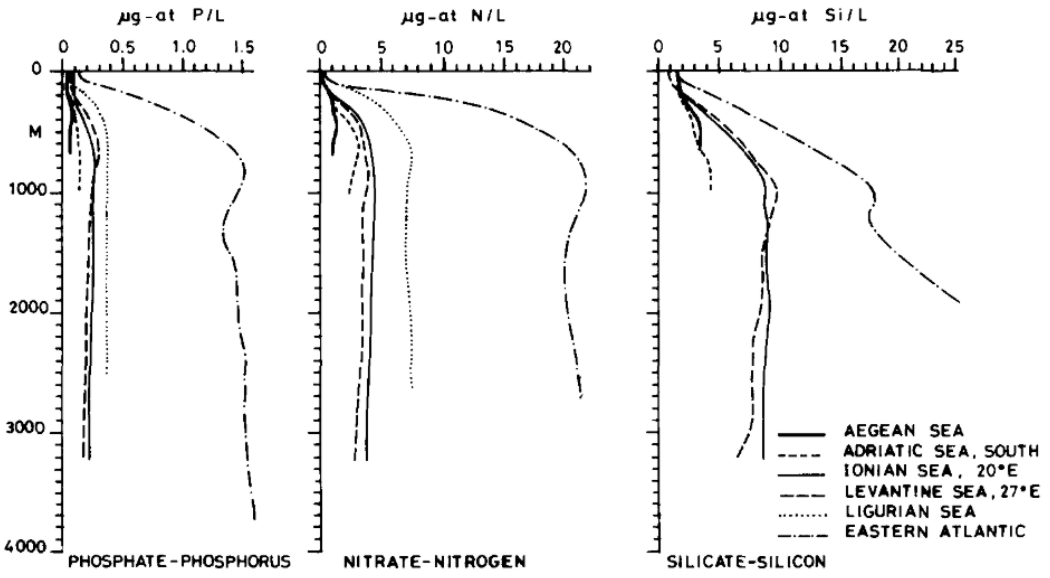

Figure 6 Vertical distribution of inorganic phosphate, nitrate and silicate in the entire Mediterranean and Eastern Atlantic (McGill, 1965). (Salihoğlu *et al*., 1990).

In the NE Mediterranean, inorganic phosphate values ranged between 0.1 and 0.2 µg-at/l, while nitrate values fluctuated between 0.5 and 1.0 µg-at/l in the euphotic zone. Also reactive silicate values were around 1.0 µg-at/l in the euphotic zone. Nutrient concentrations were higher in the aphotic zone compared to the euphotic zone (Table 1).

Table 1 The concentration range of nutrient elements in the Eastern Mediterranean (Salihoğlu *et al.*, 1990)

The concentration range of nutrient elements in the Eastern Mediterranean

Nutrient		Concentration range (in µg-atom l^{-1} $unit^{-1}$
		NE Mediterranean
Inorganic phosphate	U	<0.1-0.2
(PO_4-P)	L	0.2-0.4
Total oxidized nitrogen	U	<0.5-1.0
[(NO_3+NO_2)−N]	L	4.0-9.0
Reactive silicate	U	<1.0-1.0
[$Si(OH)_4$−Si]	L	1.0-10.0

U: euphotic zone; L: aphotic zone.

1.4 Phytoplankton

When the phytoplankton studies conducted in the Eastern Mediterranean are examined, it is observed that they are few and cover only specific sub-areas of the Cilician Basin (Kıdeyş *et al*., 1989; Avşar *et al*., 1998; Eker and Kıdeyş, 2000; Polat and Sarıhan, 2000; Uysal *et al*., 2008; Uysal *et al*., 2003; Yılmaz *et al*., 2003). Nevertheless, it is possible to find studies on seasonal phytoplankton distributions throughout the basin.

It is known that phytoplankton is more abundant and diverse in spring and late winter months. A study conducted by Uysal (2004) showed phytoplankton flowering in spring (Figure 7, 8). In late spring and early summer, phytoplankton rich surface waters were observed to expand towards offshore in Mersin Bay. This is thought to be caused by the increase in the flow of local rivers due to the melting snow during these seasons (Uysal, 2016).

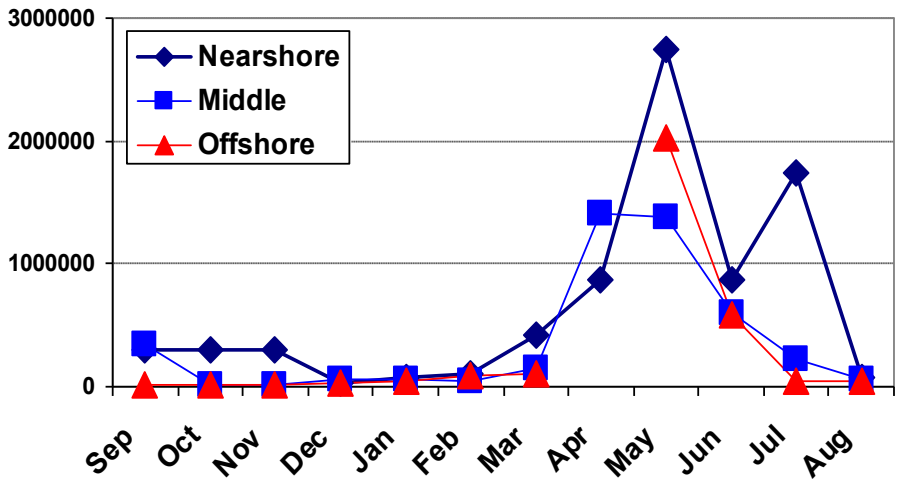

Figure 7 Monthly changes in phytoplankton cell abundances (total cell #/L) at Cilician shelf waters (Uysal, 2016).

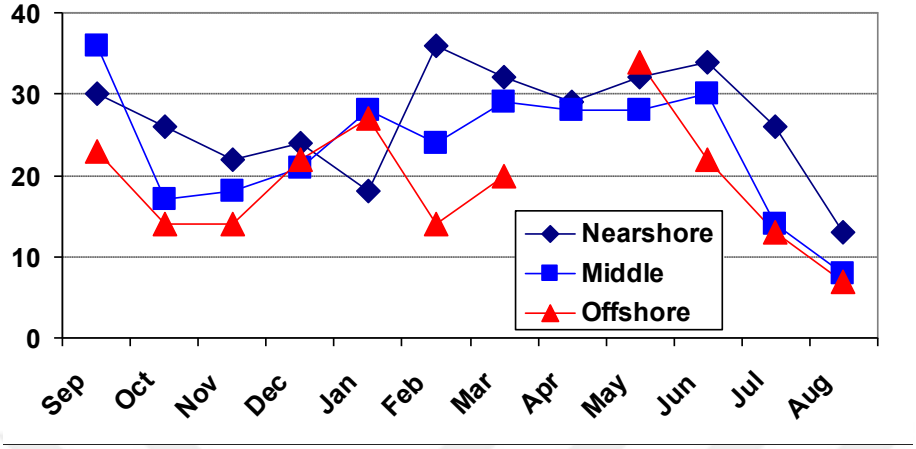

Figure 8 Monthly changes in the number of phytoplankton species observed in Cilician shelf waters (Uysal, 2016).

In this period, it was determined that the group with the highest number of species in the region was diatoms, followed by dinoflagellates and chrysophytes, respectively. Surface phytoplankton abundance and diversity decreased from inshore to offshore. Dinoflagellates were predominant in coastal areas, especially in summer. The coastal areas that obtain nutrient-rich freshwater through rivers have much higher phytoplankton densities (e.g. Mersin and İskenderun Bays) than those in close connection with oligotrophic offshore waters (Uysal, 2016). In a study conducted by Uysal and his colleges (2003), it was found that high nutrient input of waste discharges from anthropogenic sources also increased monospecific phytoplankton blooms in Mersin Bay.

2. MATERIAL AND METHODS

This study was carried out to understand the current state of the marine phytoplankton in the area affected by the Göksu River located in the Cilician Basin (northeastern Mediterranean). Sampling stations were selected from different regions representing nearshore, offshore waters as well as the Göksu River estuary. Regarding the main westward flowing current regime, samples were also collected from both sides of the river mouth to compare eastern communities drifted by currents with those supported by the freshwater inputs in the west.

2.1. Sampling Area

In this study, four seasonal cruises were performed for the measurements and sampling of ambient physical (temperature, salinity, density) and biochemical (nutrients, dissolved oxygen, chlorophyll-*a*, particulate organic matter, *situ* fluorescence, Secchi disk depth) parameters and of phytoplankton onboard R/V Bilim-2 of the Institute of Marine Sciences - Middle East Technical University. In the region of interest (Figure 9), stations were gridded horizontally and vertically around the Göksu River mouth to understand the impact of freshwater input on changes in the quality and quantity of phytoplankton in parallel to changes in other ambient physicochemical parameters temporally and spatially.

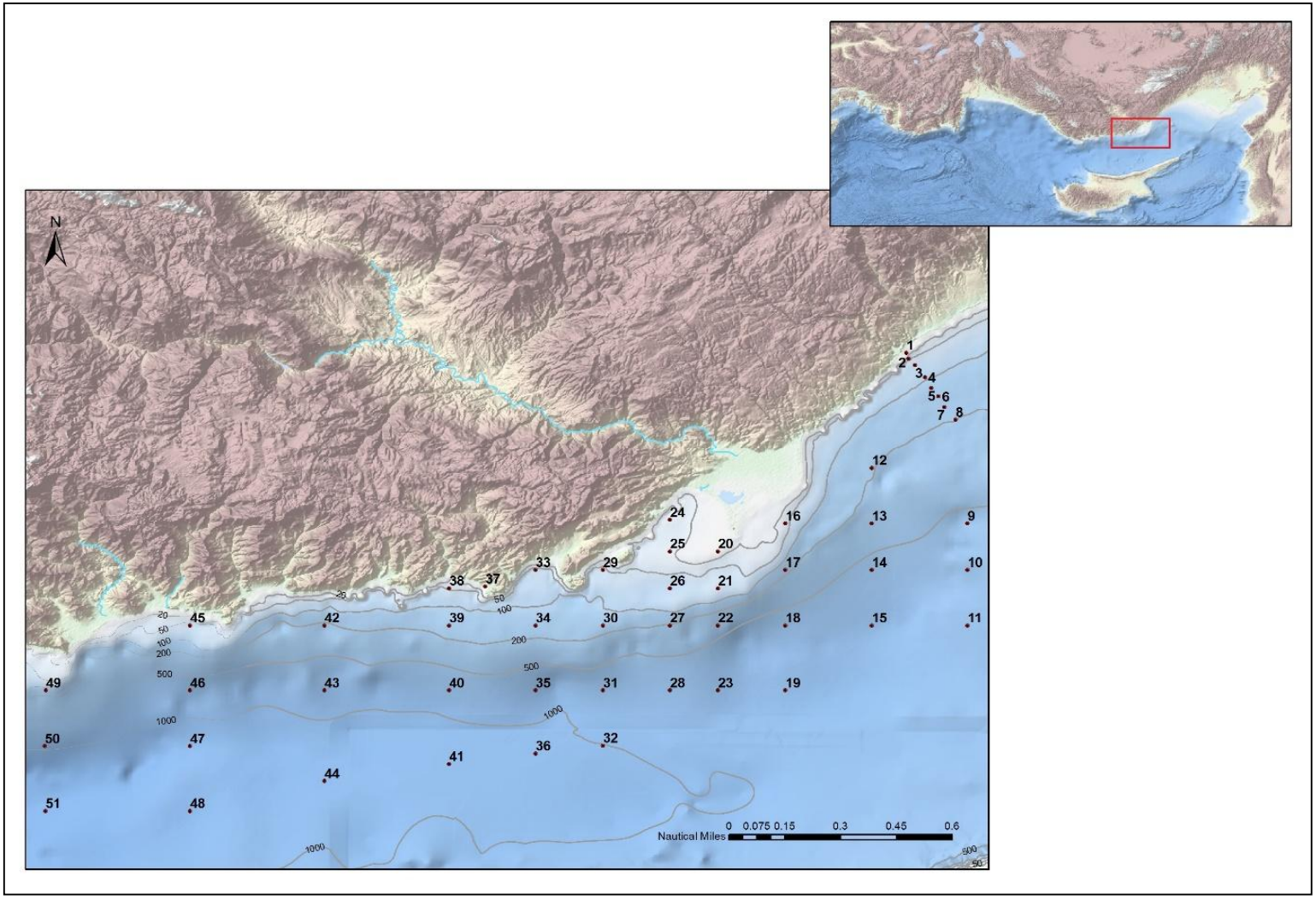

Figure 9 Location of total 51 stations covering both Göksu river estuary and the surrounding areas including Erdemli Time Series (ETS) stations in front of METU-IMS (first 9 stations).

2.2 Sampling and Analysis

In order to better describe patchy distributions of phytoplankton in the area of interest, (Figure 9) in addition to phytoplankton samples, measurements of associated ambient physical and biochemical parameters (Table 2) have also been performed during the seasonal cruises.

Table 2 Sampling plan for the TUBİTAK Project No 116Y125 Cruises in October 2017, February, April and June 2018.

Station numbers	Latitude	Longitude	CTD	Phytoplankton	Dissolved Oxygen	Nutrients	POC-PON
1	36.55870	34.26007	**P**	**P**	P	**P**	
2	36.54812	34.26428	**P**	S		**S**	
3	36.53668	34.27527	**P**	S		**S**	
4	36.51478	34.29257	**P**	P	P	**P**	
5	36.49540	34.30398	**P**	S		**S**	
6	36.48003	34.31602	**P**	S		**S**	
7	36.46118	34.32617	**P**	S		**S**	
8	36.43828	34.34553	**P**	**P**	**P**	**P**	P
9	36.25000	34.36667	**P**	S		**S**	
10	36.16667	34.36667	**P**	S		**S**	
11	36.06667	34.36667	**P**	S		**P**	
12	36.35000	34.20000	**P**	S		**P**	
13	36.25000	34.20000	**P**	S		**S**	
14	36.16667	34.20000	**P**	S		**S**	
15	36.06667	34.20000	**P**	S		**S**	
16	36.25000	34.05000	**P**	P	P	**P**	S
17	36.16667	34.05000	**P**	S		**P**	
18	36.06667	34.05000	**P**	S		**S**	
19	35.95000	34.05000	**P**	S		**S**	
20	36.20000	33.93333	**P**	P	P	**P**	P
21	36.13333	33.93333	**P**	**P**	**P**	**P**	P
22	36.06667	33.93333	**P**	S		**P**	

Table 2 *(Continued)*							
23	35.95000	33.93333	**P**	S		**P**	
24	36.25643	33.85000	**P**	S		**P**	
25	36.20000	33.85000	**P**	S		**P**	
26	36.13333	33.85000	**P**	S		**P**	
27	36.06667	33.85000	**P**	S		**S**	
28	35.95000	33.85000	**P**	S		**S**	
29	36.16667	33.73333	**P**	S		**P**	
30	36.06667	33.73333	**P**	S		**P**	
31	35.95000	33.73333	**P**	S		**S**	
32	35.85078	33.73333	**P**	S		**S**	
33	36.16667	33.61667	**P**	S		**P**	
34	36.06667	33.61667	**P**	S		**P**	
35	35.95000	33.61667	**P**	S		**S**	
36	35.83660	33.61667	**P**	S		**P**	
37	36.13687	33.52942	**P**	**P**	**P**	**P**	S
38	36.13333	33.46667	**P**	S		**P**	
39	36.06667	33.46667	**P**	S		**P**	
40	35.95000	33.46667	**P**	S		**P**	
41	35.81795	33.46667	**P**	S		**S**	
42	36.06667	33.25000	**P**	P	P	**P**	
43	35.95000	33.25000	**P**	S		**S**	
44	35.78728	33.25000	**P**	S		**S**	
45	36.06667	33.01667	**P**	S		**P**	
46	35.95000	33.01667	**P**	S		**S**	
47	35.85000	33.01667	**P**	P	P	**P**	P
48	35.73333	33.01667	**P**			**S**	
49	35.95000	32.76667	**P**	S		**P**	
50	35.85000	32.76470	**P**	S		**S**	
51	35.73333	32.76603	**P**	S	P	**P**	

S = **S**urface, **P** = **P**rofile (Surface and bottom depths)

Dissolved Oxygen: Surface, 20, 50, DCM, 75, 100, 150, 200, 250, 300, 500, 750, 1000, 1500.

Nutrients: Surface, 20, 50, DCM, 75, 100, 150, 200, 250, 300, 500, 750, 1000, 1500.

PON-POC: Surface, 20, 50, DCM, 75, 100, 150, 200

DCM: Deep Chlorophyll Maximum

2.2.1 Phytoplankton Sampling

Phytoplankton sampling was achieved by using Niskin bottles attached to the rosette during the cruises. 100 ml of samples were taken into pre-cleaned borosilicate dark bottles and fixed with 2 mL 25% glutaraldehyde and stored at room temperature in the dark on board (Murphy and Haugen, 1985).

2.2.2 Physical Parameters

High precision measurements of depth (pressure), temperature, salinity and density parameters were carried out with a SEABIRD model CTD probe coupled to a 12-Niskin Bottle (12 L capacity) Rosette System for remote-controlled water sampling at selected depths of the water column. With the CTD coupled Rosette System, water samples were taken from selected depths.

2.2.3 Chemical Parameters

2.2.3.1 Dissolved Oxygen

Dissolved oxygen measurements in seawater were performed on board by the automated Winkler titration method (Grasshoff *et al*., 1983). Using the CTD connected rosette water sampling system, water samples were collected at specified depths during the upcast. Initially, dissolved oxygen samples were taken into 100 ml glass bottles using Tygon plastic tubes to ensure that the sample remained bubble-free and thus avoid contamination with air bubbles. Immediately after sampling, solutions of manganese (II) chloride and alkaline potassium iodide were added and were shaken until all the oxygen in the samples were diffused completely. Then, samples were put in a dark place for at least 30 minutes to ensure that the reaction was completed. Finally, dissolved oxygen concentrations were measured by automated titration method by titration with 0.02 M sodium thiosulphate solution (Strickland and Parsons, 1972; Grasshoff *et al*., 1983; UNEP/MAP, 2005).

2.2.3.2 Nutrients

After oxygen samples, nutrient samples were taken into 10% HCl pre-cleaned, high-density polyethylene bottles (HDPE). Nutrient samples were then kept in -20 ° C until analysis. Nutrient concentrations (nitrate + nitrite, reactive silicate, phosphate, and ammonium) were measured at the institute laboratory by using Sea Analytical AA3 with XY3 Autosampler model four-channel Autoanalyzer with the standard colourimetric method (Grasshoff *et al*. 1983).

2.2.3.3 POC-PON

Samples of 5-10 litres of seawater collected for particulate organic carbon (POC) and particulate organic nitrogen (PON) analyses were filtered through GF / F type filter papers as soon as possible at low suction pressure. Samples were then washed with 5-10 ml of distilled water and preserved in aluminium foil in the deep freezer until analysis. These procedures performed on board immediately after sampling. At the institute laboratory, the filter paper used in the filtration, before being used, they were combusted at 450-500 ^{o}C for one hour to oxidise organic matter. The water samples were taken and filtered at selected 4 or 5 depths in the stations shown in Table 2.1. For the analysis of POC and PON, samples were dried at about 50 ^{o}C overnight in an oven and treated with stock hydrochloric acid (HCl) fume to remove inorganic carbonate content of the samples. After removing inorganic carbon from the filters, the carbonate-free filters dried again. Each filter sample then placed into the tin foil and capsuled using a special apparatus. Finally, POC and PON samples were measured by High-Temperature Dry Combustion Method, using a Vario El Cube Elementar Model CHN analyser. Calibration standards prepared from acetanilide which contains 71.09% C and 10.36% N and generally four calibration standards were used to calculate POC and PON contents of filtered seawater samples as described in Polat and Tuğrul (1995) and Çoban-Yıldız (2000).

2.3 Phytoplankton Cell Counts & Identification

In the laboratory, quantitative and qualitative analyses were performed under a reverse phase-contrast microscope. Glutaraldehyde fixed samples were kept in settling chambers (HYDRO-BIOS made with a volume of total 25 ml) over a day for settling. Following settling the whole settling area of the chamber was checked for cell counts & species identification. All specimens belonging to diatoms, dinoflagellates, coccolithophorids and remaining groups were tried to be identified at the species level. Phytoplankton sampling stations were given in Table 2.1. Cell counts were then converted to cells/l (Drebes, 1974; Pavillard, 1925; Rampi & Bernhard, 1978; Sykes, 1981; Trégouboff & Rose, 1957).

2.4 Diversity Indices

Margalef (species richness D), Shannon (diversity H') and Pielou (regularity J') (Pielou, 1966) values were determined as diversity indices.

The Margalef (Type Richness) index refers to the ratio of the number of species identified to the total number of individuals.

$d = (S - 1) / \ln N$

S: number of species,

N: the total number of individuals.

The Shannon diversity index also considers the number of species, as well as the frequency within each species.

$H' = -\sum_{i=i}^{S} pi\ log2\ pi$, pi =Ni / N

S: number of species

Ni: Number of individuals belonging to the first species

N: Total number of individuals

Pielou regularity (J ') index refers to the ratio of observed diversity to maximum diversity.

$$J' = H' (observed) / H'max$$

where is maximum possible diversity. ($H'max = \ln S$)

S: number of species

If the distribution of the species in total frequency is homogeneous, it reaches to the highest value of 1, and if there are species that dominate among individuals, values begin to fall.

2.5 Analytical Methods

In order to determine the interaction levels and potential outcomes of these interactions between physical, chemical and biological variables, data analysis was performed.

Primarily, **the test of randomness** (Index of dispersion) was applied to the data to understand the distribution of the data (normally distributed or not). If the data set shows an ideal normal distribution, the value of $s^2/\bar{x}$ ratio is 1.

$$I = s^2 (n-1) / \bar{x}$$

I: Index of dispersion

s^2: sample variance

n: Sample size

$\bar{x}$: The sample mean

Secondly, the non-parametric spearman-rank correlation test was selected for the analysis of the interactions between the variables since the data sets of the parameters were not normally distributed. **The Spearman rank-order correlation analysis** was performed between environmental parameters and cell abundances.

The formula used for the Spearman rank-order correlation coefficient is:

$$r_s = [\Sigma(y - \bar{y})(z - \bar{z})] / \sqrt{\Sigma (y - \bar{y}) \Sigma (z - \bar{z})}$$

$\bar{y}$: mean rank of the sample from variable 1,

$\bar{z}$: mean rank of the sample from variable 2,

Degrees of freedom = n-2, where n = sample size.

If $\boldsymbol{r_s \geq r_{s\ critical}}$: significant result and if $\boldsymbol{r_s \leq r_{s\ critical}}$: non-significant result.

Lastly, **Multi-Dimensional Scaling (MDS**) technique was used for detection of the possible phytoplankton patches and environmental factors contributing to these patchy formations by analysing all relevant data.

The raw abundance data consists of abundant species and rare species. For that reason, root-root transformations were applied to regulate the weight of abundant species. This transformation is advantageous over logarithmic transformation when using the Bray-Curtis coefficient for similarity analysis.

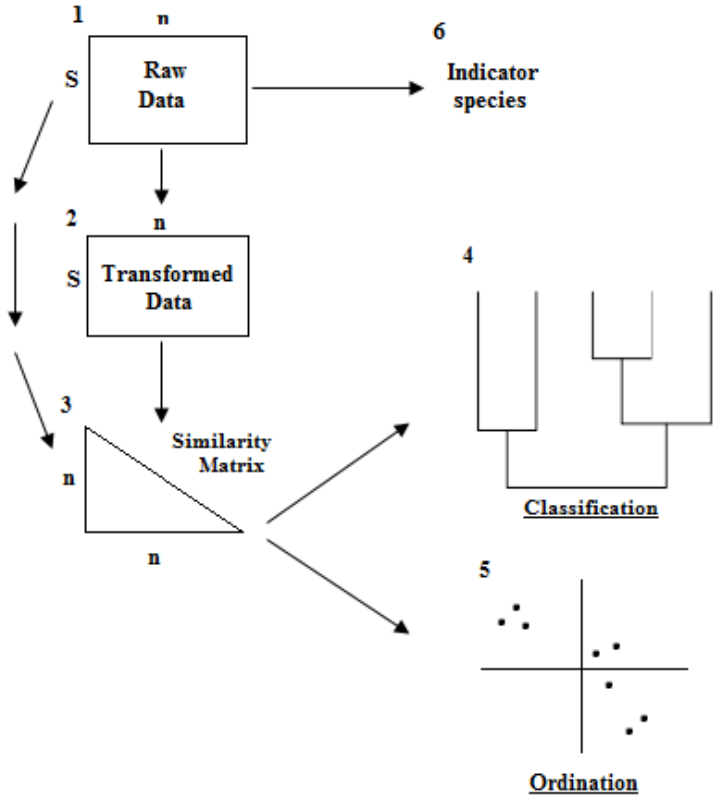

Figure 10 Schematic representation of stages of the MDS analysis based on (dis)similarity coefficients (Field *et al*., 1982).

The formula used for the transformation is;

$$Y_{ij} = \sqrt{\sqrt{X_{ij}}} = {X_{ij}}^{1/4}$$

where X_{ij} = raw data score of the ith species in the jth sample

Y_{ij} = matching transformed score

Similarity (S) can be assessed with similarity coefficients by using direct countings, biomass or presence/ absence data. Similarity measure usually described in the range (0-1) or (0-100 %).

S = 1 means that samples are entirely similar, S = 0 means that samples are entirely dissimilar. Bray- Curtis coefficient was selected to assess similarity since it is the most useful measure for the ecological survey analysis. Coefficient calculations were done with transformed abundance data.

The formula used for the calculation of the Bray-Curtis coefficient is;

The similarity between j^{th} and k^{th} samples is:

$$S_{jk} = 100\left(1 - \frac{\sum_{i=1}^{p} |y_{ij} - y_{ik}|}{\sum_{i=1}^{p} |y_{ij} + y_{ik}|}\right)$$

$$= 100\,\frac{\sum_{i=1}^{p} 2\min\,(y_{ij}, y_{ik})}{\sum_{i=1}^{p}(y_{ij} + y_{ik})}$$

where Y_{ij} = count for i^{th} species in a j^{th} sample,

Y_{ik} = count for i^{th} species in a k^{th} sample.

Species similarity matrices are formed by calculating similarity coefficients of species abundance between every pair of samples in a lower triangular array. To better understand the structure of natural group formations, hierarchical clustering was applied based on the Bray- Curtis similarity matrix.

Group-average linking was selected as the sorting strategy for the construction of a dendrogram from the similarity matrix. This strategy unites two groups together at the average rank of similarity between all components of one group and all components of the other.

To better visualize the relationship between the groups, dendrogram groups were classified in the relevant ordination. Multi-dimensional scaling (MDS) technique was preferred as ordination method. MDS tries to produce an ordination by using the information of similarity levels of n groups in a given number of dimensions as sample 1 closer in similarity to sample 3 than sample 5. MDS plot can be plotted as scaled, located,

rotated or inverted optionally. It gives relative positions of the samples to each other. However, in case of high, the number of samples and lower-dimensional ordination, distortion or stress between dissimilarities and corresponding distances in the MDS plot emerges.

Non-metric MDS algorithm works with an iterative process. This procedure can be explained in the following steps:

1- Set the number of dimensions for MDS plot (= m)
2- In m dimensions built a base map for n samples
3- Regress interpoint distances (d_{jk}) from the base map on the corresponding dissimilarities(δ_{jk})
4- "Goodness-of-fit" measurements done with the stress formula:

$$STRESS = \sum j \sum k \left(d_{jk} - \hat{d}_{jk}\right)^2 / \sum j \sum k \, d_{jk}^2$$

where $\hat{d}_{jk}$ = distance given by the fitted regression line for dissimilarity (δ_{jk})

Stress = 0 means that the rank order of the dissimilarities is maintained. Stress value increases when the map is unrelated to the dissimilarities.

5- Find a convenient position for the current sample on the map, which decreases the stress.
6- Repeat steps 3 and 5 until no further reduction is possible in stress.

To identify indicator species responsible for these natural group formations, the contribution to average dissimilarity ($\bar{\delta}$) or similarity ($\bar{S}$) from ith species are calculated.

Based on the $\delta = 100 - S$ formula, contribution to (δ_{jk}) from ith species is:

$$\delta_{jk}(i) = 100.\left|y_{ij} - y_{ik}\right| / \sum_{i=1}^{p} \left(y_{ij} + y_{ik}\right)$$

Its standard deviation showed as SD ($\bar{\delta}_i$) in the result part. Higher $\bar{\delta}_i$ value and $\bar{\delta}_i$/ SD ($\bar{\delta}_i$) ratio express the distinctive species. The same goes for $\bar{S}_i$ value and $\bar{S}_i$ / SD ($\bar{S}_i$) ratio.

3. RESULTS

In this part, seasonal observations of physical and chemical parameters that affect abundance and distribution of phytoplankton were evaluated spatially and temporally.

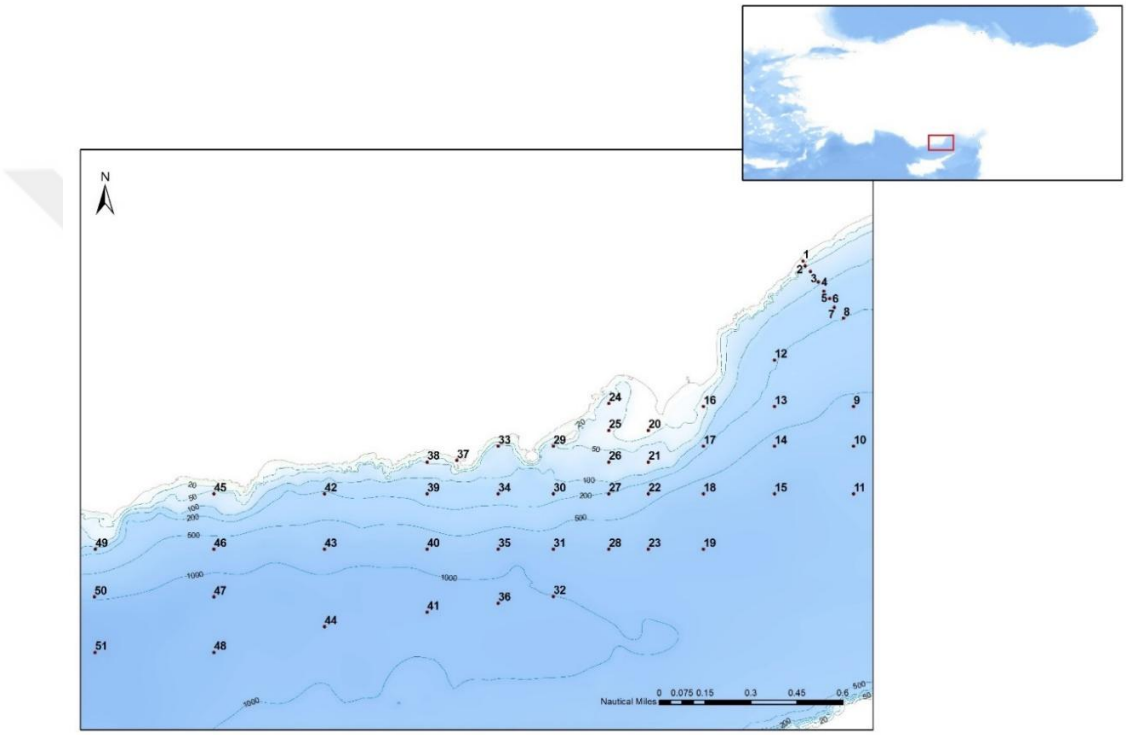

Figure 11 Location of seasonal sampling stations with depth contours.

During the four cruises which took place in October 2017, February, April and June 2018, environmental parameters were collected from all designated stations (Figure 11). In October, 47 stations were sampled missing stations 19, 49, 50 and 51. In February, environmental parameters were collected from 49 stations lacking stations 11 and 51. In April, 47 stations were sampled, and stations 11, 49, 50 and 51 were not sampled. In June, except the 11th station, all stations were sampled (Figure 12).

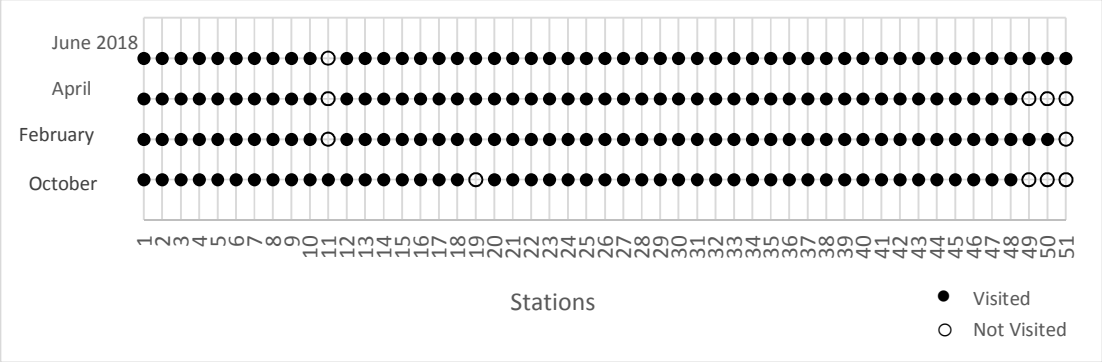

Figure 12 Sampled stations during all four seasons. (October 2017, February, April and June 2018)

3.1 Physical Parameters

In this study, temperature, salinity, density and PAR data were collected from the stations during maritime cruises to determine the effect of physical parameters.

3.1.1 Temperature

The temperature in the surface waters varied from 17.26 to 27.41□ in the study area. As expected, the highest temperatures recorded during summer (June-2018) whereas, the lowest vales were obtained in winter (February-2018) (Table 3).

The temperatures in the surface waters showed significant decreasing values in their seasonally arithmetic means in the order summer > fall > spring > winter. Beginning from the lowest, the mean the surface water temperature was 18.48 □ in winter, ranging between 17.26 and 19.04 □ (February 2018) (Table 3). For this season, the lowest temperatures were observed near the Göksu River mouth whilst the highest values were recorded at stations 5 and 12 situated at the east (Figure 13b). From winter to spring (April 2018), the surface water temperatures denoted gradually increase, varying from 19.58 to 21.50□ with an arithmetic mean of 20.26 □ (Table 3). The highest value were observed at station 27 located at offshore of the Göksu River while the lowest temperature was observed at station 44 (>1000m depth) located at the deeper west (Figure 13c).

In fall (October 2017), the mean surface temperature increased and reached value of 25.89□, fluctuating between 24.84 and 26.83□ (Table 3). In general, it denoted decrease from east to west (Figure 13a). In summer, the surface temperature reached its peak with a mean of 26.30 □, ranging from 24.93 to 27.41 □ (June 2018) (Table 3). The highest temperature was recorded at station 1 and the lowest temperature was detected at station 29, later being influenced by direct runoff from the Göksu River (Figure 13d).

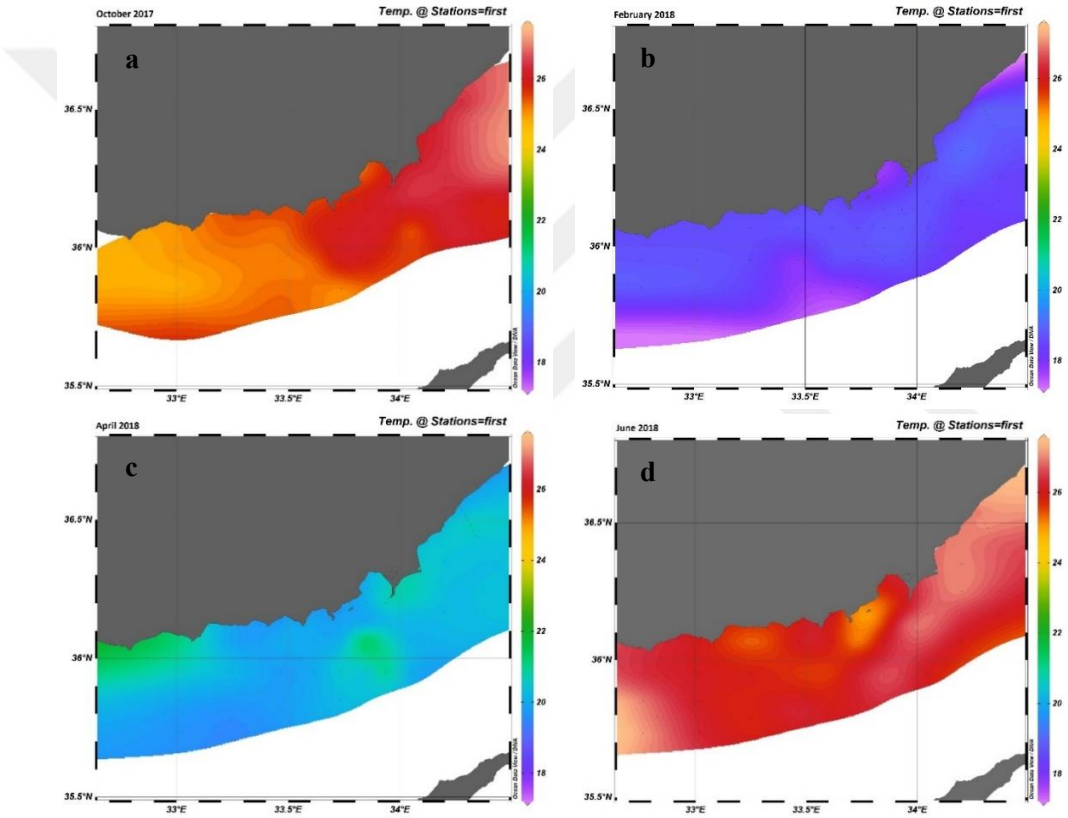

Figure 13 Surface temperature(□) distributions for all seasons; Fall -October (a), Winter-February (b), Spring-April (c), Summer-June (d) (ODV/DIVA Gridding/Interpolation).

Table 3 Minimum, maximum and mean surface temperature values recorded in each season.

	Temperature (□)		
	Minimum	**Maximum**	**Mean**
October 2017	24.84	26.83	25.89
February 2018	17.26	19.04	18.48
April 2018	19.58	21.50	20.26
June 2018	24.93	27.41	26.30

3.1.2 Salinity

The salinity in the surface waters varied from 38.23 - 39.80 psu in the study area. The highest temperatures recorded during fall whereas, the lowest vales were obtained in spring (Table 4).

The salinities in the surface waters showed decreasing values in their seasonally arithmetic means in the order fall > summer > winter > spring. Beginning from the lowest, the mean the surface water salinity was 39.16 psu in spring, ranging between 38.23 and 39.43 psu (Table 4). For this season, the lowest salinities were observed at ETS-4 station located at the east whilst the highest values were recorded at station 30 (Figure 14c). In winter, the mean surface salinity increased and reached value of 39.35 psu, fluctuating between 38.47 - 39.46 psu (Table 4). For this season, the lowest salinities were observed at shallow ETS-2 station located at the east whilst the highest values were recorded at station 12, a deep station situated at the east (Figure 14b). In summer, the surface water salinities increased, varying from 39.23 and 39.52 psu with an arithmetic mean of 39.52 psu (Table 4). The lowest values were observed at ETS-1 station located at coastal eastern side of the sampling area while the highest salinity was observed at ETS-7 station located at the deeper east. Further offshore surface salinity showed a sudden increase at stations ETS-5, 6, 7 (Figure 14d).

In fall, the mean surface salinity increased and reached value of 39.75 psu, fluctuating between 39.63 - 39.80 psu (Table 4). For this season, the lowest temperatures were observed at station 20 near the Göksu River mouth whilst the highest values were recorded at station 24 situated at the Taşucu Bay (Figure 14a).

Table 4 Minimum, maximum and mean surface salinity values recorded in each season

Seasons	**Salinity (psu)**		
	Minimum	**Maximum**	**Mean**
October 2017	39.63	39.80	39.75
February 2018	38.47	39.46	39.35
April 2018	38.23	39.43	39.16
June 2018	39.23	39.62	39.52

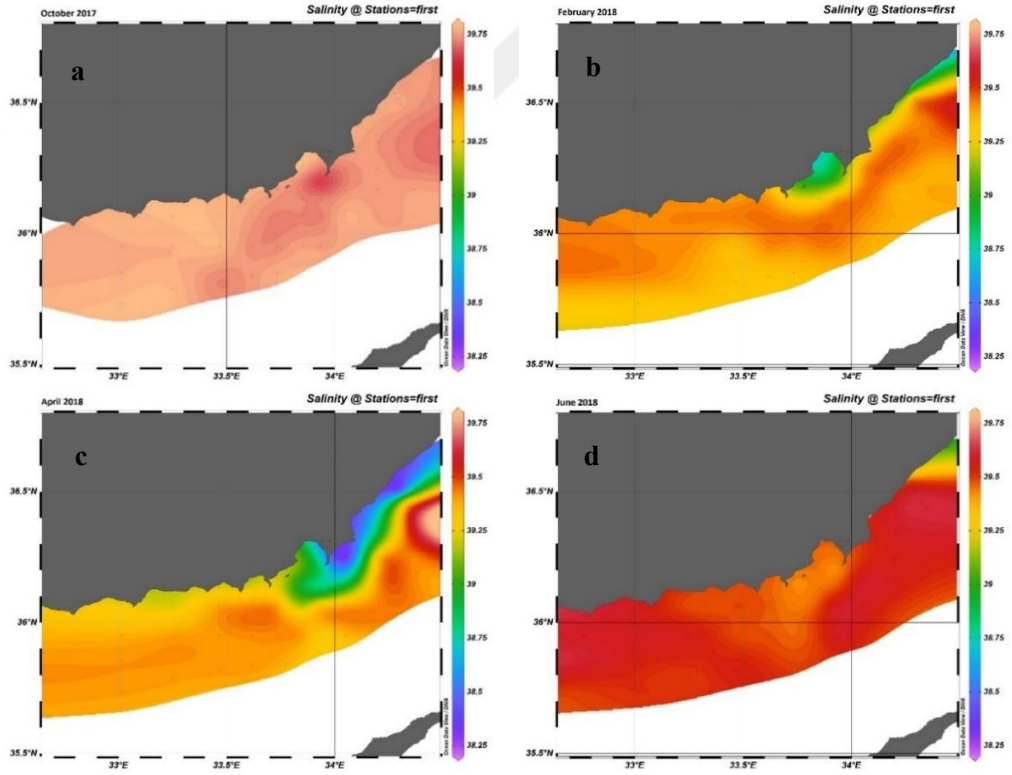

Figure 14 Surface salinity (psu) distributions for all seasons; Fall-October (a), Winter-February (b), Spring-April (c), Summer-June (d) (ODV/DIVA Gridding/Interpolation).

3.1.3 Density

The density in the surface waters varied from 25.77 - 28.68 kg/m^3 in the study area. The highest densities recorded during winter whereas, the lowest vales were obtained in summer (Table 5).

The densities in the surface waters showed decreasing values in their seasonally arithmetic means in the order winter > spring > fall > summer. Beginning from the lowest, the mean the surface water density 26.35 kg/m^{3}in summer, ranging between 25.77 and 26.72 kg/m^3 (Table 5). For this season, the lowest densities were observed at ETS-1 station located at the east whilst the highest values were recorded at station 30 at 100-200m depth contour line off the Taşucu Bay (Figure 15d). In fall, the mean surface density increased and reached value of 26.66 kg/m^3, fluctuating between 26.34 and 27.00 kg/m^3 (Table 5). For this season, the lowest temperatures were observed at at ETS-8 station on 200m depth contour line at the east whilst the highest values were recorded at station 47 on the >1000m depth contour line at the (Figure 15a). The mean the surface water density was 27.87 kg/m^3 in spring, ranging between 27.04 to 28.24 kg/m^3 (Table 5). For this season, the lowest densities were observed at station 16 , later being influenced by direct runoff from the Göksu River whilst the highest values were recorded at station 44 on the >1000m depth contour line at the west (Figure 15c). In winter, the mean surface density increased and reached value of 28.48 kg/m^3, fluctuating between 28.12 - 28.68 kg/m^3 (Table 5). For this season, the lowest densities were observed at shallow ETS-2 station located at the east whilst the highest values were recorded at station 48, one of the deepest (>1000m) stations at the west (Figure 15b).

Table 5 Minimum, maximum, and mean surface density values for each season.

Seasons	Density (kg /m3)		
	Minimum	**Maximum**	**Mean**
October 2017	26.34	27.00	26.66
February 2018	28.12	28.68	28.48
April 2018	27.04	28.24	27.87
June 2018	25.77	26.72	26.35

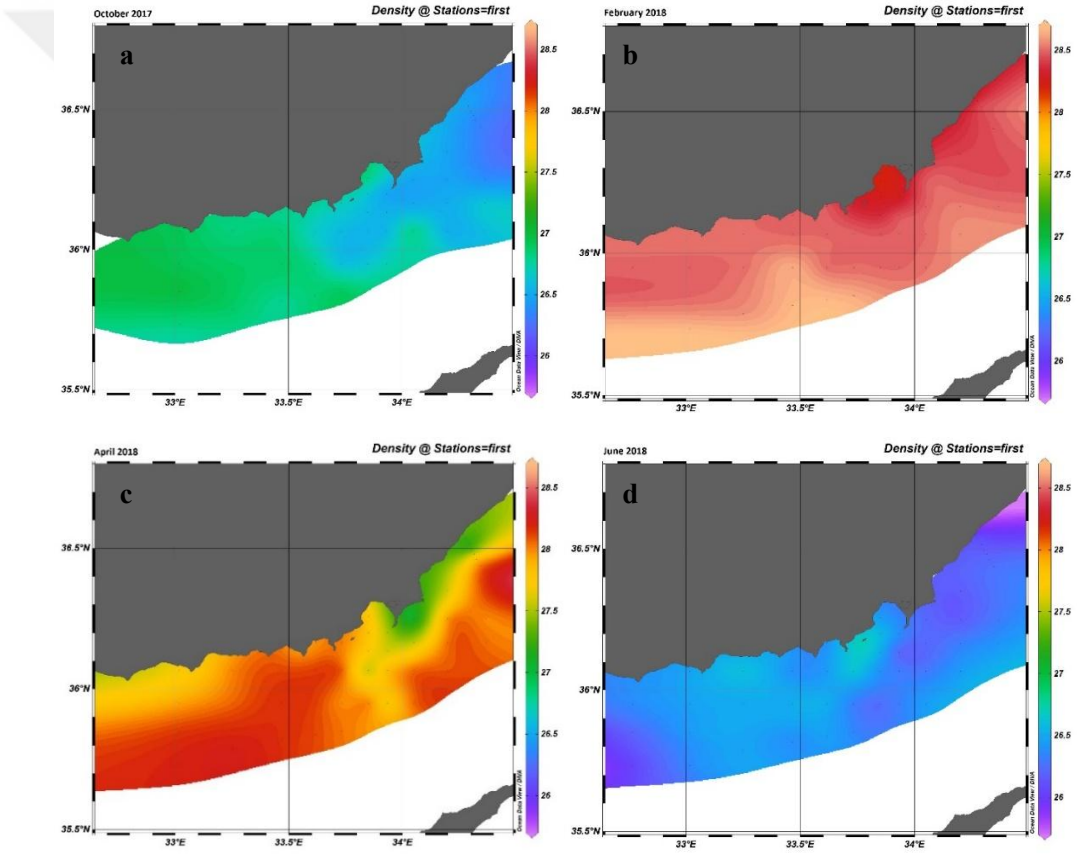

Figure 15 Changes in surface density with seasons; Fall -October (a), Winter-February (b), Spring-April (c), Summer-June (d) (ODV/DIVA Gridding/Interpolation).

3.2 Chemical Parameters

3.2.1 Nutrient Salts

3.2.1.1 Phosphate

The lowest phosphate concentrations in the surface waters was observed at the detection limit of the instrument (0.02 μM) and maximal concentration was 0.11μM in the study area. The highest temperatures recorded during fall and spring (Table 6).

Table 6 Minimum, maximum, and mean surface phosphate concentrations (μM) measured in each season.

Seasons	Phosphate (μM)		
	Minimum	**Maximum**	**Mean**
October 2017	0.020	0.110	0.030
February 2018	0.020	0.100	0.034
April 2018	0.020	0.110	0.040
June 2018	0.020	0.090	0.040

The phosphate concentrations in the surface waters showed decreasing values in their seasonally arithmetic means in the order summer = spring > winter > fall. Beginning from the lowest, the mean surface water phosphate value was 0.03μM in fall, ranging between 0.02 and 0.11μM (Table 6). For this season, by checking whole phosphate data from the stations indicates that while for the majority of phosphate values were between 0.02 and 0.04μM; stations ETS-8, 16 and 20 have displayed slightly higher values ranging between 0.05 and 0.06 μM. High phosphate values were also detected at stations ETS-4 and 30 (Figure 16a, Figure 17). From fall to winter, the surface water phosphate values denoted gradually increase, varying from 0.02 and 0.1μM with an arithmetic mean of 0.03μM (Table 6). For this season, phosphate values were mostly between 0.02-0.04μM. The coastal stations 29, 33, 37, 38 and 39 have displayed phosphate values between 0.05 - 0.06 μM, higher than the overall mean level.

This was also the case for stations 49 and 50 located at the west. The highest value was obtained at coastal station 25 (Figure 16b, Figure 17).In the spring, the surface water phosphate values denoted gradually increase, varying from 0.02 and 0.11μM with an arithmetic mean of 0.04μM (Table 6). For this season, phosphate values showed a more patchy distributions. At ETS stations 1 through 10, phosphate values showed high fluctuations between 0.02-0.11 μM. The highest values were obtained at coastal stations ETS-1and ETS-6. Concentrations fluctuated between 0.02-0.07μM at stations 12 through 20, including the area, being influenced by direct runoff from the Göksu River. Phosphate values were measured between 0.02 - 0.04μM at stations 24 through 36, while data distribution was stable. For stations 37 through 48, phosphate values varied between 0.02-0.08μM, while stations 38 (at 50m depth contour line) and 44 (at > 1000m depth contour line) showed noticeably higher values than other stations in this region (Figure 16c, Figure 17). In the summer, the surface water phosphate values were varying from 0.02 and 0.09μM with an arithmetic mean of 0.04μM (Table 6). For this season, ETS stations 1 through 11, phosphate values showed high fluctuations between 0.03-0.08 μM. The highest values were obtained at coastal station ETS-1. Phosphate values ranged from 0.02 to 0.09μM at stations 7 through 11, while the highest value for this season observed at coastal station 37. Stations 38 through 49 had phosphate contents between 0.02 and 0.05μM and showed small fluctuations (Figure 16d, Figure 17).

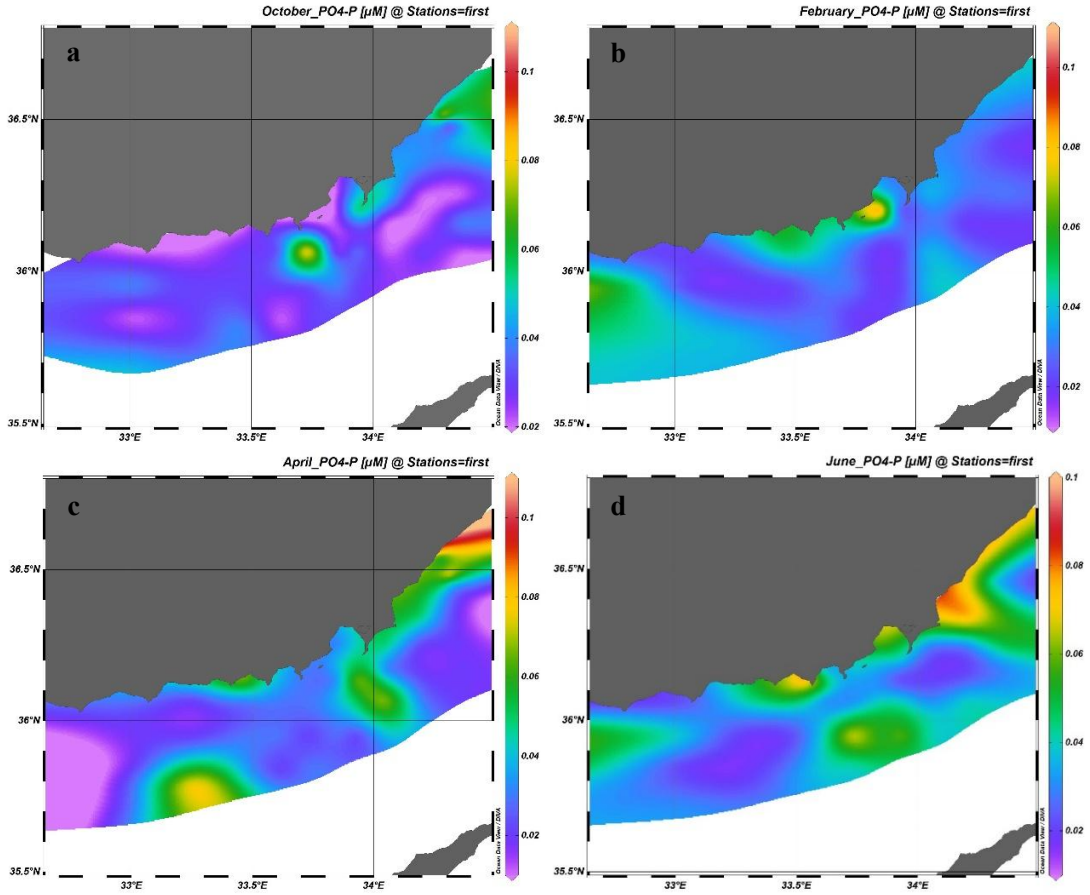

Figure 16 Surface phosphate (µM) distribution in each season; Fall -October (a), Winter-February (b), Spring-April (c), Summer-June (d) (ODV/DIVA Gridding/Interpolation).

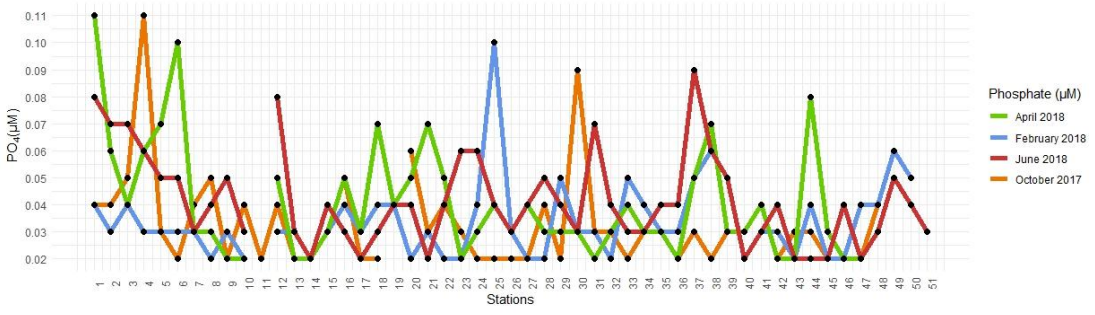

Figure 17 Phosphate concentrations (µM) measured at stations for all seasons.

3.2.1.2 Nitrate

The nitrate concentrations in the surface waters varied from 0.05-1.74µM in the study area. The highest values recorded during winter whereas, the lowest values were obtained in fall and spring (Table 7).

Table 7 Minimum, maximum and mean surface nitrate concentrations (µM) measured in each season.

Seasons	**Nitrate (µM)**		
	Minimum	**Maximum**	**Mean**
October 2017	0.05	1.08	0.16
February 2018	0.24	1.74	0.47
April 2018	0.08	0.58	0.19
June 2018	0.05	1.27	0.19

The nitrate concentrations in the surface waters showed decreasing values in their seasonally arithmetic means in the order winter > spring = summer > fall. Beginning from the lowest, the mean surface water nitrate value was 0.16µM in fall, ranging between 0.05 and 1.08µM (Table 7). For this season, nitrate concentrations were mostly below 0.05µM. Relatively higher concentrations were retained at stations 12, 16 and 38. The noticeably high nitrate value was observed at station 12 (Figure 18a, Figure 19). In spring, the mean surface water nitrate value was 0.19µM, ranging between 0.08 and 0.58µM (Table 7). For this season, nitrate values were mostly lower than 0.40µM and fluctuated within a small range. The highest value was observed at station ETS-1. A high value of 0.57µM was observed at station 30 and 16 (Figure 18c, Figure 19). From spring to summer, the mean nitrate value observed to be same as 0.19µM, ranging between 0.05 and 1.27µM (Table 7). For this season, nitrate values ranged between 0.12-1.00 µM at ETS stations. ETS-1 station displayed the highest value. At stations 12 through 42, nitrate values were mostly lower than 0.25µM with less fluctuation. At stations 45 through 49, values varied between 0.06-1.27 µM. Measurements made at these stations show high variability in terms of nitrate values. The highest value for this season was obtained at station 46 (Figure 18d, Figure 19).

In winter, the mean surface nitrate concentrations increased and reached value of 0.47µM, fluctuating between 0.24 and 1.74µM (Table 7). For this season, the highest value measured and even for whole year was obtained at coastal station 24. At ETS stations, nitrate values showed a decrease from inshore to offshore, and values ranged between 0.25-1.31µM. To the highest value was obtained at coastal stations ETS-1. In the region being influenced by direct runoff from the Göksu River, nitrate value decreased from inshore to offshore. The concentrations obtained from stations 33 through 49, at the west, was below 0.05µM with no apparent significant fluctuations (Figure 18b, Figure 19).

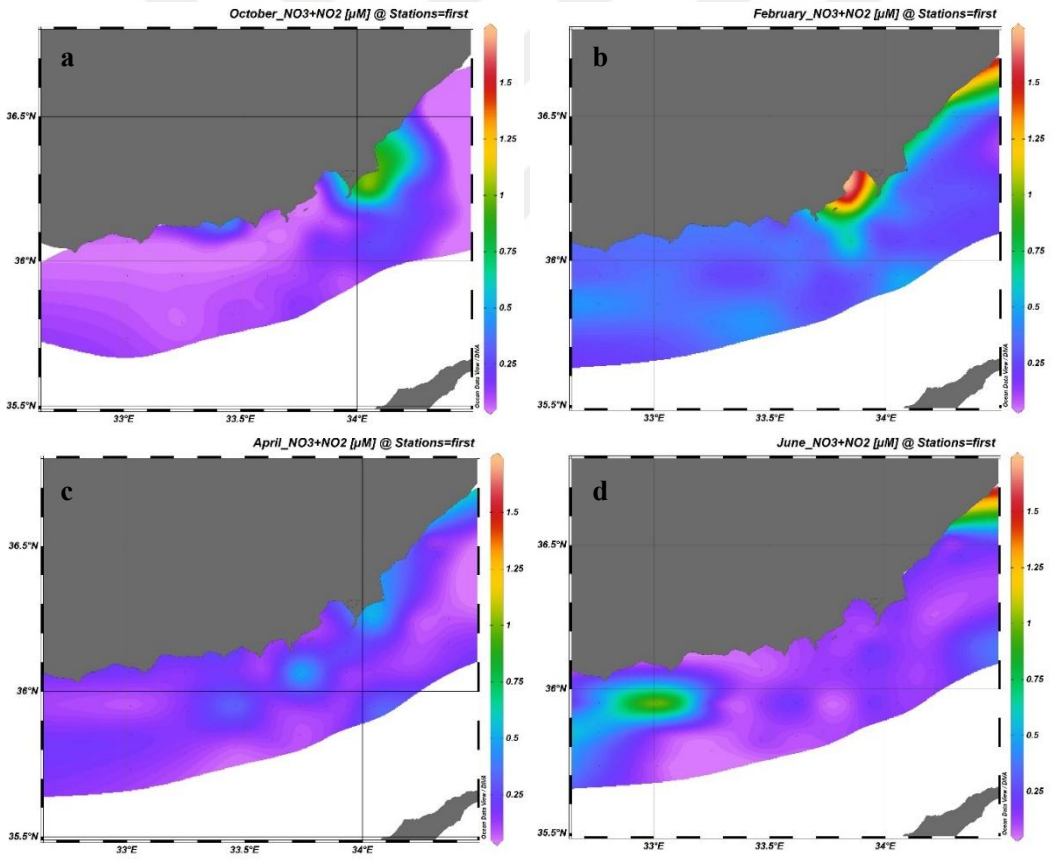

Figure 18 Surface nitrate (µM) distribution in each season; Fall -October (a), Winter-February (b), Spring-April (c), Summer-June (d) (ODV/DIVA Gridding/Interpolation).

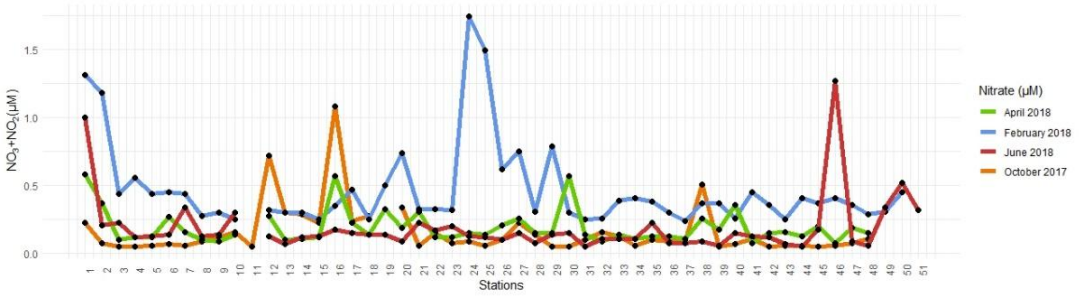

Figure 19 Nitrate concentrations (µM) measured at stations for all seasons.

3.2.1.3 Silicate

The silicate concentrations in the surface waters varied from 0.35-2.93µM in the study area. The highest values recorded during winter whereas, the lowest values were obtained in summer (Table 8).

Table 8 Minimum, maximum, and mean surface silicate concentrations (µM) measured in each season.

Seasons	**Silicate (µM)**		
	Minimum	**Maximum**	**Mean**
October 2017	0.50	1.56	0.86
February 2018	0.79	2.93	1.36
April 2018	0.43	1.24	0.59
June 2018	0.35	1.10	0.62

The silicate concentrations in the surface waters showed decreasing values in their seasonally arithmetic means in the order winter > fall > summer > spring. Beginning from the lowest, the mean surface water silicate value was 0.59µM in spring, ranging between 0.43-1.24µM (Table 8). For this season, according to the data, 96% of the values were between 0.43µM and 0.90µM. During this period, two stations attract attention with their high values compared to other stations. Offshore stations 10 and 16 displayed the highest values (Figure 20, Figure 21c).

In summer, the mean surface water silicate value was 0.62µM, ranging between 0.35µM and 1.10µM (Table 8). For this season, 96% of the silicate values measured were between 0.35µM-0.91µM. ETS-1 coastal station displayed the highest concentration, and coastal station 20 has a considerably higher value than the rest. Not only for this season but also for the whole year, the lowest value was obtained from offshore station 49 (Figure 20, Figure 21d). In fall, the mean surface water silicate value was 0.86µM, ranging between 0.50 and 1.56µM (Table 8). For this season, the majority of the data were between 0.50-1.11µM. Relatively higher silicate concentrations were measured at stations 13, 14, 20, 26, and 34. However, stations 16 and 17 have displayed significantly higher values for this season (Figure 20, Figure 21a). From fall to winter, the surface water silicate values denoted gradually increase, varying from 0.79 to 2.93µM with an arithmetic mean of 1.36µM (Table 8). For this season, the highest silicate of the year measured in this month. 82% of the silicate measurement results for this month were between 0.79 and 1.88µM. Slightly higher silicate values were obtained at coastal stations 16, 20, 24, 25 and 29, later being influenced by direct runoff from the Göksu River. Stations namely ETS-1, 40, 47 and 48 attract exceptional attention with their high values obtained from different points of the sampling area (Figure 20, Figure 21b).

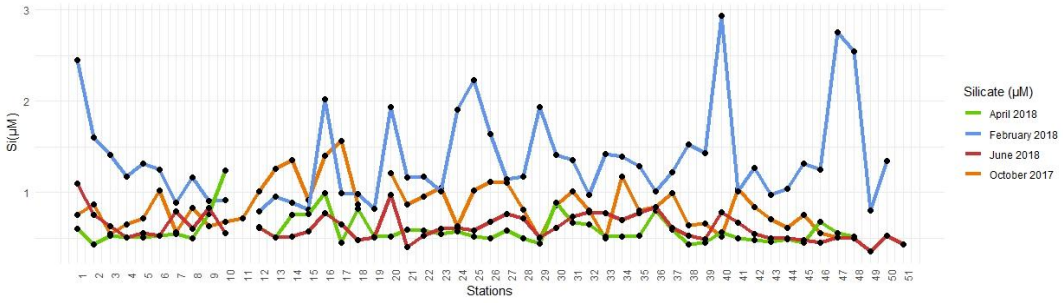

Figure 20 Silicate concentrations (µM) measured at stations for all seasons.

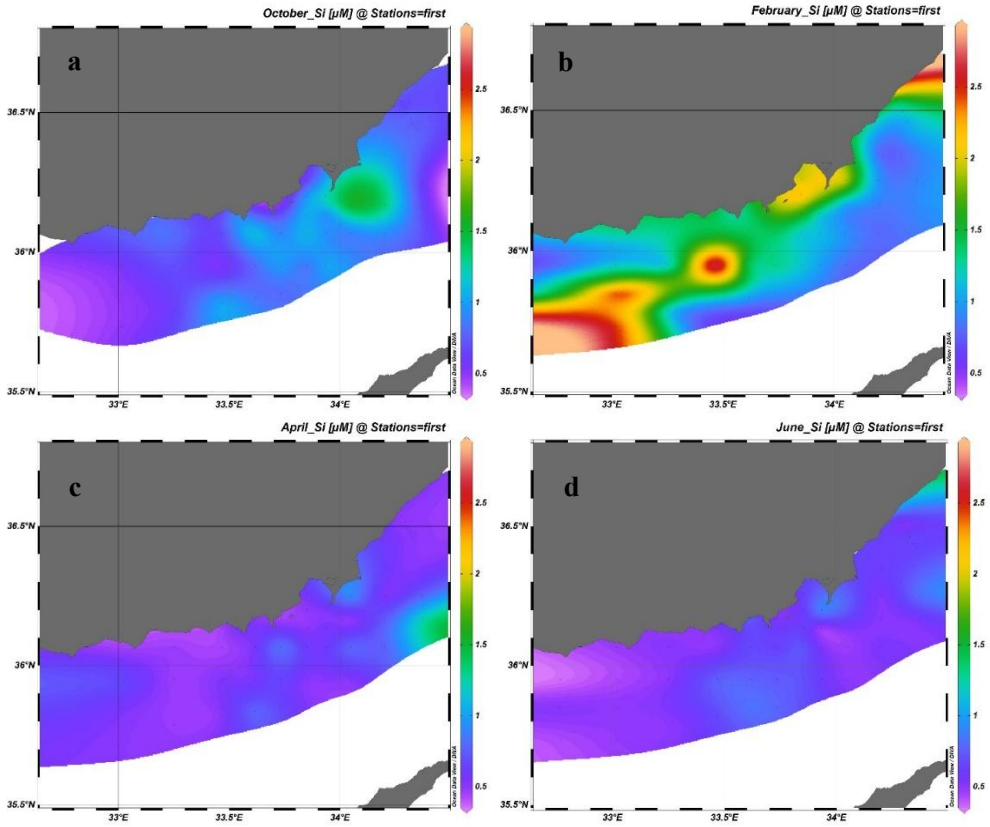

Figure 21 Silicate (µM) distributions for all seasons; Fall -October (a), Winter-February (b), Spring-April (c), Summer-June (d) (ODV/DIVA Gridding/Interpolation).

3.2.1.4 Si: N: P Stoichiometry

The N: P ratios in the surface waters varied from 0.5 to 43.5 in the study area. The highest values recorded during winter whereas, the lowest values were obtained in fall. Furthermore, the Si: N ratios in the surface waters varied from 0.4 to 19.5 in the study area. The highest values recorded during fall whereas, the lowest values were obtained in summer (Table 9).

Table 9 Seasonally N: P and Si: N ratios of the sampling area

	NOx/PO4			Si/NOx		
	Minimum	**Maximum**	**Mean**	**Minimum**	**Maximum**	**Mean**
October 2017	0.5	25.5	5.4	1.3	19.5	8.8
February 2018	4.8	43.5	14.7	1.1	11.3	3.5
April 2018	1.6	19.0	5.4	1.0	8.9	3.9
June 2018	0.7	31.8	5.1	0.4	14.6	5.0

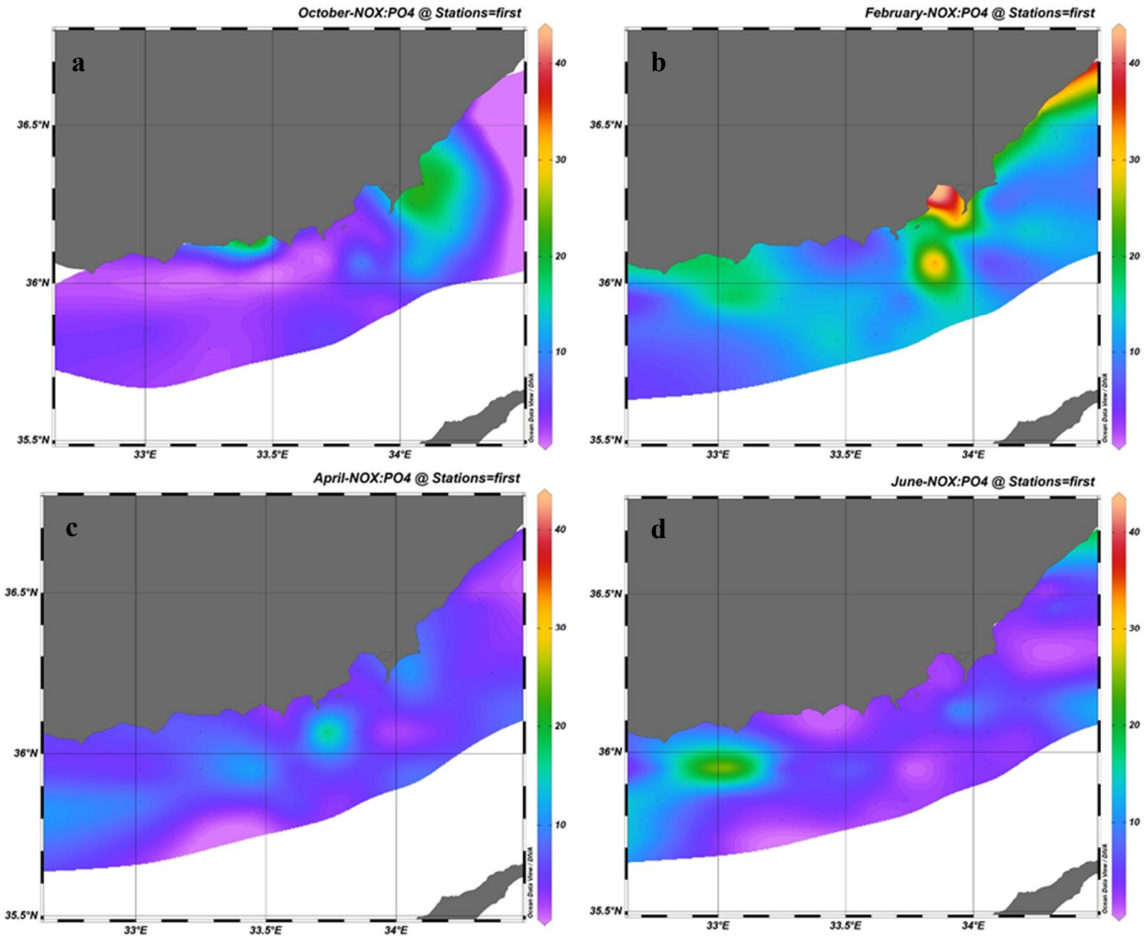

Figure 22 NO_x: PO_4 ratio distributions for all seasons; Fall -October (a), Winter-February (b), Spring-April (c), Summer-June (d) (ODV/DIVA Gridding/Interpolation).

The nitrate: phosphate ratios in the surface waters showed decreasing values in their seasonally arithmetic means in the order winter > spring = fall > summer (Table 9). Beginning from the lowest, the mean value was 5.1 in summer, ranging between 0.7 and 31.8 (Table 9). For this season, high N: P ratio above 25 was observed at station 46 (500-1000m depth) located at the west. The most of the stations were found at low ratios below 10 (Figure 22d). From summer to fall, N: P-ratios denoted gradually increase, varying from 0.5 to 25.5 with an arithmetic mean of 5.4 (Table 9). High N: P-ratios observed around stations influenced by direct runoff from the Göksu River and the highest was recorded at the coastal station 38, for this season. The most of the stations were found at low ratios below 10 (Figure 22a). In spring, the mean N: P ratio observed to be same as 5.4, fluctuating between 1.6 and 19.0 (Table 9). In general, the most of the stations were found at low ratios below 10. The highest N: P ratio observed at station 30 located at mesotrophic shelf in this season (Figure 22c). In winter, N: P ratios increased and reached the mean value of 14.7, fluctuating between 4.8 and 43.5 (Table 9). The highest N: P ratios obtained from the stations near the Göksu River mouth and inside the Taşucu Bay (Figure 22b).

The silicate: nitrate ratios in the surface waters showed decreasing values in their seasonally arithmetic means in the order fall > summer > spring > winter (Table 9). Beginning from the lowest, the mean value was 3.5 in winter, ranging between 1.1 and 11.3 (Table 9). For this season, Si: N ratios were found high ratios above Redfield ratio (Si: N = 16:16) at all stations. The highest value was obtained at offshore station 40 (Figure 23b). In spring, the mean Si: N ratio was 3.9, fluctuating between 1.0 and 8.9 (Table 9). In general, all of the stations were found at high ratios above 1. The highest Si: N ratio observed at stations 9, 10 and 37 located at offshore waters in this season (Figure 23c). From spring to summer, Si: N-ratios denoted gradually increase, varying from 0.4 to 14.6 with an arithmetic mean of 5 (Table 9). As seen in spring, most of the stations were found at high ratios above 1, except offshore station 46 located at the west. The highest value obtained at offshore station 31 (Figure 23d).

In fall, Si: N ratios increased and reached the mean value of 8.8, fluctuating between 1.3 and 19.5 (Table 9). The highest Si: N ratios obtained from the stations 25, 30, 34 and 42 on the coastal shelf whilst the lowest values obtained at stations 12 and 16 influenced by direct runoff from the Göksu River (Figure 23a).

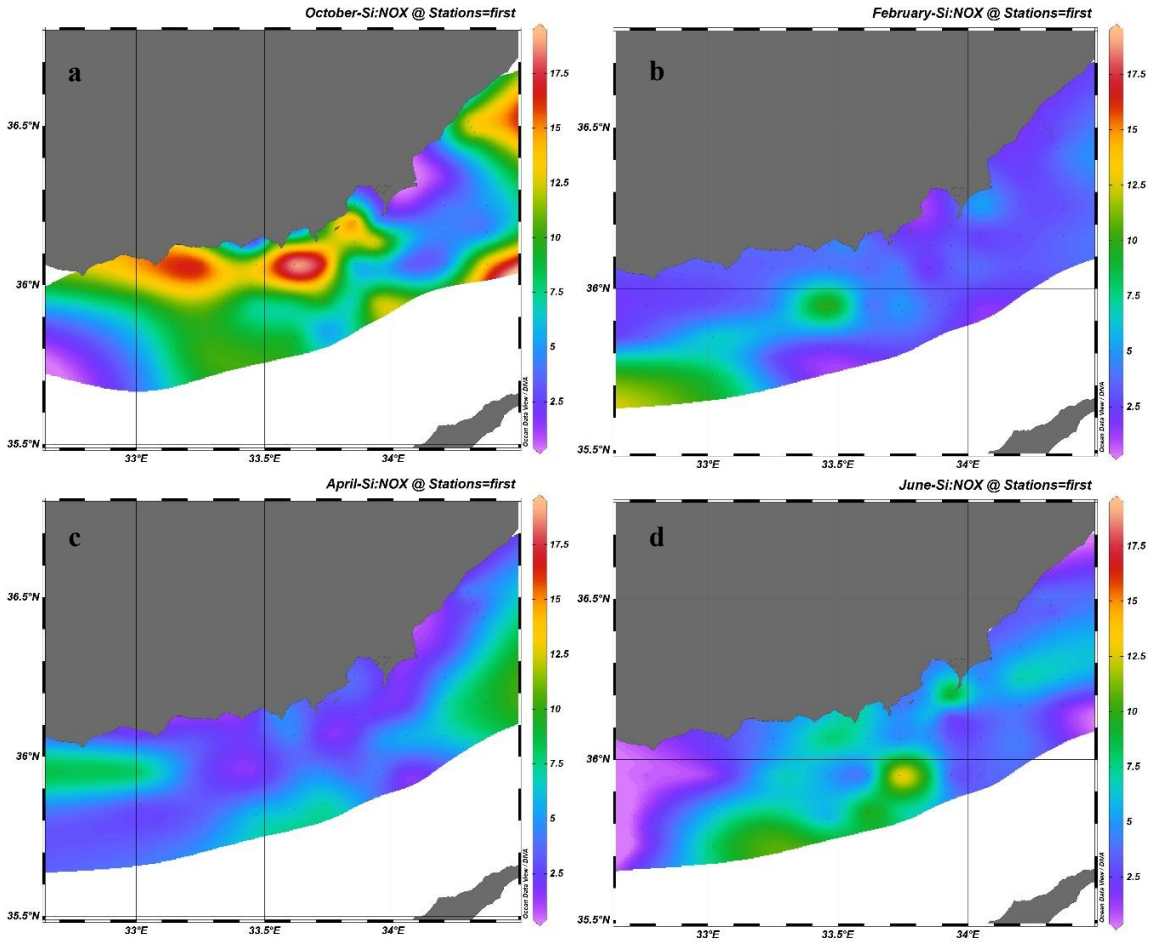

Figure 23 Si: NO_x ratio distributions for all seasons; Fall -October (a), Winter-February (b), Spring-April (c), Summer-June (d) (ODV/DIVA Gridding/Interpolation).

3.2.2 Dissolved Oxygen

The dissolved oxygen measurements in the surface waters varied from 202.78 to 242.15µM in the study area. The highest values recorded during winter whereas, the lowest values were obtained in summer (Table 10).

Table 10 Minimum, maximum and mean surface dissolved oxygen (µM) concentrations recorded in each season.

Seasons	Dissolved Oxygen (µM)		
	Minimum	**Maximum**	**Mean**
October 2017	204.18	213.70	207.99
February 2018	224.79	242.15	229.71
April 2018	231.99	237.07	234.92
June 2018	202.78	216.32	206.94

The dissolved oxygen values in the surface waters showed decreasing values in their seasonally arithmetic means in the order spring > winter > fall > summer. Beginning from the lowest, the mean surface water silicate value was 207µM in summer, ranging between 203-216µM (Table 10). For this season, the majority (94%) of all measurements from the stations were between 199-215µM within the confidence interval of two SD. Station 37 has a noticeably higher value than the mean level (Figure 24d). In fall, the mean surface water dissolved oxygen values was 208µM, ranging between 204.2-213.7µM (Table 10). For this season, all the measurements from the stations were between the confidence interval of two SD as 204.2-213.7µM. The offshore stations 46 and 47 have displayed slightly higher measurements; however, inshore stations 20 and 21 have slightly lower measurements (Figure 24a). From fall to winter, the surface water silicate values denoted gradually increase, varying from 225 to 242µM with an arithmetic mean of 230µM (Table 10). For this season, the 89% of all measurements fell between 219-240µM/L within the confidence interval of two SD. The coastal station ETS-1 has exceptionally the highest measurement both for this season and for the whole year (Figure 24b). In spring, the mean surface water dissolved oxygen values was 235µM, ranging between 232-237µM (Table 10). For this season, all the measurements from the stations were between the 232-238µM within the confidence interval of two SD (Figure 24c).

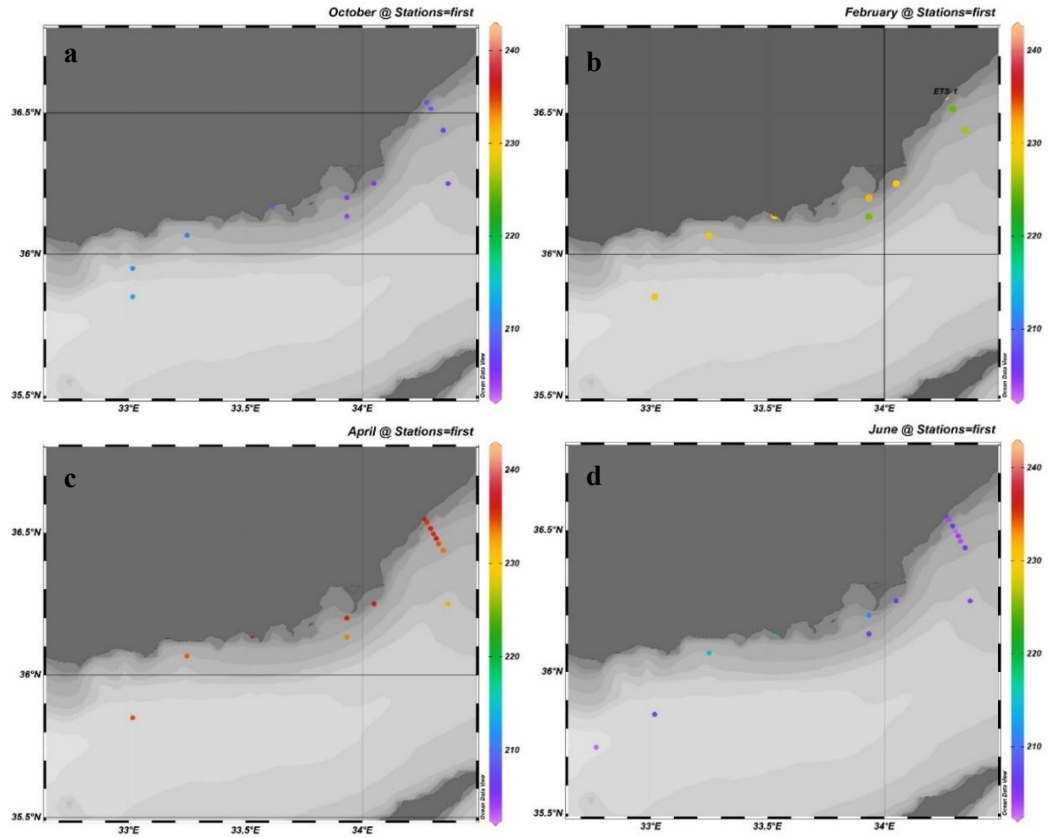

Figure 24 Dissolved Oxygen (µM) measurements for all seasons; Fall -October (a), Winter-February (b), Spring-April (c), Summer-June (d) (ODV).

3.3 Biological Parameters

3.3.1 Phytoplankton Distribution and Composition

3.3.1.1 Abundance

Surface cell abundances varied between 10704-1245504 cells per litre in the study area with maximal and minimal population densities retained in winter and fall, respectively.

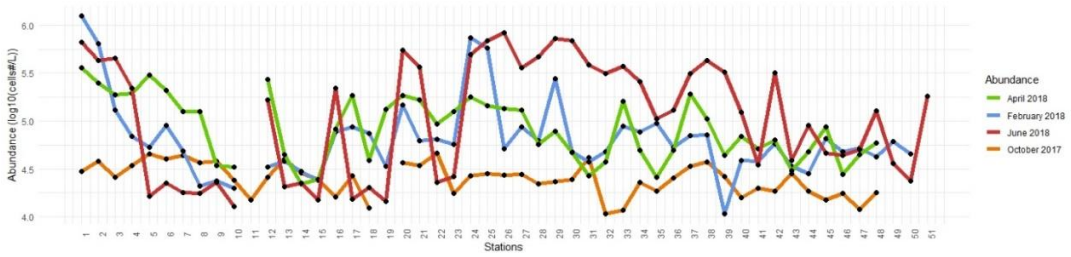

Figure 25 Abundance (cell numbers l^{-1}) distribution at stations for all seasons.

In fall, abundance values ranged between 10704-46352 cells per litre with a mean value of 25862 cells per litre. Ninety-eight per cent of these values found between 10704-46125 cells per litre within the confidence interval of two SD. Significantly higher abundance was observed at station 22 (Figure 25, Figure 26a). In winter, values ranged between 10800-1245504 cells per litre at the stations, with an average of 122159 cells per litre. Ninety-two per cent of values observed in between 10800-566409 cells per litre within the confidence interval of two SD. Nonetheless, four stations have displayed remarkably higher abundance values compared to the rest of the stations. Stations ETS-1, ETS-2, 24 and 25 have retained the highest population densities (Figure 25, Figure 26b). In spring, abundance values varied between 22080-363680 cells per litre at the stations, with an average of 109421 cells per litre. Ninety-six per cent of these values detected between 22080-273240 cells per litre within the confidence interval of two SD. The highest abundance values were detected from the station ETS-1 and ETS-5 (Figure 25, Figure 26c). In summer sampling, abundance values ranged between 12928-837600 cells per litre at the stations, with the mean value of 227333 cells per litre. Ninety-four per cent of these values found between 12928-693031 cells per litre within the confidence interval of two SD. Stations 25, 26 and 29 showed extremely higher values compared to their surrounding areas. The highest value was obtained from a coastal station 26 for this season (Figure 25, Figure 26d).

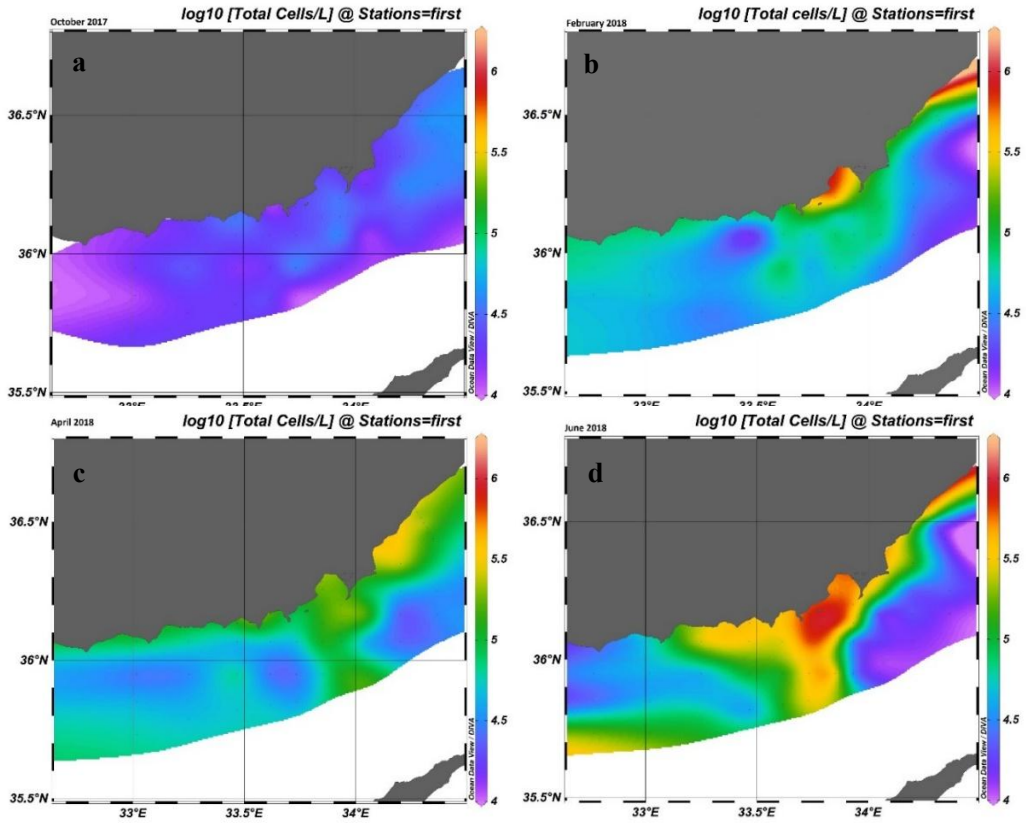

Figure 26 Log transformed abundance (Cell Number L^{-1}) distribution for all seasons; Fall-October (a), Winter-February (b), Spring-April (c), Summer-June (d) (ODV/DIVA Gridding/Interpolation).

3.3.1.2 Species Variety

The number of phytoplankton species identified at surface ranged between 13 and 47 at stations. The population was found most species diverse during spring and least in summer.

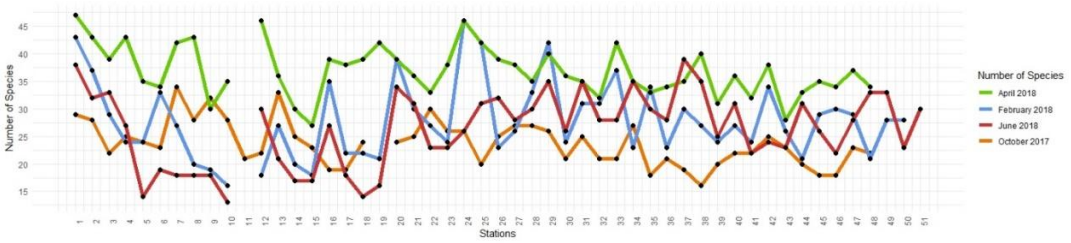

Figure 27 Number of phytoplankton species observed at stations during all sampling periods.

In fall, the number of the phytoplankton species observed varied between 16 and 34, with an average of 24 species at the stations. ETS-7, ETS-9 and station 29 have retained a more diverse community than the rest of the stations (Figure 27, Figure 28a). In winter, the number of phytoplankton species varied between 16 and 46, with an average of 28 species. Stations that were rich in species were ETS-1, 24, 25 and 29 (Figure 27, Figure 28b). In spring, the number of the phytoplankton species ranged between 27 and 47, with an average of 37 species at the stations. Similar to winter, ETS-1 station displayed the highest phytoplankton variety in spring. Offshore station 15 has the lowest number of phytoplankton species for this season (Figure 27, Figure 28c). In summer, the number of the phytoplankton species ranged between 13 and 39, with an average of 26 species at the stations. Offshore ETS stations and offshore stations 14, 15, 17, 18 and 19 were slightly low in variety for this sampling period. In contrast, coastal stations ETS-1 and station 39 have the highest number of different phytoplankton species (Figure 27, Figure 28d).

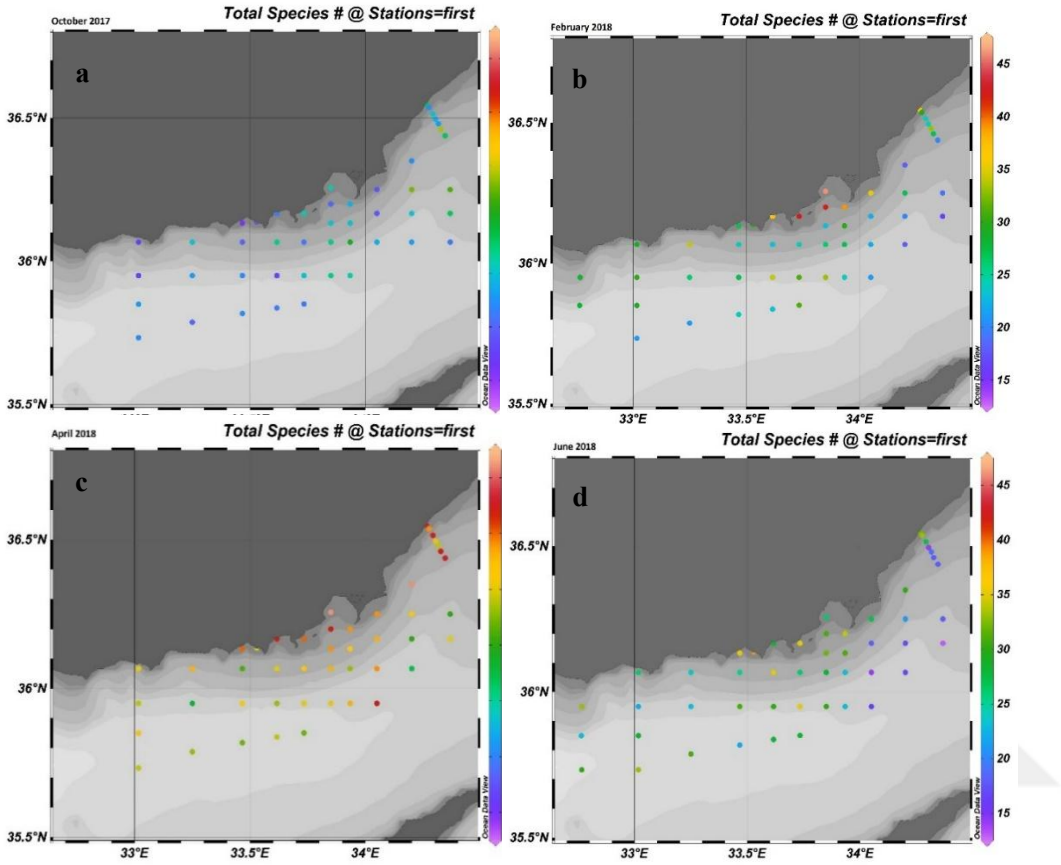

Figure 28 Number of phytoplankton species present at stations for all seasons; Fall -October (a), Winter-February (b), Spring-April (c), Summer-June (d) (ODV).

3.3.1.3 Phytoplankton Compositions

In fall, the phytoplankton species in the class of Prymnesiophyceae accounted for 38.3 per cent of the total abundance and has the highest abundance for this season. The class of Bacillariophyceae (diatoms) drew attention with a high abundance with a rate of 24.6 per cent. Pyrrophyceae composed 21.7%, and the class of Cryptophyceae 15.4% of the total abundance. In this period, Euglenophyceans contributed to the total abundance with 0.01 per cent (Figure 29a). *Emiliania huxleyi* which belongs to Prymnesiophyceae class was detected as the most dominant species (38%) in this period among all species.

As the members of Bacillariophyceae; *Nitzschia* sp. (6%), *Nitzschia tenuirostris* (5%) and *Thalassiosira* sp. (7%) were observed as the dominant species in this period. *Heterocapsa* sp., which belongs to Pyrrophyceae group, has 11% of the total abundance among all species. *Hillea fusiformis* detected in 15% of the total abundance among all species as a representative of Cryptophyceae. The abundance percentage of species below 3 per cent were included in the group others, and the total abundance ratio of this group was 18 per cent (Figure 30a).

In winter, diatoms were the dominating group (77.3%) compared to other groups. This was followed by Prymnesiophyceans (15.7%), Cryptophyceans (3.7 %) and lastly by Pyrrophyceans (3.2 %). Two more classes contributed to the abundance in this period, albeit with a small percentage; Euglenophyceae (of 0.8%) and Chlorophyceae (of 0.001%) (Figure 29b). Diatom species *Skeletonema costatum* (23%), *Chaetoceros socialis* (21%), *Chaetoceros curvisetus* (7%), *Nitzschia tenuirostris* (5%), *Pseudo-nitzschia delicatissima* (5%) and *Asterionella japonica* (3%) have made a significant contribution to total abundance among all species. Coccolithophorid *Emiliania huxleyi* formed 15% of the total abundance among all species. *Hillea fusiformis*, which belongs to the Cryptophyceae group, made up 4% of the total abundance among all species. Species with a minor contribution (<3%) were included in the group, others with an overall contribution of 18% (Figure 30b).

In spring, diatoms accounted for 78.93 % of the total abundance and have the highest abundance for this season. Respectively; the class of Prymnesiophyceae contributed to the total abundance with 8.3 %, the group of Pyrrophyceae with 7.16%, the class of Cryptophyceae with 4.98%, the class of Chrysophyceae with 0.52% and last and least the class of Euglenophyceae with 0.26% (Figure 29c). Among the diatom species *Pseudo-nitzschia delicatissima* (18%), *Chaetoceros* sp. (15%), *Proboscia alata forma gracillima* (14%), *Chaetoceros rostratus* (12%) and *Chaetoceros curvisetus* (6%) have contributed significantly to total abundance among all species. Contribution of *Emiliania huxleyi* to the bulk was 8% among all species. *Hillea fusiformis* composed 5% of the total abundance among all species as a representative of Cryptophyceae class. *Heterocapsa* sp., which

belongs to Pyrrophyceae group, made 3% of the total abundance among all species. Species with a minor contribution (<3%) were included in the group, others with an overall contribution of 20% (Figure 30c).

In summer, diatoms accounted for 91.3 per cent of the total abundance and retained the highest abundance for this season. Respectively; the class of Prymnesiophyceae contributed to the total abundance with 3.85%; the group of Pyrrophyceae with 3.53%; the class of Cryptophyceae with 1.36%; the classes of Euglenophyceae and Ebriophyceae both with 0.004% (Figure 29d). Among the diatom species; *Leptocylindrus danicus* with (77%) as the highest, *Rhizosolenia styliformis* (5%) and *Pseudo-nitzschia delicatissima* (4%) have contributed significantly to total abundance among all species. Contribution of *Emiliania huxleyi* to the bulk *was* 4% among all species. Species with a minor contribution (<3%) were included in the group, others with an overall contribution of 11% (Figure 30d).

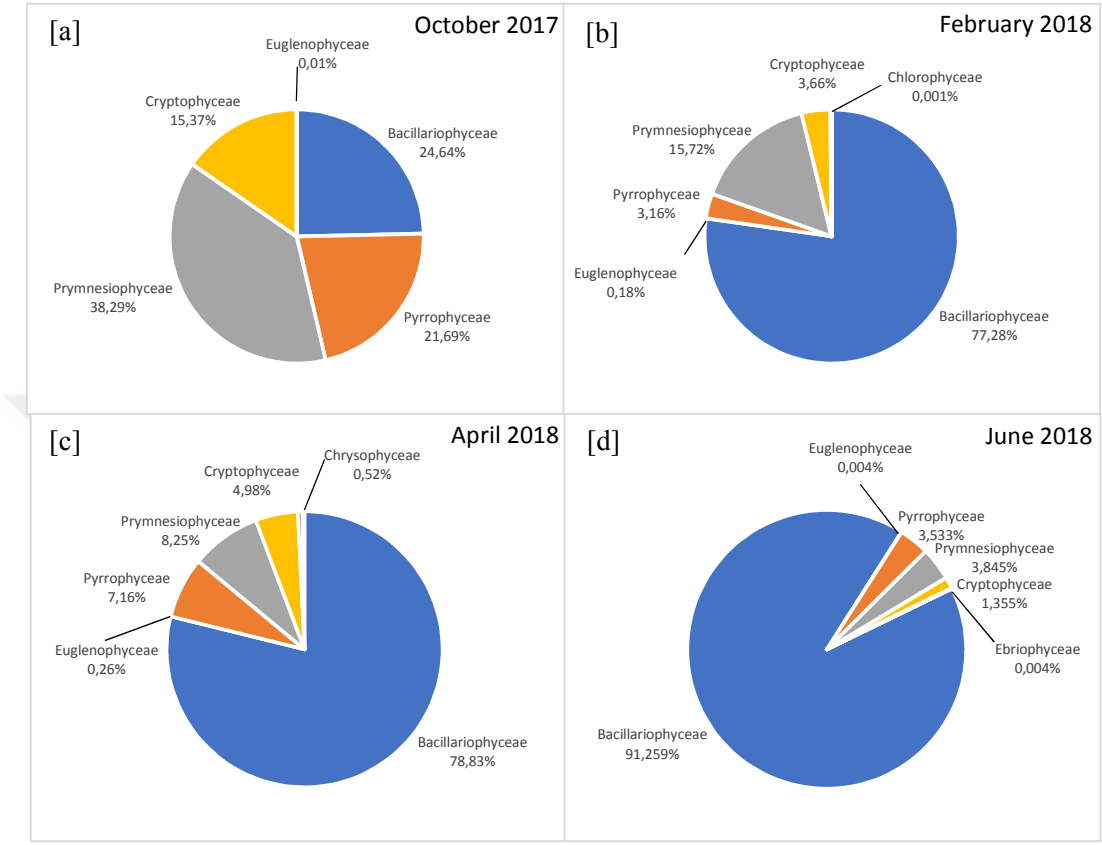

Figure 29 Pie charts of phytoplankton group abundances from all stations during four seasons; Fall -October [a], Winter-February [b], Spring-April [c], Summer-June [d]. The same colours for each chart reflect the same groups.

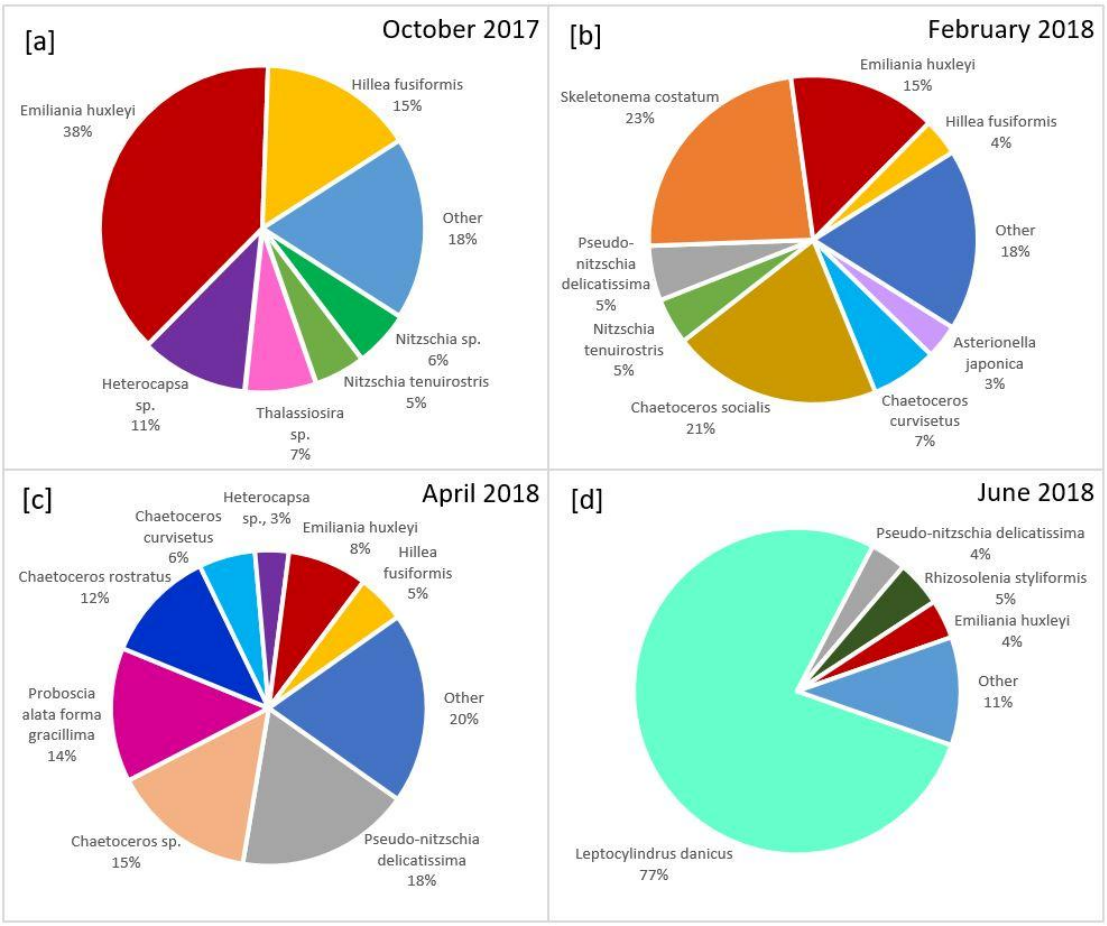

Figure 30 Pie charts of phytoplankton species and abundance from all stations during four seasons; Fall -October [a], Winter-February [b], Spring-April [c], Summer-June [d]. The same colours for each chart reflect the same species. The other group contains the species that contributes less than 3 per cent of the total abundance.

3.3.2 Ratio of Ditom and Dinoflagellate Community

The Dia/ Dino index in the surface waters varied from 0.2 to 0.9 in the study area. The highest values recorded during winter and summer whereas, the lowest values were obtained in fall (Table 11).

Table 11 Mean Abundace of Dinoflagellate, Diatom Comunities with Dia/Dino index for each season.

Seasons	Mean Abundance (cells /L)		
	Dinoflagellate	Diatom	Dia/Dino
October-2017	5609	6373	0.53
February-2018	3865	94408	0.96
April-2018	7831	86262	0.92
June-2018	8032	207461	0.96

The Dia/ Dino indeces in the surface waters showed decreasing values in the order winter = summer > spring > fall. Beginning from the lowest, index was 0.53, in the fall. For this season, ecosystem was co-dominated by diatoms and dinoflagellates. In spring, the Dia/ Dino index increased and reached the value of 0.92. For this season, diatoms were dominating group. In summer and winter, the Dia/ Dino index further increased and reached the value of 0.96. As in spring, diatoms were the dominant group by increasing its presence (See Table 11 and Figure 31).

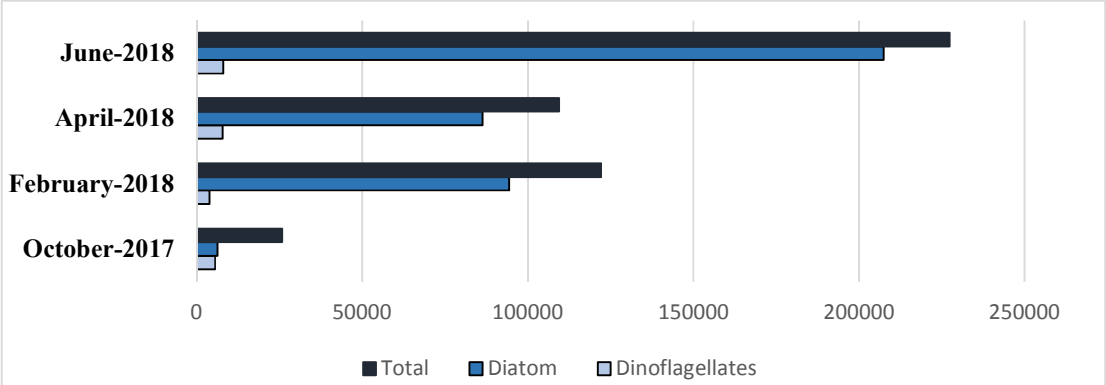

Figure 31 Diatom, Dinoflagellate and total mean abundances (cells / L) from all stations for each season.

3.3.3 Identified Harmful Algal Bloom (HAB) Species

In fall, as the members of Bacillariophyceae class; *Cylindrotheca closterium* and *Pseudo-nitzschia delicatissima,* also as the members of Pyrrophyceae class; *Dinophysis ovum, Gonyaulax spinifera, Phalacroma rotundatum* and *Prorocentrum lima* detected as HAB species. In winter, as the members of Bacillariophyceae class; *Cylindrotheca closterium, Pseudo-nitzschia delicatissima* and *Pseudo-nitzschia multistriata,* also as the members of Pyrrophyceae class; *Dinophysis fortii* were observed as HAB species. In spring, as the members of Bacillariophyceae class; *Cylindrotheca closterium, Pseudo-nitzschia delicatissima* and *Pseudo-nitzschia seriata,* also as the members of Pyrrophyceae class; *Cochlodinium polykrikoides and Karenia papilionacea* obtained as HAB species. In summer, as the members of Bacillariophyceae class; *Cylindrotheca closterium* and *Pseudo-nitzschia delicatissima,* also as the members of Pyrrophyceae class; *Cochlodinium polykrikoides* and *Karenia mikimotoi* detected as HAB species (Table 12).

Table 12 Identified HAB Species for each season.

Species	**October 2017**	**February 2018**	**April 2018**	**June 2018**
Diatoms				
Cylindrotheca closterium	+	+	+	+
Pseudo-nitzschia delicatissima	+	+	+	+
Pseudo-nitzschia multistriata		+		
Pseudo-nitzschia seriata			+	
Dinoflagellates				
Cochlodinium polykrikoides			+	+
Dinophysis fortii		+		
Dinophysis ovum	+			
Gonyaulax spinifera	+			
Karenia mikimotoi				+
Karenia papilionacea			+	
Phalacroma rotundatum	+			
Prorocentrum lima	+			

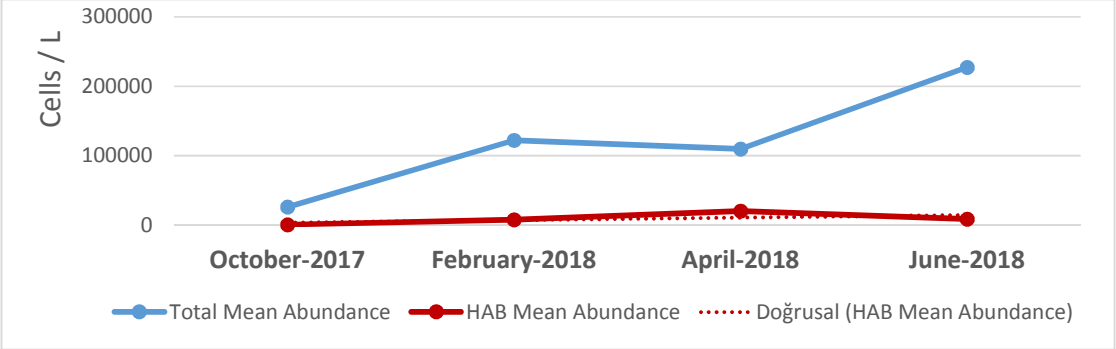

Figure 32 Mean Abundance of Total and HAB Species for each season.

The mean abundance of HAB species in the surface waters showed decreasing values in the order spring > summer > winter > fall. Beginning from the lowest, mean abundance was 159 cells/L, in the fall (Figure 32). For this season, these species observed at 13 stations in total of 47 (Figure 33). In winter, mean abundance of HAB species was 7348 cells/L (Figure 32). For this season, the frequency of occurrence of hab species increased and these species observed at 32 stations in total of 49 stations (Figure 33). In summer, mean abundance of HAB species was 8158 cells/L (Figure 32). As in winter, HAB species were observed at all 50 stations (Figure 33). In spring, mean abundance of HAB species was 20057 cells/L (Figure 32) and these species were observed at all 47 stations (Figure 33).

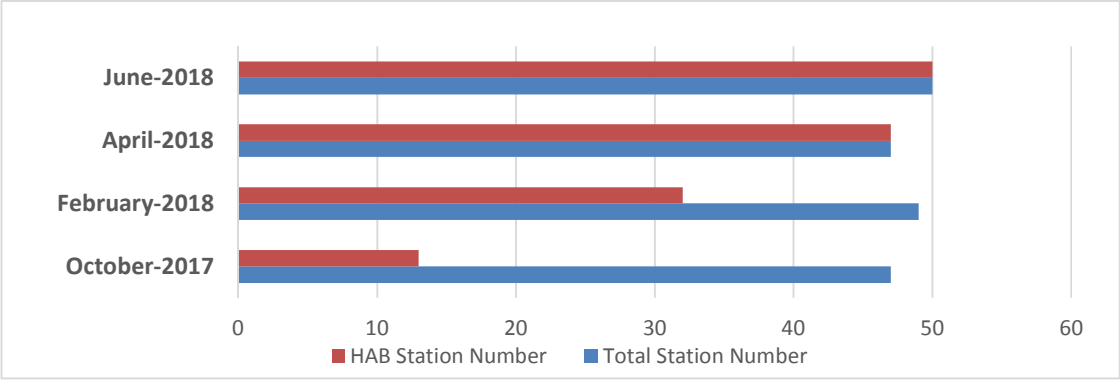

Figure 33 Number of stations in total and HAB species detected for each season.

3.3.4. Biological Diversity Indices

Margalef (species richness D), Shannon (diversity H') and Pielou (regularity J') values were determined as diversity indices.

The maximal (3.7) and minimal (1.3) Margalef Index values wobserved at station 24 in spring and at station 10 in summer (Figure 34).

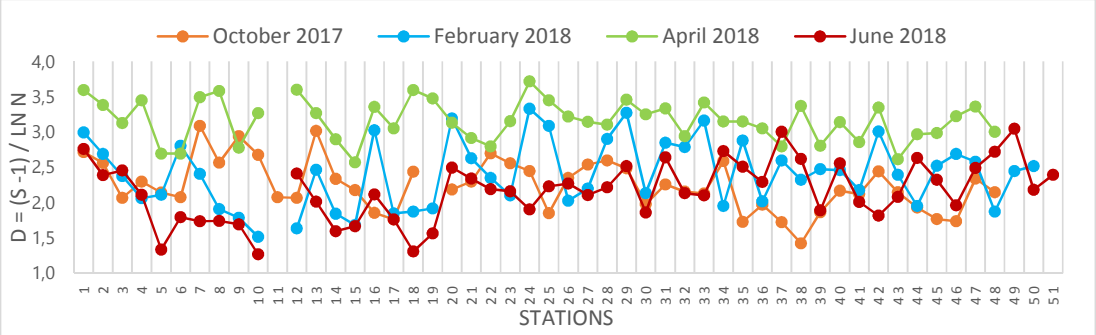

Figure 34 Changes in Margalef Index values at stations in time.

In fall, richness values ranged between 1.4 and 3.1, with a mean value of 2.2 at all stations. The highest richness was obtained at station ETS-7. Besides that, station 13 also displayed a high level of 3. The lowest richness value was detected at coastal station 38 for this sampling period (Figure 34, Figure 35a). In winter, phytoplankton richness varied between 1.5 and 3.3, with an average value of 2.4. High levels were obtained at coastal stations ETS-1, 16, 20, 24, 25, 29 and 33, most of being influenced by direct runoff from the Göksu River (Figure 34, Figure 35b). In spring, phytoplankton richness was higher during this season than other seasons; it changed between 2.6 and 3.7 with a mean value of 3.2. In contrast, two offshore stations 15 and 43 have slightly low richness for this season (Figure 34, Figure 35c).

In summer, richness values ranged between 1.3 and 3.1, with a mean value of 2.2 at the stations. Offshore station 10 has the lowest richness both for this season and the whole year. Furthermore, the offshore station 18 displayed significantly low richness from the rest. Contrary to coastal stations 37 and 49 have notably high richness values in this sampling period (Figure 34, Figure 35d).

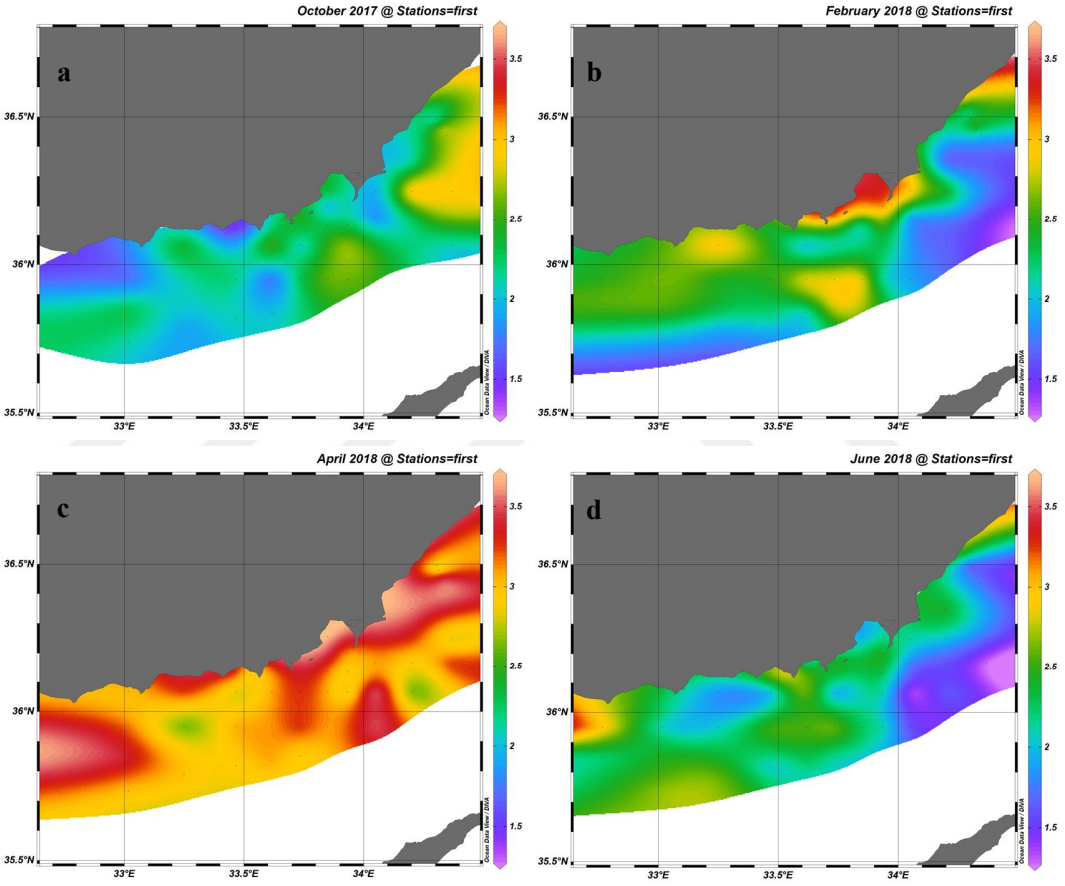

Figure 35 Spatial changes in Margalef Index values in October 2017 (a), February (b), April (c), June 2018 (d) (ODV/DIVA Gridding/Interpolation).

The maximal (2.7) and minimal (0.4) Shannon Index values were observed at station 29 in spring and at station 25 in summer (Figure 36).

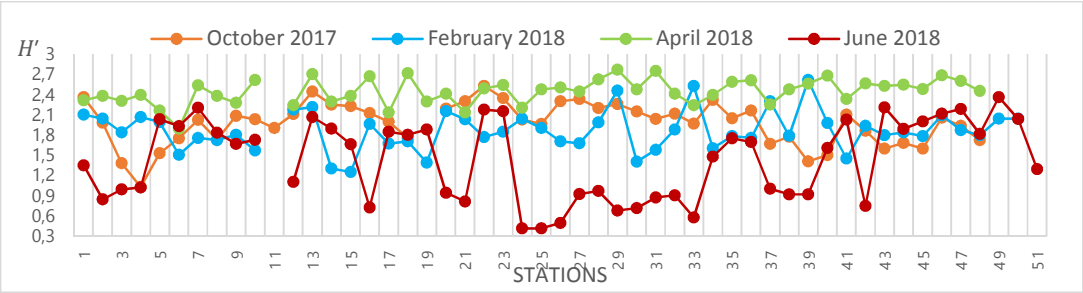

Figure 36 Changes in Shannon Index values at stations in time.

In fall, Shannon diversity index values ranged between 1.0 and 2.5, with an average diversity of 1.9. High diversity measures were retained at stations ETS-1 13, 21, 22 and 23. Apart from these, lower diversity values detected at stations ETS-3, 4 and 5 situated around the 100m depth contour line to the eastern side of the sampling area (Figure 36, Figure 37a). In winter, diversities changed between 1.3 and 2.6, with a mean of 1.9. Significantly high diversity detected from stations 29 and 33 situated on the 50m depth contour line. Besides, station 39 also had considerably high diversity in this season. On the other hand, offshore stations 13 and 14 have explicitly low diversity compared to the overall of the season (Figure 36, Figure 37b). In spring, diversity was markedly higher than other months, and it altered between 1.9 and 2.8, with a high mean value of 2.4. The highest diversity detected at station 29 both for this month and the whole year. Nevertheless, station ETS-6, stations 17 and 21 have noticeably low diversity than general distribution (Figure 36, Figure 37c). In summer, Shannon diversity index values varied between 0.4 and 2.4, with a mean value of 1.4. When the region is analysed as zones, the area centered on the Göksu River discharge has low diversity. Especially, coastal parts around the Göksu River discharge area have more specifically low diversity values, even the lowest diversity of the year was retained at station 25 in this region. The diversity in coastal stations 43, 44, 46 and 49 in the western part of the sampling area is higher than the rest (Figure 36, Figure 37d).

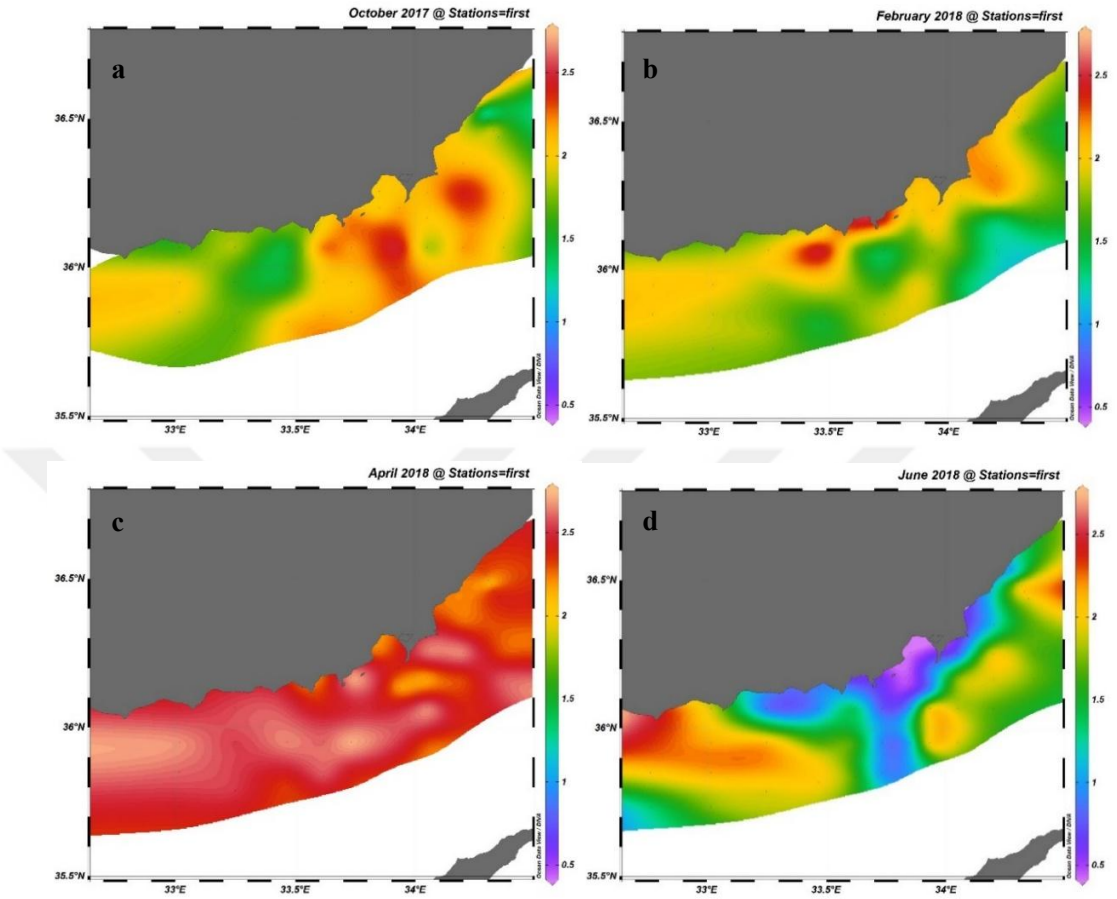

Figure 37 Spatial changes in Shannon Index values in October 2017 (a), February (b), April (c), June 2018 (d) (ODV/DIVA Gridding/Interpolation).

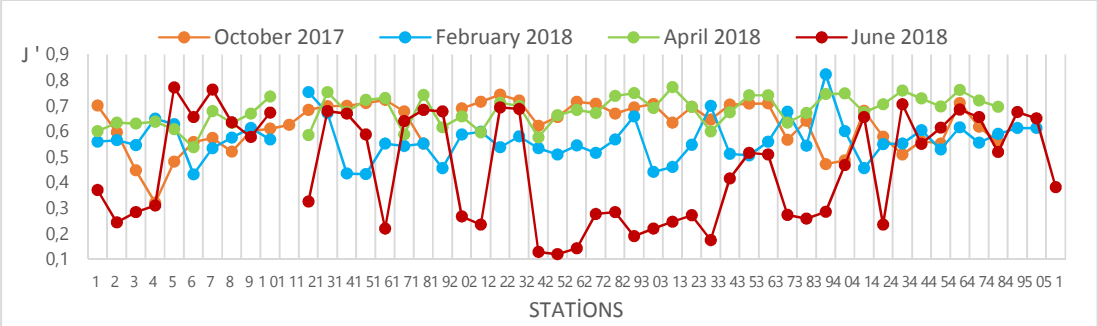

Figure 38 Changes in Pielou Index values at stations in time.

The maximal (0.8) and minimal (0.1) Pielou Index values were observed at station 39 in winter and at station 25 in summer (Figure 38).

In fall, evenness values lined between 0.3-0.7, with a mean value of 0.6. Evenness data was generally between normal ranges without showing many outlying values. However, ETS-4 station has significantly low evenness from the rest of the stations in this season (Figure 38, Figure 39a). In winter, the same situation occurred as not having many outlying values. Total data ranged between 0.4-0.8, with an average of 0.6. In this season, two stations (station 12 and 39) remarks with their high evenness. Station 39 has the highest evenness both for this sampling period and for the whole year (Figure 38, Figure 39b). Evenness values for spring were commonly higher than other sampled months. Values were between 0.5-0.8, with a mean value of 0.7. Similar to the previous two months, evenness values were generally in a confidence interval of two SD. However, ETS-6 station has notably lower evenness than the rest (Figure 38, Figure 39c). In summer, evenness varied between 0.1-0.8, with a mean value of 0.5. Compared to other months, the evenness values of the stations showed high fluctuations from station to station. The middle part of the sampling area has low evenness; mainly, coastal stations being influenced by direct runoff from the Göksu River have more significantly low evenness, in fact; the lowest evenness value of the year was at station 25 in this region (Figure 38, Figure 39d).

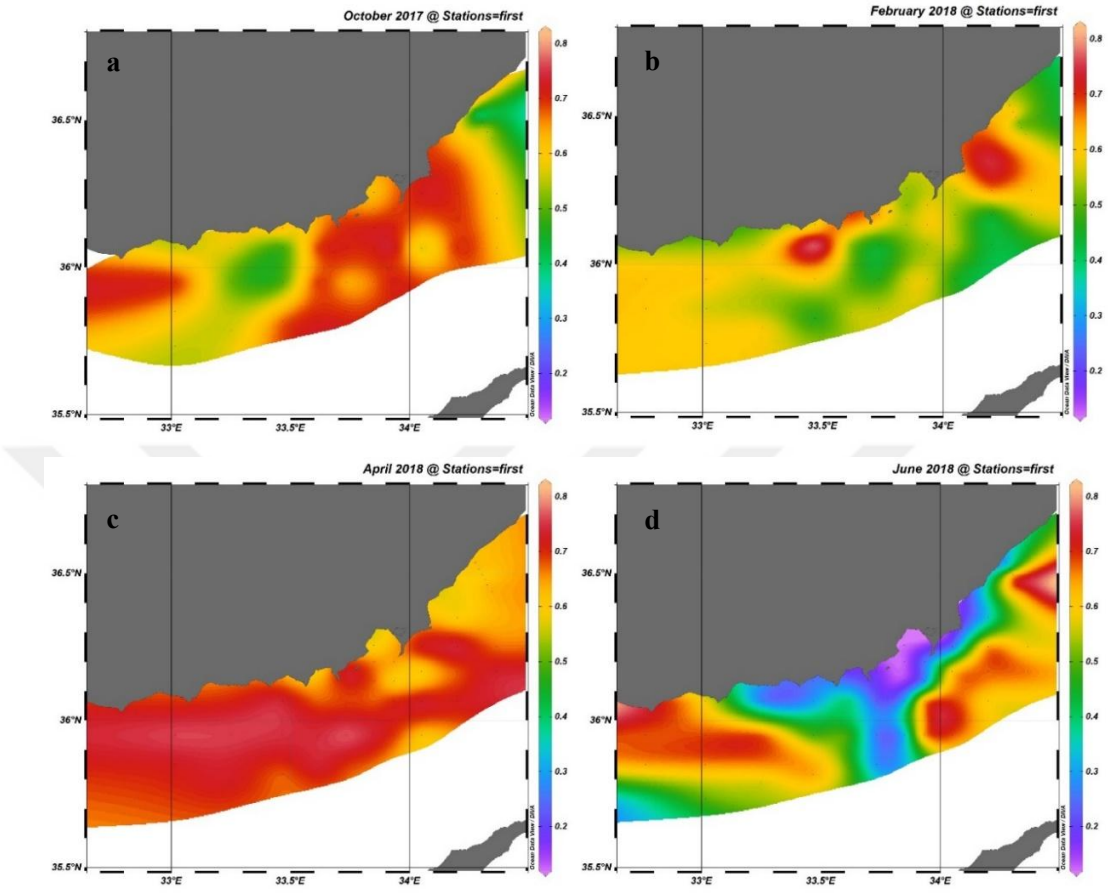

Figure 39 Spatial changes in Pielou Index values in October 2017 (a), February (b), April (c), June 2018 (d) (ODV/DIVA Gridding/Interpolation).

3.3.5. Statistical Analysis

3.3.2.1 Correlation Analysis

In the beginning, concerned parameters were checked to identify whether the data were normally distributed or not. This process was accomplished by employing a randomness test for all parameters. As none of the data set followed a normal distribution, then for the correlation analysis, non-parametric Spearman rank-order correlation test was applied to look for associations between phytoplankton abundance and environmental physical and chemical variables.

In fall, phytoplankton abundance was correlated with a high significance level at $p < 0.01$ with temperature, salinity and density. Phytoplankton abundance was positively correlated with temperature and negatively correlated with salinity and density, whereas no significant correlation was present with phosphate, nitrate and silicate. Also, abundance was significantly ($p < 0.05$) and negatively correlated with dissolved oxygen. In winter, abundance was highly correlated ($p < 0.01$) with density and silicate; in detail, it was negatively correlated with density and positively correlated with silicate. There was no correlation between abundance and temperature, salinity and phosphate. Besides, abundance significantly ($p < 0.05$) positively correlated with nitrate, N: P, Si: N-ratio and dissolved oxygen. It was positively correlated with nitrate and N: P-ratio and negatively correlated with Si: N-ratio and dissolved oxygen. In spring, phytoplankton abundance was correlated with a high significance level at $p < 0.01$ with salinity, density, phosphate, nitrate and Si: N ratio. It was negatively correlated with salinity, density and Si: N-ratio, while it was positively correlated with phosphate and nitrate. No significant correlation existed between abundance and temperature, silicate and dissolved oxygen. In summer, abundance was negatively correlated with salinity at a high significance level ($p < 0.01$). Also, it was significantly correlated with temperature, phosphate and dissolved oxygen ($p < 0.05$). While phytoplankton abundance had a negative correlation with temperature, it had a positive correlation with phosphate and dissolved oxygen. There was no significant correlation between abundance and density, nitrate and silicate (Table 13)

Table 13 Spearman's rank-order correlation between phytoplankton abundance and environmental parameters.

Variables	October-2017		February-2018		April-2018		June-2018	
	r	*P-value*	*r*	*P-value*	*r*	*P-value*	*r*	*P-value*
Temperature	0.67457	0.00020**	-0.04347	0.76620	0.11999	0.42180	-0.32873	0.01976*
Salinity	-0.39785	0.00562**	-0.12020	0.40950	-0.80569	<0.0001**	-0.80045	<0.0001**
Density	-0.67759	0.00017**	-0.49143	0.00040**	-0.69577	0.00020**	0.20759	0.14770
Phosphate	0.11859	0.42720	0.28106	0.05043	0.65441	0.00061**	0.28259	0.04677*
Nitrate	0,08724	0.55980	0.58469	0.01027*	0.37730	0.00894**	-019936	0.16510
Silicate	0.25697	0.08122	0.49427	0.00031**	-0.27501	0.06137	0.27160	0.05640
NO_X:PO_4	-0.02751	0.8544	0.35440	0.01247*	-0.17656	0.2351	-0.27373	0.05441
Si:NO_4	0.06829	0.6483	-0.30122	0.03586*	-0.48737	0.0005**	0.26340	0.06457
DO	-0.69702	0.01176*	0.71667	0.03687*	0.34915	0.20210	0.54118	0.03271*

*Correlation is significant at P <0.05, **Correlation is significant at P <0.01.

3.3.2.1 Multi-Dimensional Scaling (MDS) Analysis

In fall, there were ten main phytoplankton group formations based on the Bray-Curtis Similarity measure at an arbitrary similarity level of 57% (Figure 3.24). Group-1 formed the largest patch among others. It consisted of stations 5, 6, 15, 17, 21, 25, 26, 29, 30, 32, 33, 34, 35, 36, 37, 38, 39, 40, 41, 43, 44, 45, 46, 47 and 48. Group-2 included single station, 42. Group-3 contained stations from 7 to 14 and 18. Group-4 contained stations 3 and 4. Group-5 covered stations 22, 23 and 31. Group-6 included single station 28, and group-7 also included station 27 only. Stations 1 and 2 were included in group 8. Group-9 contained stations 16 and 20. Lastly, group-10 included only station 24 (Figure 40).

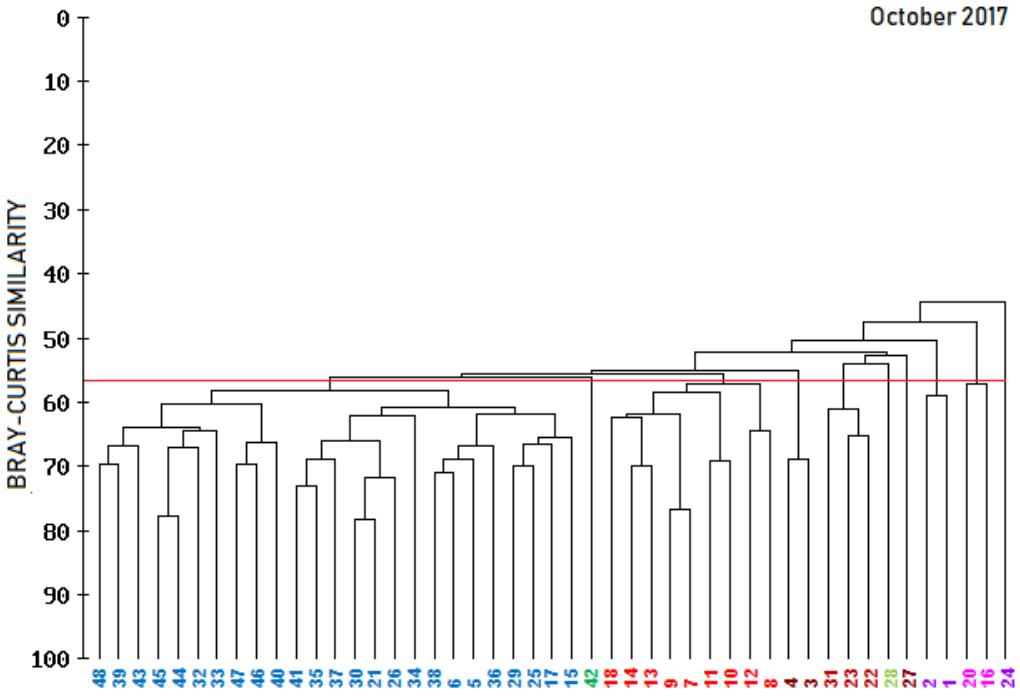

Figure 40 Dendrogram showing classification based on Bay-Curtis Similarity measure for surface samples in October-2017.

Seen from the MDS ordination diagrams, group-10 in terms of composition was quite different from the others. Also, Group-1 in the middle of this diagram was more similar to groups 2 and 3 than other groups (Figure 41).

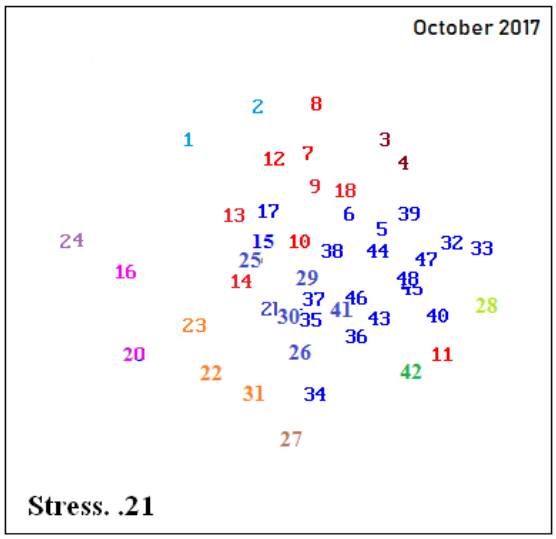

Figure 41 Two-Dimensional non-metric MDS ordination of all stations sampled in October-2017.

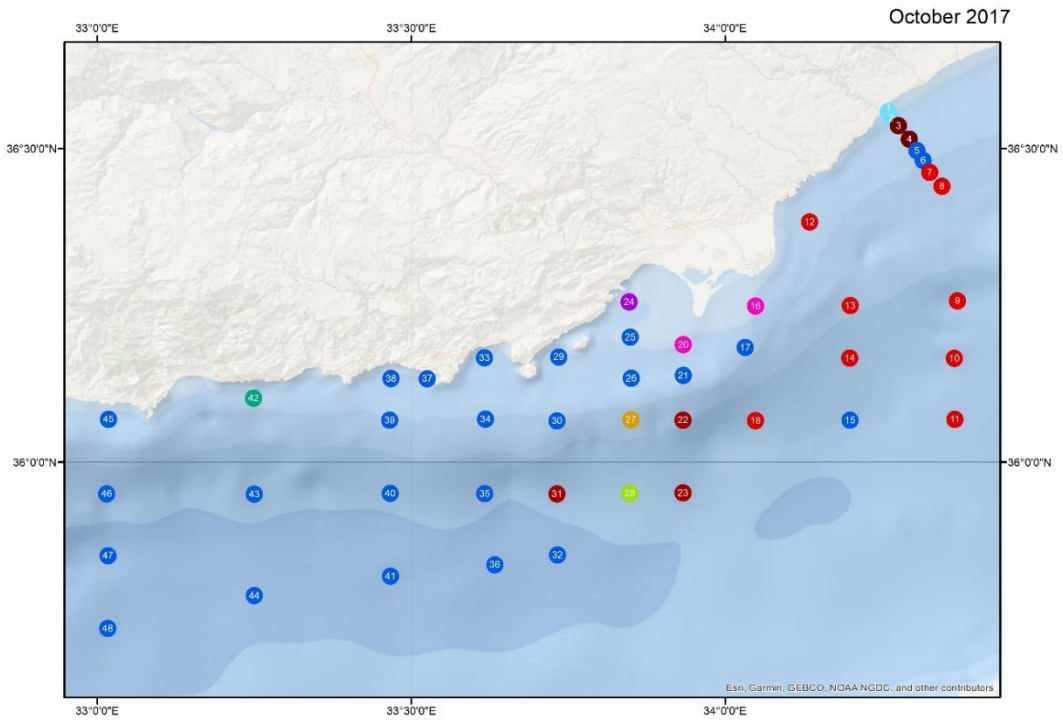

Figure 42 Phytoplankton patches observed in October-2017.

In fall Group-1 composed mainly the stations in the western half of the study area. More stress was present offshore Göksu River and at the easternmost part of the shelf at stations ETS 1 through 8. The eastern side of the sampling area was dominated by group-3. In reality, one would expect westward expansion of Group 3 towards the west due to the persisting current regime in the basin. We assume that only an eddy formation in the east can block westward transfer of flora via Asia Minor Current. ETS stations were divided into four patches (groups 8, 4, 1 and 3) from inshore to offshore (Figure 42). Another major factor for such a great distinction within groups in the area across Göksu River was the cruise track that was followed throughout the cruise. Due to bad weather conditions, a break was given in Taşucu Bay and then the cruise was continued westward following the shallow coastal stations. This was followed by the offshore stations in the west and in return stations that were missed in the east were visited. This eventually led to a change in ambient flora within a few days. This indicates that the flora of the study area was very sensitive and respond quickly to changes in ambient physicochemical factors.

Table 14 Species Contributions to Similarity within the groups in October-2017.

Group	***Species***	$\overline{S}_i$	**SD** (S_j)	$\overline{S}_i$ / **SD** (S_j)	$\Sigma\overline{S}_i$ **%**
	Emiliania huxleyi	9,10	1,27	7,10	14,95
1	*Hillea fusiformis*	7,60	0,94	8,13	27,51
	Heterocapsa sp.	7,00	0,78	9,03	39,12
	Thalassiosira sp.	4,70	1,58	2,99	46,91
*60.58	*Nitzschia* sp.	4,10	2,05	1,97	53,61
	Emiliania huxleyi	8,00	0,81	9,80	13,27
3	*Heterocapsa* sp.	5,50	0,96	5,71	22,44
	Hillea fusiformis	5,50	0,99	5,52	31,51
	Thalassiosira sp.	4,40	0,69	6,37	38,79
*60.06	*Nitzschia tenuirostris*	4,10	1,18	3,45	45,57
4					
*68.79					
	Hillea fusiformis	6,90	0,55	12,67	11,07
5	*Emiliania huxleyi*	5,90	0,94	6,20	20,45
	Thalassiosira sp.	5,50	0,44	12,42	29,25
	Nitzschia sp.	5,00	0,97	5,18	37,32
*62.42	*Heterocapsa* sp.	4,80	0,72	6,69	45,01
8					
*58.93					

Table 14(*Continued*)

9					
*57.10					

* average similarity within the group

The species that contribute to the similarity within groups are given in table 14. Species with a high average of contribution ($\bar{S}_i$) and high ratio of $\bar{S}_i$ / SD(S_i) are consistently noticeable in groups. Although the species in the groups were same, the dominance of these species within the group contributed to the similarity of the groups. In group-1, *Emiliania huxleyi* was the dominant species by having the highest contribution, and then *Hillea fusiformis* makes the highest contribution to the similarity. In group-3, again *Emiliania huxleyi* has the highest contribution to the similarity but unlike the first group, this time, the second-highest contribution made by *Heterocapsa* sp. In group-5, this time *Hillea fusiformis* as a member of the Cryptophyceae class made the most significant contribution to the similarity of the group followed by the coccolithophorid *Emiliania huxleyi.*

The species that play an essential role in the differentiation of the groups are tabulated below (Table 15). Species of *Nitzschia tenuirostris, Gyrodinium estuariale, Choanoflagellate, Chaetoceros* sp. and *Bacteriastrum delicatulum* displayed a significant role in differentiating the groups.

Table 15 Species Contributions to Dissimilarity within the groups in October-2017.

Group	***Species***	$\bar{\delta}_i$	**SD (δ_i)**	$\bar{\delta}_i$ **/ SD (δ_i)**	$\Sigma\bar{\delta}_i$ **%**
	Katodinium sp.	2,24	0,87	2,58	5,10
2 & 1	*Amphidinium* sp.	1,56	1,05	1,49	8,64
	Gonyaulax polygramma	1,52	0,10	15,55	12,11
	Pronoctiluca pelagica	1,52	0,10	15,55	15,58
*43.94	*Pyrophacus horologium*	1,47	0,32	4,60	18,93
	Nitzschia tenuirostris	1,49	1,09	1,36	3,36
3 & 1	*Oxytoxum variabilis*	1,42	0,57	2,49	6,56
	Amphidinium sp.	1,38	0,97	1,43	9,67
	Chaetoceros sp.	1,37	1,10	1,24	12,75
*44.37	*Gyrodinium estuariale*	1,26	0,83	1,51	15,59

Table 15 (*Continued*)

3 & 2	*Katodinium* sp.	2,51	0,28	8,83	5,33
	Oxytoxum variabilis	1,60	0,23	7,01	8,71
	Gyrodinium estuariale	1,55	0,73	2,13	11,99
	Chaetoceros sp.	1,44	1,14	1,27	15,05
* 47.16	*Nitzschia tenuirostris*	1,39	0,87	1,60	17,99
4 & 1	*Gyrodinium estuariale*	1,76	1,46	1,21	3,94
	Oxytoxum variabilis	1,61	0,63	2,58	7,55
	Amphidinium sp.	1,61	1,07	1,50	11,16
	Pronoctiluca pelagica	1,58	0,11	14,77	14,69
*44.70	*Prorocentrum lima*	1,58	0,11	14,77	18,22
4 & 2	*Katodinium* sp.	2,82	0,06	46,83	6,16
	Chaetoceros curvisetus	2,16	0,05	46,83	10,89
	Oxytoxum sp.	1,82	0,04	46,83	14,86
	Oxytoxum variabilis	1,82	0,04	46,83	18,83
* 45.76	*Proboscia alata* forma *gracillima*	1,82	0,04	46,83	22,80
4 & 3	*Gyrodinium estuariale*	1,54	0,83	1,85	3,40
	Proboscia alata forma *gracillima*	1,53	0,58	2,63	6,78
	Oxytoxum viride	1,52	0,60	2,53	10,14
	Thalassiosira sp.	1,45	0,59	2,47	13,35
* 45.32	*Prorocentrum lima*	1,40	0,16	8,75	16,45
5 & 1	*Choanoflagellate*	1,97	1,57	1,26	4,24
	Chaetoceros sp.	1,90	1,37	1,39	8,33
	Nitzschia tenuirostris	1,71	1,15	1,49	12,01
	Dactyliosolen sp.	1,67	0,22	7,44	15,61
*46.53	*Rhizosolenia styliformis*	1,61	0,51	3,16	19,07
5 & 2	*Choanoflagellate*	2,06	1,80	1,15	3,96
	Chaetoceros sp.	1,97	1,72	1,15	7,75
	Bacteriastrum delicatulum	1,80	0,27	6,70	11,22
	Rhizosolenia styliformis	1,67	0,39	4,32	14,44
*51.97	*Gyrodinium estuariale*	1,65	0,46	3,61	17,61
5 & 3	*Nitzschia tenuirostris*	2,47	0,70	3,52	5,08
	Choanoflagellate	1,90	1,43	1,33	8,98
	Dactyliosolen sp.	1,51	0,24	6,21	12,09
	Chaetoceros sp.	1,43	0,94	1,51	15,03
*48.66	*Nitzschia* sp.	1,43	0,99	1,44	17,96
5 & 4	*Choanoflagellate*	2,12	1,65	1,28	3,84
	Thalassiosira sp.	2,10	0,28	7,52	7,64
	Bacteriastrum delicatulum	1,85	0,25	7,35	11,00
	Nitzschia tenuirostris	1,83	0,56	3,27	14,32
*55.13	*Chaetoceros* sp.	1,75	1,21	1,45	17,50

Table 15 (*Continued*)

6 & 1	*Pseudo-nitzschia delicatissima*	2,56	0,39	6,59	5,52
	Rhizosolenia styliformis	1,89	0,45	4,22	9,58
	Nitzschia tenuirostris	1,80	1,21	1,48	13,45
	Leptocylindrus mediterraneus	1,78	0,63	2,85	17,28
* 46.50	*Pronoctiluca pelagica*	1,69	0,10	16,63	20,92
6 & 2					
* 47.46					
6 & 3	*Nitzschia tenuirostris*	2,58	0,73	3,52	5,32
	Proboscia alata forma *gracillima*	1,82	0,89	2,06	9,07
	Amphidinium sp.	1,54	0,53	2,92	12,24
	Oxytoxum variabilis	1,50	0,21	7,07	15,32
* 48.62	*Gyrodinium estuariale*	1,46	0,68	2,13	18,31
6 & 4	*Pseudo-nitzschia delicatissima*	2,63	0,05	50,20	5,32
	Thalassiosira sp.	2,04	0,04	50,20	9,44
	Rhizosolenia styliformis	2,02	0,04	50,20	13,52
	Ceratium kofoidii	2,02	0,04	50,20	17,60
* 49.43	*Nitzschia tenuirostris*	1,92	0,73	2,64	21,48
6 & 5	*Pseudo-nitzschia delicatissima*	2,29	0,20	11,44	4,98
	Choanoflagellate	1,94	1,69	1,15	9,21
	Bacteriastrum delicatulum	1,69	0,25	6,85	12,90
	Gyrodinium sp.	1,63	0,45	3,64	16,46
* 45.94	*Gyrodinium estuariale*	1,56	0,44	3,54	19,84
7 & 1	*Choanoflagellate*	2,96	1,35	2,20	6,10
	Oxytoxum variabilis	2,77	0,57	4,89	11,81
	Dactyliosolen fragilissimus	2,14	0,12	17,27	16,22
	Chaetoceros tortissimus	2,14	0,12	17,27	20,63
* 48.56	*Chaetoceros* sp.	1,99	0,84	2,37	24,72
7 & 2					
* 60.22					
7 & 3	*Choanoflagellate*	2,92	0,97	3,01	5,89
	Nitzschia tenuirostris	2,50	0,71	3,50	10,94
	Dactyliosolen fragilissimus	1,93	0,20	9,75	14,84
	Chaetoceros tortissimus	1,93	0,20	9,75	18,75
*49.48	*Nitzschia* sp.	1,76	1,07	1,65	22,31
7 & 4	*Choanoflagellate*	3,58	0,07	52,20	7,27
	Chaetoceros tortissimus	2,15	0,04	52,20	11,62
	Leptocylindrus danicus	1,94	0,04	52,20	15,56
	Nitzschia tenuirostris	1,84	0,70	2,65	19,31
* 49.24	*Nitzschia* sp.	1,81	0,28	6,56	22,99

Table 15 (*Continued*)

7 & 5	*Oxytoxum variabilis*	2,21	0,61	3,59	4,66
	Chaetoceros tortissimus	1,90	0,18	10,57	8,69
	Dactyliosolen fragilissimus	1,88	0,16	11,81	12,66
	Bacteriastrum delicatulum	1,64	0,24	6,94	16,12
*47.28	*Gyrodinium* sp.	1,58	0,43	3,67	19,46
7 & 6					
* 47.44					
8 & 1	*Cylindrotheca closterium*	2,35	0,50	4,68	4,69
	Nitzschia tenuirostris	1,90	1,19	1,61	8,49
	Gymnodinium sanguineum	1,72	0,17	9,97	11,92
	Thalassiosira sp.	1,72	1,10	1,56	15,35
*50.15	*Gyrodinium estuariale*	1,65	0,75	2,20	18,63
8 & 2	*Katodinium* sp.	2,38	0,01	185,94	4,46
	Cylindrotheca closterium	2,38	0,01	185,94	8,93
	Nitzschia tenuirostris	2,17	0,15	14,66	13,01
	Gyrodinium estuariale	2,10	0,38	5,50	16,95
*53.35	*Chaetoceros curvisetus*	1,83	0,01	185,94	20,37
8 & 3	*Cylindrotheca closterium*	1,99	0,75	2,65	4,25
	Thalassiosira sp.	1,74	0,89	1,96	7,95
	Choanoflagellate	1,54	1,53	1,00	11,23
	Gymnodinium sanguineum	1,44	0,45	3,20	14,31
* 46.90	*Proboscia alata* forma *gracillima*	1,31	0,50	2,63	17,11
8 & 4	*Cylindrotheca closterium*	2,45	0,04	63,24	5,45
	Ceratium kofoidii	1,87	0,13	14,13	9,61
	Nitzschia tenuirostris	1,78	0,51	3,48	13,57
	Gymnodinium sanguineum	1,73	0,17	10,36	17,41
* 44.94	*Choanoflagellate*	1,62	1,87	0,87	21,02
8 & 5	*Nitzschia tenuirostris*	3,13	0,25	12,29	5,87
	Thalassiosira sp.	2,28	0,80	2,84	10,14
	Cylindrotheca closterium	2,15	0,16	13,54	14,18
	Bacteriastrum delicatulum	1,59	0,20	7,83	17,16
* 53.32	*Gymnodinium sanguineum*	1,52	0,18	8,53	20,01
8 & 6	*Nitzschia tenuirostris*	3,27	0,15	22,47	5,99
	Pseudo-nitzschia delicatissima	2,25	0,01	197,21	10,11
	Cylindrotheca closterium	2,25	0,01	197,21	14,23
	Thalassiosira sp.	2,23	1,03	2,16	18,32
* 54.54	*Gyrodinium estuariale*	1,98	0,36	5,49	21,96
8 & 7	*Nitzschia tenuirostris*	3,16	0,14	22,56	6,02
	Cylindrotheca closterium	2,17	0,01	203,93	10,16
	Gyrodinium estuariale	1,92	0,35	5,49	13,82
	Chaetoceros tortissimus	1,84	0,01	203,93	17,33
*52.46	*Dactyliosolen fragilissimus*	1,84	0,01	203,93	20,84

Table 15 (*Continued*)

9 & 1	*Chaetoceros* sp.	3,21	1,12	2,88	6,13
	Bacteriastrum delicatulum	2,50	1,03	2,42	10,89
	Nitzschia sp.	2,06	1,28	1,60	14,82
	Rhizosolenia styliformis	1,96	0,50	3,95	18,55
* 52.43	*Leptocylindrus mediterraneus*	1,92	0,69	2,78	22,22
9 & 2	*Chaetoceros* sp.	3,53	0,71	4,95	6,09
	Bacteriastrum delicatulum	2,72	0,95	2,85	10,79
	Prorocentrum sp.	2,31	0,99	2,33	14,76
	Chaetoceros curvisetus	2,10	0,24	8,87	18,39
* 58.00	*Rhizosolenia styliformis*	2,03	0,16	12,32	21,88
9 & 3	*Bacteriastrum delicatulum*	2,18	0,99	2,20	4,27
	Chaetoceros sp.	1,80	1,03	1,74	7,80
	Choanoflagellate	1,74	1,78	0,98	11,21
	Dactyliosolen sp.	1,71	0,19	8,79	14,56
*51.01	*Gyrodinium estuariale*	1,55	0,72	2,16	17,61
9 & 4	*Bacteriastrum delicatulum*	2,82	0,82	3,45	5,08
	Chaetoceros sp.	2,66	1,33	2,00	9,87
	Prorocentrum sp.	2,38	0,83	2,88	14,16
	Thalassiosira sp.	2,30	0,93	2,48	18,31
* 55.45	*Rhizosolenia styliformis*	2,09	0,14	15,26	22,08
9 & 5	*Nitzschia* sp.	2,61	1,07	2,44	5,45
	Prorocentrum sp.	2,06	0,72	2,85	9,74
	Choanoflagellate	1,75	1,77	0,99	13,39
	Nitzschia tenuirostris	1,73	0,33	5,20	17,01
* 47.88	*Gyrodinium estuariale*	1,66	0,43	3,87	20,48
9 & 6	*Nitzschia* sp.	2,73	1,27	2,16	4,70
	Pseudo-nitzschia delicatissima	2,56	0,27	9,49	9,11
	Bacteriastrum delicatulum	2,54	0,87	2,91	13,48
	Prorocentrum sp.	2,16	0,94	2,30	17,19
* 58.15	*Ceratium kofoidii*	1,97	0,21	9,49	20,57
9 & 7	*Nitzschia* sp.	3,07	1,25	2,45	5,84
	Bacteriastrum delicatulum	2,44	0,83	2,94	10,50
	Chaetoceros tortissimus	2,09	0,21	9,85	14,48
	Dactyliosolen fragilissimus	2,09	0,21	9,85	18,47
* 52.53	*Prorocentrum* sp.	2,08	0,91	2,28	22,43
9 & 8	*Thalassiosira* sp.	2,48	1,18	2,09	4,45
	Cylindrotheca closterium	2,39	0,19	12,43	8,75
	Bacteriastrum delicatulum	2,37	0,65	3,63	13,01
	Chaetoceros sp.	2,11	1,20	1,76	16,80
*55.64	*Gyrodinium estuariale*	2,11	0,36	5,92	20,60

Table 15 (*Continued*)

10 & 1	*Nitzschia tenuirostris*	3,02	1,37	2,20	5,57
	Choanoflagellate	2,63	1,18	2,24	10,44
	Nitzschia sigmoidea	2,03	0,12	16,45	14,20
	Pleurosigma normanii	1,98	0,32	6,17	17,86
*54.13	*Gymnodinium* sp.	1,92	0,78	2,47	21,40
10 & 2					
*57.43					
10 & 3	*Choanoflagellate*	2,64	0,67	3,94	4,65
	Pleurosigma normanii	1,83	0,20	9,31	7,87
	Nitzschia sigmoidea	1,83	0,20	9,31	11,09
	Nitzschia tenuirostris	1,73	1,06	1,63	14,15
* 56.71	*Pseudosolenia calcar-avis*	1,70	0,18	9,31	17,15
10 & 4	*Choanoflagellate*	3,16	0,06	49,63	5,22
	Nitzschia tenuirostris	2,91	0,64	4,57	10,02
	Pleurosigma normanii	2,04	0,04	49,63	13,39
	Nitzschia sigmoidea	2,04	0,04	49,63	16,76
*60.57	*Pseudosolenia calcar-avis*	1,90	0,04	49,63	19,89
10 & 5	*Nitzschia tenuirostris*	4,21	0,37	11,33	7,23
	Chaetoceros sp.	1,88	1,64	1,15	10,45
	Nitzschia sigmoidea	1,77	0,16	11,33	13,50
	Pleurosigma normanii	1,77	0,16	11,33	16,54
*58.23	*Bacteriastrum delicatulum*	1,71	0,25	6,83	19,48
10 & 6					
* 60.21					
10 & 7					
* 63.86					
10 & 8	*Cylindrotheca closterium*	2,27	0,01	195,31	4,13
	Gyrodinium estuariale	2,00	0,36	5,49	7,78
	Thalassiosira sp.	1,97	1,04	1,89	11,37
	Pleurosigma normanii	1,74	0,01	195,32	14,54
*54.86	*Nitzschia sigmoidea*	1,74	0,01	195,32	17,71
10 & 9	*Chaetoceros* sp.	3,34	0,65	5,11	5,98
	Nitzschia tenuirostris	2,88	0,08	33,99	11,13
	Bacteriastrum delicatulum	2,57	0,89	2,90	15,73
	Nitzschia sigmoidea	1,99	0,21	9,38	19,29
*55.87	*Pleurosigma normanii*	1,99	0,21	9,38	22,85

* average dissimilarity within groups.

In winter, there were eight main phytoplankton group formations based on the Bray-Curtis Similarity measure at an arbitrary similarity level of 55%. Group-1 has the largest patch among the sampling area. It included stations 4 to 7, 12, 13, 17, 18, 21 to 23, 26 to 28, 31, 34, 35, 37, 38, 42 to 48 and 50. Group-2 included stations 36, 40, 41 and 49. Group-3 contained stations 9, 10, 14, 15, 19 and 30. Group-4 consisted of a single station 8, and group-5 also contained single station 32. Group-6, which covered a relatively large area, consisted of stations 1, 2, 16, 20, 24, 25, 29 and 33. Lastly, group-7 included a single station 3, and group-8 station 39 (Figure 43).

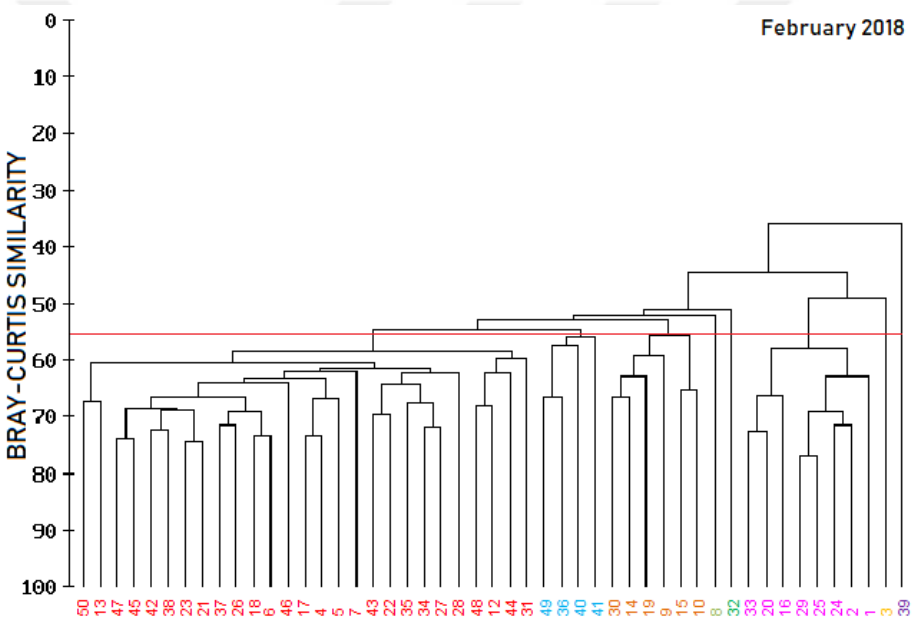

Figure 43 Dendrogram showing classification based on Bay-Curtis Similarity measure for surface samples in February-2018

As seen from the MDS ordination diagrams, group-8 in terms of composition was different from the others. Also, Group-1 in the middle of this diagram was more similar to groups 2 and 3 than other groups. Groups 6 and 7 were closer to each other than the rest. (Figure 44).

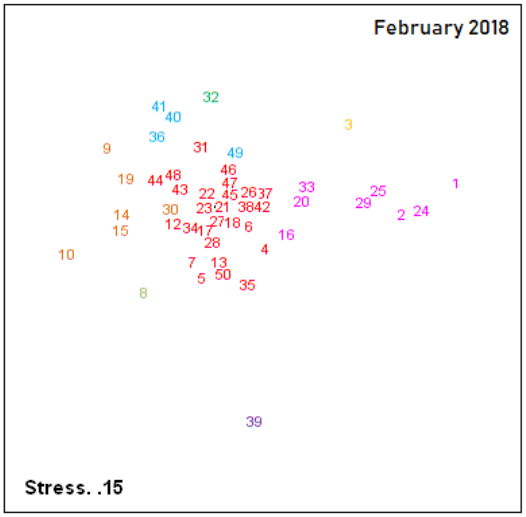

Figure 44 Two-Dimensional non-metric MDS ordination of all stations sampled in February-2018

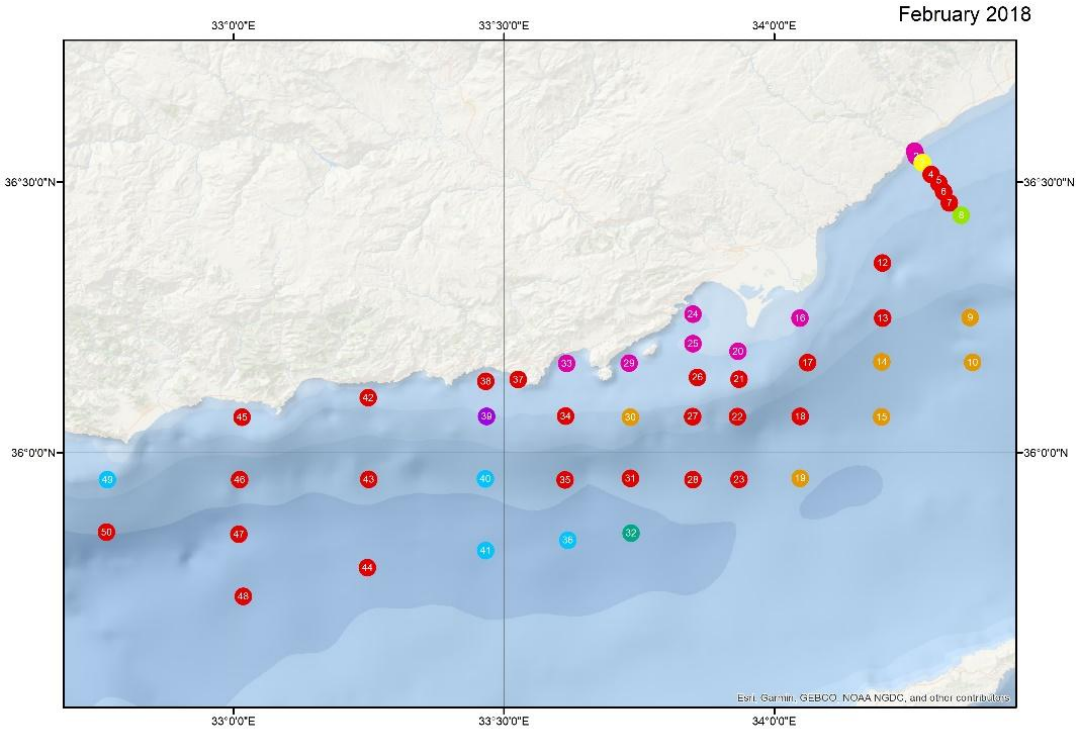

Figure 45 Phytoplankton patches observed in February-2018.

In this season, Group-1 was scattered throughout the sampling area as a prevalent group. Group-2 mainly included offshore waters in the west. Group 6 composed of stations that are mainly influenced by the Göksu River discharges including Taşucu Bay. ETS stations formed four distinct groups along to transect including groups 6, 7, 1 and 4. In the east, deep offshore waters formed the Group-3 (Figure 45).

The species that contribute to the similarity within groups are given in the table below (Table 16). For the first three groups, *Emiliania huxleyi* was the most contributing to intra-group similarity. However, unlike each other; in the first group, the second most significant contribution was made by *Chaetoceros socialis*, while in the second and third groups, *Hillea fusiformis* made this contribution. In the group-2, apart from these species *Nitzschia tenuirostris*, *Amphidinium* sp. and *Calciosolenia brasiliensis* contributed to the similarity. In the group-3, in addition to those mentioned, *Nitzschia tenuirostris, Leptocylindrus mediterraneus* and *Bacteriastrum delicatulum* contributed to the similarity. In group 6, *Chaetoceros socialis* made the most considerable contribution to similarity, while *Skeletonema costatum* made the second major contribution.

Table 16 Species Contributions to Similarity within the groups in February-2018.

Group	*Species*	$\overline{S}_i$	SD (S_j)	$\overline{S}_i$ / SD(S_j)	$\Sigma \overline{S}_i$ %
1	*Emiliania huxleyi*	8,10	0,93	8,70	13,07
	Chaetoceros socialis	7,40	2,40	3,08	25,00
	Nitzschia tenuirostris	5,80	0,84	6,90	34,34
	Hillea fusiformis	5,30	1,00	5,29	42,92
* 61.95	*Bacteriastrum delicatulum*	3,70	0,55	6,63	48,83
2	*Emiliania huxleyi*	9,70	0,80	12,13	16,64
	Hillea fusiformis	5,30	0,94	5,64	25,72
	Nitzschia tenuirostris	4,60	0,52	8,93	33,67
	Amphidinium sp.	4,50	1,44	3,12	41,39
*58.19	*Calciosolenia brasiliensis*	4,40	0,28	15,47	48,94
3	*Emiliania huxleyi*	11,90	1,00	11,96	20,29
	Hillea fusiformis	7,70	1,16	6,65	33,49
	Nitzschia tenuirostris	7,00	0,68	10,24	45,41
	Leptocylindrus mediterraneus	5,10	0,44	11,60	54,13
*58.68	*Bacteriastrum delicatulum*	4,40	0,78	5,66	61,64
6	*Chaetoceros socialis*	5,10	1,24	4,16	8,23
	Skeletonema costatum	4,80	1,27	3,79	15,95
	Emiliania huxleyi	4,00	0,70	5,62	22,27
	Pseudo-nitzschia delicatissima	3,60	0,76	4,74	28,05
* 62.54	*Asterionella japonica*	3,10	0,68	4,54	33,01

* average similarity within the group

The species that play an essential role in the differentiation of the groups are tabulated below (Table 17). For this season, species of *Chaetoceros socialis, Skeletonema costatum, Heterocapsa* sp. *and Chaetoceros decipiens* played a notable role in the discrimination of groups.

Table 17 Species Contributions to Dissimilarity within the groups in February-2018.

Group	*Species*	$\overline{\delta}_i$	SD (δ_i)	$\overline{\delta}_i$ / SD (δ_i)	$\Sigma\,\overline{\delta}_i$ %
2 & 1	*Chaetoceros socialis*	2,03	1,76	1,15	4,48
	Syracosphaera sp.	1,44	0,89	1,62	7,66
	Rhabdosphaera tignifer	1,27	0,77	1,66	10,47
	Heterocapsa sp.	1,23	1,06	1,16	13,19
* 45.37	*Amphidinium* sp.	1,21	0,92	1,31	15,84
3 & 1	*Chaetoceros socialis*	3,84	1,75	2,20	8,20
	Calciosolenia brasiliensis	1,64	1,07	1,53	11,71
	Heterocapsa sp.	1,53	1,14	1,34	14,97
	Chaetoceros diversus	1,52	0,99	1,53	18,21
* 46.88	*Chaetoceros decipiens*	1,40	1,05	1,33	21,20
3 & 2	*Chaetoceros socialis*	2,54	1,72	1,48	5,20
	Syracosphaera sp.	2,37	0,70	3,39	10,04
	Calciosolenia brasiliensis	1,80	1,09	1,65	13,73
	Syracosphaera pulchra	1,66	0,35	4,74	17,12
* 48.88	*Heterocapsa* sp.	1,62	1,14	1,42	20,43
4 & 1	*Chaetoceros socialis*	3,10	0,83	3,75	6,60
	Heterocapsa sp.	2,16	1,31	1,65	11,20
	Amphidinium sp.	1,89	1,16	1,62	15,23
	Thalassiothrix frauenfeldii	1,57	0,85	1,84	18,57
*46.89	*Distephanus speculum*	1,57	0,53	2,93	21,91
4 & 2	*Amphidinium* sp.	3,14	0,98	3,21	5,74
	Syracosphaera sp.	2,35	0,77	3,07	10,05
	Chaetoceros socialis	2,16	0,54	4,01	14,01
	Heterocapsa sp.	2,08	1,57	1,33	17,83
*54.59	*Cylindrotheca closterium*	1,85	0,68	2,71	21,22
4 & 3	*Pseudo-nitzschia delicatissima*	2,71	0,20	13,37	5,71
	Amphidinium sp.	2,40	0,86	2,80	10,77
	Chaetoceros diversus	2,17	1,30	1,66	15,34
	Torodinium teredo	1,98	0,18	11,01	19,51
* 47.46	*Chaetoceros danicus*	1,98	0,15	13,37	23,69

Table 17 (*Continued*)

5 & 1	*Chaetoceros socialis*	4,06	1,02	3,99	8,44
	Rhabdosphaera tignifer	2,82	0,19	15,07	14,31
	Oxytoxum variabilis	2,00	0,13	15,07	18,46
	Chaetoceros diversus	1,60	0,53	3,05	21,79
* 48.14	*Leptocylindrus danicus*	1,58	0,72	2,20	25,07
5 & 2	*Chaetoceros socialis*	2,55	1,75	1,46	5,49
	Oxytoxum variabilis	2,05	0,12	17,62	9,90
	Syracosphaera sp.	1,88	0,60	3,14	13,96
	Chaetoceros decipiens	1,86	0,11	17,62	17,98
*46.38	*Rhabdosphaera tignifer*	1,68	0,72	2,34	21,60
5 & 3	*Rhabdosphaera tignifer*	3,34	0,19	17,23	6,48
	Chaetoceros decipiens	2,15	0,13	17,23	10,66
	Oxytoxum variabilis	2,15	0,53	4,03	14,82
	Rhabdosphaera stylifer	1,81	0,11	17,23	18,34
* 51.57	*Thalassiothrix frauenfeldii*	1,67	0,81	2,05	21,57
5 & 4 *58.33					
6 &1	*Skeletonema costatum*	3,71	1,35	2,74	7,07
	Pseudo-nitzschia delicatissima	2,48	0,94	2,64	11,79
	Chaetoceros curvisetus	2,14	1,33	1,61	15,86
	Asterionella japonica	1,93	1,06	1,83	19,54
* 52.44	*Lauderia* sp.	1,74	0,78	2,25	22,87
6 & 2	*Skeletonema costatum*	3,85	1,39	2,77	6,35
	Pseudo-nitzschia delicatissima	2,84	0,71	4,01	11,02
	Chaetoceros decipiens	2,50	0,53	4,68	15,15
	Chaetoceros curvisetus	2,35	1,36	1,73	19,02
*60.67	*Chaetoceros socialis*	2,28	1,42	1,60	22,77
6 & 3	*Skeletonema costatum*	4,70	1,08	4,35	7,53
	Chaetoceros socialis	3,63	1,34	2,71	13,35
	Pseudo-nitzschia delicatissima	3,38	0,59	5,76	18,78
	Asterionella japonica	2,91	0,84	3,47	23,44
* 62.35	*Chaetoceros decipiens*	2,75	0,55	4,97	27,85
6 & 4	*Skeletonema costatum*	4,68	1,13	4,15	7,36
	Chaetoceros socialis	3,13	0,91	3,43	12,29
	Asterionella japonica	2,90	0,88	3,31	16,85
	Chaetoceros decipiens	2,74	0,58	4,76	21,16
* 63.61	*Chaetoceros curvisetus*	2,57	1,54	1,67	25,20
6 & 5	*Skeletonema costatum*	4,08	1,06	3,84	6,72
	Chaetoceros socialis	3,87	0,85	4,55	13,08
	Chaetoceros curvisetus	2,25	1,37	1,64	16,79
	Pseudo-nitzschia delicatissima	2,06	0,73	2,83	20,18
* 60.76	*Rhabdosphaera tignifer*	1,92	0,32	5,96	23,35

Table 17 (*Continued*)

7 & 1	*Chaetoceros* sp.	5,06	0,53	9,57	9,35
	Chaetoceros socialis	3,75	0,94	3,98	16,29
	Skeletonema costatum	3,63	1,09	3,35	23,00
	Lithodesmium undulatum	2,00	0,12	16,34	26,69
*54.10	*Pseudo-nitzschia delicatissima*	1,89	0,91	2,08	30,18
7 & 2	*Chaetoceros* sp.	5,29	0,28	19,10	8,30
	Skeletonema costatum	3,83	1,28	2,98	14,30
	Chaetoceros socialis	2,35	1,61	1,46	17,99
	Pseudo-nitzschia delicatissima	2,35	0,55	4,26	21,67
* 63.79	*Amphidinium* sp.	2,31	0,69	3,34	25,29
7 & 3	*Chaetoceros* sp.	5,42	0,97	5,61	8,82
	Skeletonema costatum	4,99	0,26	18,87	16,95
	Pseudo-nitzschia delicatissima	3,04	0,16	18,87	21,90
	Asterionella japonica	2,58	0,14	18,87	26,10
* 61.47	*Gymnodinium* sp.	2,56	0,14	18,87	30,26
7 & 4 *53.76					
7 & 5 *62.16					
7 & 6	*Chaetoceros socialis*	3,66	0,80	4,58	7,18
	Chaetoceros sp.	2,69	1,05	2,56	12,46
	Chaetoceros curvisetus	2,14	1,32	1,62	16,65
	Heterocapsa sp.	1,55	0,23	6,69	19,70
*50.96	*Lithodesmium undulatum*	1,39	0,22	6,31	22,43
8 & 1	*Emiliania huxleyi*	4,91	0,57	8,58	8,19
	Chaetoceros socialis	4,86	1,21	4,00	16,30
	Nitzschia tenuirostris	3,61	0,54	6,66	22,32
	Hillea fusiformis	3,35	0,56	6,04	27,91
* 59.99	*Heterocapsa* sp.	2,08	1,26	1,65	31,38
8 & 2	*Emiliania huxleyi*	5,56	0,50	11,11	8,25
	Hillea fusiformis	3,22	0,50	6,40	13,02
	Chaetoceros socialis	3,05	2,09	1,46	17,55
	Amphidinium sp.	3,02	0,93	3,23	22,02
* 67.38	*Nitzschia tenuirostris*	2,85	0,41	7,03	26,25
8 & 3	*Emiliania huxleyi*	6,08	0,42	14,60	8,56
	Hillea fusiformis	3,90	0,62	6,31	14,05
	Nitzschia tenuirostris	3,74	0,55	6,86	19,33
	Chaetoceros decipiens	3,18	0,23	13,97	23,81
* 70.95	*Tropidoneis* sp.	2,90	0,21	13,97	27,90
8 &4 * 66.04					
8 & 5 *66.59					

Table 17 (*Continued*)

8 & 6	*Chaetoceros socialis*	4,36	0,98	4,43	6,28
	Skeletonema costatum	3,33	1,33	2,50	11,08
	Emiliania huxleyi	3,12	0,62	5,07	15,57
	Asterionella japonica	2,83	0,86	3,30	19,65
*69.47	*Chaetoceros curvisetus*	2,51	1,51	1,67	23,27
8 & 7					
* 67.12					

* average dissimilarity within groups.

In spring, there were two widely distributed primary phytoplankton group formations based on the Bray-Curtis Similarity measure at an arbitrary similarity level of 58%. Group-1 comprise mainly the deep offshore waters of the study area beyond shelf whereas group 2 covers mainly the coastal & shelf areas. (Figure 46).

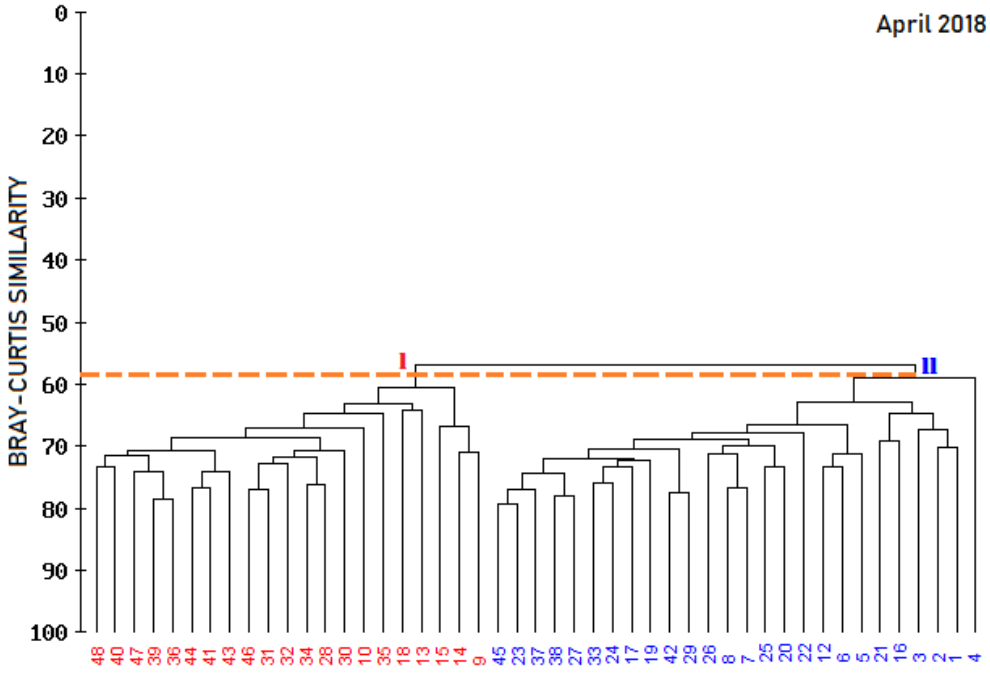

Figure 46 Dendrogram showing classification based on Bay-Curtis Similarity measure for surface samples in April-2018

According to the MDS ordination diagrams, these two main groups were separated from each other (Figure 47).

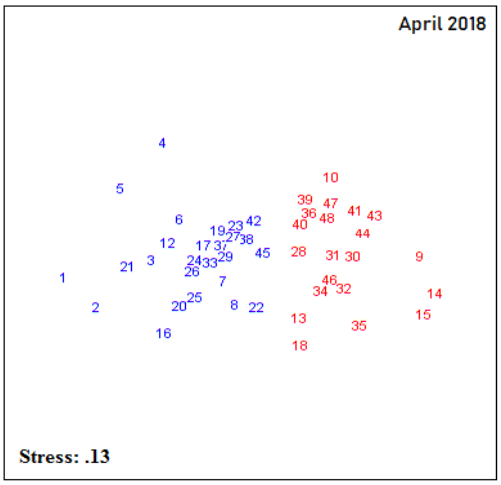

Figure 47 Two-Dimensional non-metric MDS ordination of all stations sampled in April-2018

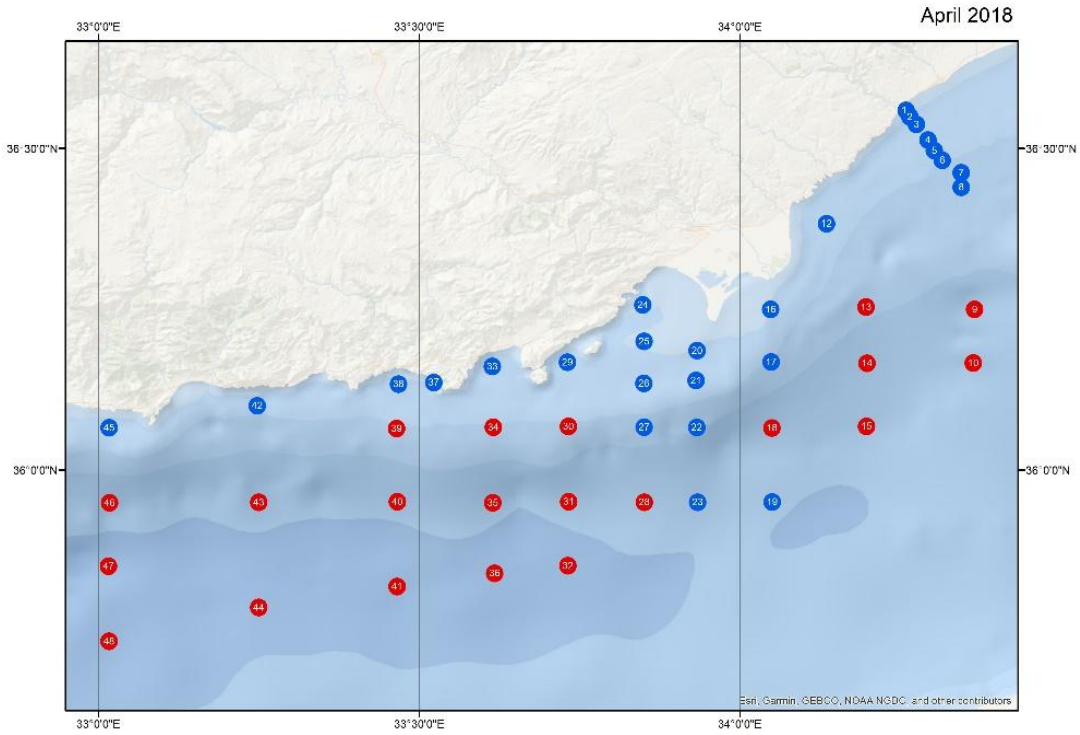

Figure 48 Phytoplankton patches observed in April-2018.

In this season, Group-1 was scattered throughout the sampling area as divided into two-parts and dominated the open areas of the sampling area except where the Göksu River discharges. Group-2 was distributed through coastal waters as a whole, and expand over the offshore waters by covering the impact area of the Göksu River and ETS stations (Figure 48).

Table 18 Species Contributions to Similarity within the groups in April-2018.

Group	Species	$\overline{S}_i$	SD (S_j)	$\overline{S}_i$ / SD(S_j)	$\Sigma\overline{S}_i$ %
1	*Emiliania huxleyi*	5,60	0,56	9,86	8,44
	Heterocapsa sp.	4,90	0,48	10,31	15,90
	Pseudo-nitzschia delicatissima	4,80	0,58	8,26	23,11
	Proboscia alata forma *gracillima*	4,60	0,43	10,88	30,15
* 65.99	*Hillea fusiformis*	4,60	0,59	7,83	37,15
2	*Proboscia alata* forma *gracillima*	5,10	0,50	10,21	7,64
	Pseudo-nitzschia delicatissima	4,50	1,99	2,27	14,45
	Chaetoceros rostratus	4,30	1,38	3,08	20,86
	Chaetoceros sp.	4,00	1,83	2,17	26,83
* 66.44	*Emiliania huxleyi*	3,80	1,17	3,23	32,51

* average similarity within the group

The species that contribute to the similarity within groups are given in the table above (Table 18). For the first group, *Emiliania huxleyi* was the dominant species by having the highest contribution, and then *Heterocapsa sp.* made the highest contribution to the similarity. Also, *Pseudo-nitzschia delicatissima*, *Proboscia alata* forma *gracillima* and *Hillea fusiformis* contributed to intra-group similarities. In group-2, *Proboscia alata* forma *gracillima* made the most significant contribution followed by *Pseudo-nitzschia delicatissima*. Besides, *Chaetoceros rostratus, Chaetoceros* sp. and *Emiliania huxleyi* contributed to the similarity.

The species that play an essential role in the differentiation of the groups are tabulated below (Table 19). In spring, there were two groups distinct from each other. Species of *Chaetoceros rostratus, Chaetoceros* sp., *Chaetoceros curvisetus, Dactyliosolen fragilissimus and Pseudo-nitzschia delicatissima* displayed a crucial role in the discrimination of groups.

Table 19 Species Contributions to Dissimilarity within the groups in April-2018.

Group	*Species*	$\overline{\delta}_i$	SD (δ_i)	$\overline{\delta}_i$ / SD (δ_i)	$\Sigma\overline{\delta}_i$ %
2 & 1	*Chaetoceros rostratus*	1,71	0,63	2,74	3,97
	Chaetoceros sp.	1,66	0,88	1,89	7,81
	Chaetoceros curvisetus	1,52	0,93	1,64	11,33
	Dactyliosolen fragilissimus	1,51	0,68	2,21	14,83
* 43.18	*Pseudo-nitzschia delicatissima*	1,30	0,62	2,10	17,85

* average dissimilarity within groups.

In summer surface flora was divided into three groups of varying patch size. The largest first group covered mainly the west part of the study area including coastal shelf waters in the east. The relatively smaller third group was formed mainly of offshore waters in the east. The smallest second group contained only the shallowest station ETS1 in the east. The reason why it was separated from the rest was the time delay due to cruise timing. The summer cruise involved two legs due to loss of grab sampler at station ETS2 and damage on e-frame in the mids of the cruise. In the second leg, almost all of the stations covered in the first leg have been revisited except station ETS1. Almost a week gap between the sampling of two consecutive stations (ETS1 and the rest) separated ETS1 from the rest of the stations. Change in the composition of shallow coastal flora was very rapid due to inputs from the nearby Lamas creek at station ETS1 (Figure 49, Figure 51).

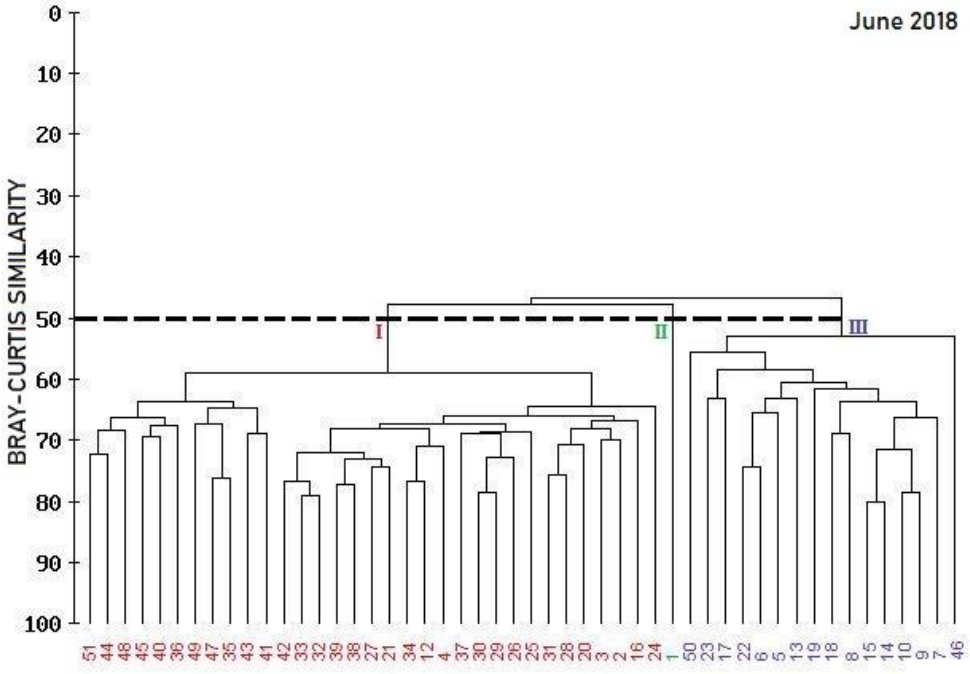

Figure 49 Dendrogram showing classification based on Bay-Curtis Similarity measure for surface samples in June-2018

Due to the MDS ordination diagrams, Group-2 was different from the others in terms of the composition. Also, there was a clear separation between group-1 and group-3 (Figure 50).

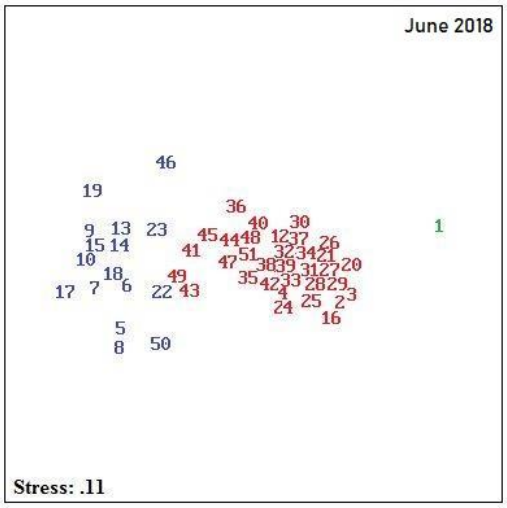

Figure 50 Two-Dimentional non-metric MDS ordination of all stations sampled in June-2018.

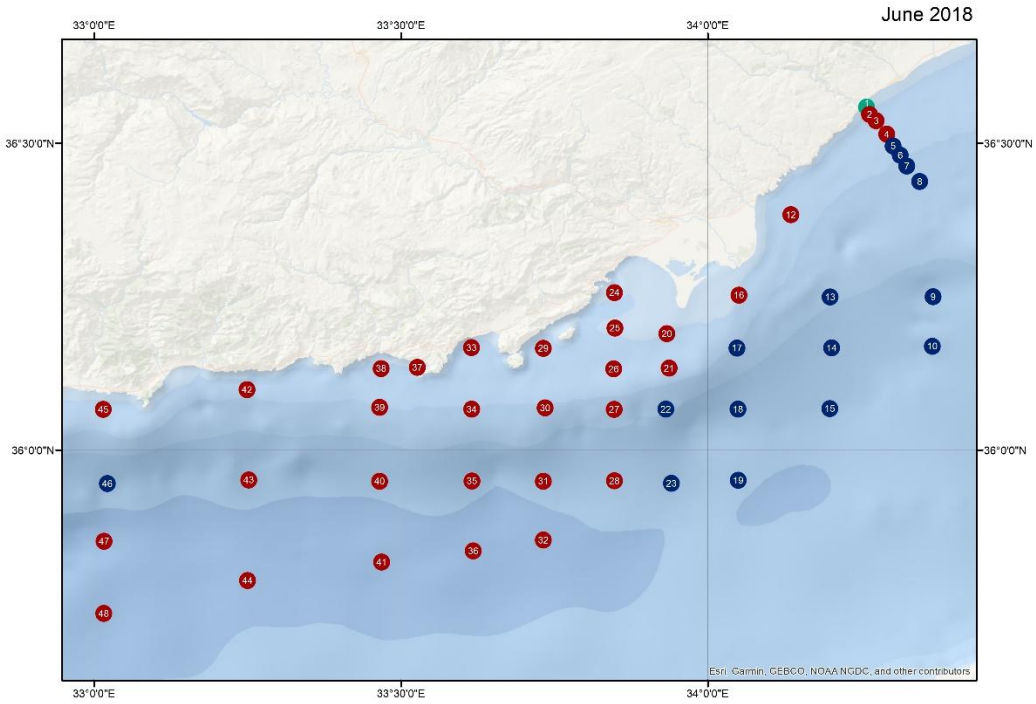

Figure 51 Phytoplankton patches observed in June-2018.

The species that contribute to the similarity within groups are given in the table below (Table 20). For the first group, the highest contribution was made by *Leptocylindrus danicus,* and then *Rhizosolenia styliformis* made the second-highest contribution to the similarity. Besides, *Emiliania huxleyi*, *Pseudo-nitzschia delicatissima* and *Hillea fusiformis* contributed to intra-group similarities. In group-2, *Emiliania huxleyi* has the most notable contribution, and *Pseudo-nitzschia delicatissima* followed as second. Also, *Hillea fusiformis, Heterocapsa* sp.and *Rhizosolenia styliformis* contributed to the similarity.

Table 20 Species Contributions to Similarity within the groups in June-2018.

Group	***Species***	$\overline{S}_i$	**SD** (S_j)	$\overline{S}_i$ / SD(S_j)	$\Sigma\,\overline{S}_i$ %
	Leptocylindrus danicus	9,60	3,13	3,05	15,08
1	*Rhizosolenia styliformis*	5,80	0,65	8,84	24,22
	Emiliania huxleyi	5,30	0,86	6,16	32,60
	Pseudo-nitzschia delicatissima	5,20	0,88	5,88	40,79
*63.34	*Hillea fusiformis*	4,00	0,62	6,46	47,11
	Emiliania huxleyi	10,10	1,31	7,72	16,87
2	*Pseudo-nitzschia delicatissima*	7,20	1,36	5,29	28,85
	Hillea fusiformis	6,90	2,94	2,36	40,37
	Heterocapsa sp.	6,70	2,86	2,33	51,45
* 60.13	*Rhizosolenia styliformis*	5,60	2,39	2,34	60,74

* average similarity within the group

The species that play an essential role in the differentiation of the groups are tabulated below (Table 21). In this season, there were three main groups different from each other. Species of *Leptocylindrus danicus, Cerataulina pelagica, Chaetoceros curvisetus and Chaetoceros* sp. played a significant role in the discrimination of groups.

Table 21 Species Contributions to Dissimilarity within the groups in June-2018.

Group	*Species*	$\overline{\delta}_i$	SD (δ_i)	$\overline{\delta}_i$ / SD (δ_i)	$\Sigma\,\overline{\delta}_i$ %
2 & 1	*Leptocylindrus danicus*	6,06	2,53	2,40	11,48
	Ceratium pelagica	1,96	0,68	2,89	15,19
	Rhizosolenia styliformis	1,90	0,93	2,05	18,78
	Nitzschia sp.	1,73	1,20	1,44	22,06
* 52.82	*Nitzschia tenuirostris*	1,72	1,17	1,47	25,31
3 & 1	*Chaetoceros* sp.	3,54	0,95	3,73	6,77
	Cerataulina pelagica	2,56	0,25	10,25	11,65
	Chaetoceros didymus var protuberans	2,17	0,60	3,59	15,80
	Hillea fusiformis	1,83	0,29	6,38	19,29
* 52.33	*Coscinodiscus* sp.	1,77	0,19	9,34	22,67
3 & 2	*Leptocylindrus danicus*	6,49	0,97	6,70	9,02
	Chaetoceros sp.	5,36	0,72	7,49	16,46
	Cerataulina pelagica	3,25	0,16	20,81	20,98
	Chaetoceros didymus var protuberans	3,12	0,35	9,05	25,32
* 71.97	*Rhizosolenia styliformis*	2,83	0,69	4,11	29,25

* average dissimilarity within groups.

4. DISCUSSION

The Eastern Mediterranean is defined as one of the oligotrophic basins among the world's seas (Azov, 1991), also recognised by having low productivity due to the inadequate source of nutrients at the surface layer (Dugdale and Wilkerson, 1988). As against the adjacent Atlantic Ocean, the Mediterranean Sea limited in terms of both nitrate and phosphate due to nutrient-depleted surface waters flowing from Gibraltar to the Mediterranean (Krom *et al*., 1991). It is argued that phosphorus is a limiting factor in the upper zone, especially in terms of algal production (Yılmaz and Tuğrul, 1998). The reason for this limitation is suggested to be the high rate of diazotrophic N2 fixation in the Eastern Mediterranean Sea (Krom *et al*., 2010). The nutrient limitation may vary by season and region. According to the studies done by Yücel (2013) and Kress (2005), the co-limitation of nitrogen and phosphorus was recorded, and it is argued that coastal waters may be limited to silicate in the future (Koçak *et al.*, 2010).

It is known that N, P and Si concentration and elemental ratios highly affect phytoplankton assemblages (Harris, 1988). The observational definition of these factors those required for balanced development is the Redfield ratios as N: P: Si, 16: 1: 16 (Justić *et al*., 1995; REDFIELD, 1960). Due to the deviations occurring at these ratios, lesser nutrients in the system become limiting for phytoplankton growth. Since the loading of N, P and Si is affected by human activities, these rates in rivers change (Turner *et al*., 2003). The Mediterranean is a very variable system respecting nutrient concentrations and stoichiometry (Millot *et al*. 2006; Béthoux *et al*. 1998). Nutrient concentrations are generally measured at the detection limit, and therefore N: P ratios are not precise.

4.1. Physical and Biochemical Parameters

In fall, high temperature, low salinity, as well as, low-density values carried by the Asia Minor Current (AMC), defined as the extension of the Cilician Current, enters the region in the northeast-southwest direction (Kamel, 1999). According to the results of the fall period, the surface water temperature and salinity values of the Cilician

Basin of the northeastern Mediterranean did not significantly change spatially. Surface water temperature values decreased in the same direction following the east-west direction of the current. Coastal zone surface waters under the influence of local rivers were colder than open sea due to faster cooling (Poulos *et al*., 1997). Salinity values in coastal waters, outside the delta area, were similar to offshore waters. Biochemical parameters, dissolved inorganic nutrients and total phosphorus (TP) concentrations were low during this season, excluding the Göksu River impact area, which did not significantly change spatially. Relatively high nitrate and silicate values were measured in the coastal area affected by the Göksu River and the Lamas River. Dissolved oxygen values measured at this limited station ranged from 6.53 to 6.84 mg/L in surface waters, and seawater was fully saturated with oxygen in accordance with the typical eastern Mediterranean characteristics (Kress & Herut, 2001).

According to surface distribution maps produced from the physical and biochemical measurement results, obtained from the winter period field study, the spatial changes were more prominent. Surface water temperature values decreased significantly in the winter period due to the decrease in air temperature and cooling of surface waters (Poulos *et al*., 1997). Göksu and Lamas river waters, which are both colder than the sea, directly influenced the coastal area where the lowest temperature values were observed (Tornés, Pérez, Durán, & Sabater, 2014). Salinity values were measured between 38.47 - 38.74 in coastal surface waters where the water temperature was lower due to increased rainfall and river flow rates (Poulos *et al*., 1997). When comparing to fall results, the upper layer/surface layer waters temperature significantly decreased, whereas density values increased slightly.

It is known that in spring, the extension of the AMC observed during winter months in Erdemli and Anamur is not as strong as previous months; however, the effects of river inputs in the region are strongly felt. In this month, surface temperature, salinity and density graphs show that salinity and density decrease, extending to the openings of the Göksu River mouth. Additionally, during this season, the effects of the Lamas, Seyhan and Ceyhan Rivers' transport to the region by coastal currents are also observed in salinity and density profiles collected from the east of the Göksu River. When examining surface water temperature and salinity values in this season,

spatial changes are significant as in the winter period. In the Gulf-Cyprus region, which has a broad continental shelf, the temperature distributions decreased in an east-west direction. Throughout this period, salinity values of the coastal area waters affected by regional Lamas and Göksu rivers are lower due to the increase in flow rates (Lane *et al*., 2007). Density values calculated in spring are slightly lower than in the winter period. According to biochemical analysis results of spring, which represents the spring period; salinity shows a significant spatial change, and nutrient salts and total phosphorus (TP) show a similar spatial distribution to Cilician Basin waters. In the coastal region where the Göksu and Lamas Rivers have relatively low flow rate, salinity values decreased, and nutrient salt values increased (Akçay &Tuğrul, 2018). The dissolved oxygen values measured at the limited station ranged from 7.42 - 7.6 mg/L in surface waters and the seawater was fully saturated with oxygen following typical eastern Mediterranean characteristic (Kress & Herut, 2001).

In the summer season, stations 1, 9, 10, 13, 14, 15, 18 and 19 were sampled on the 25th of June, and other stations were sampled on the 2nd, 3rd and 4th of July due to failure of the ship during June. When examining these stations, possible changes in water properties during the week between the end of June and the beginning of July should be considered.

When physical properties of surface water are examined during summer, the presence of the AMC, which proceeds westward, carries high temperature, high salinity and low-density surface waters. According to this period's results, the physical characteristics of the Cilician basin continental shelf waters showed spatial changes due to river inputs and current regime as in other seasons. The lowest salinity values were measured in the shallow coastal area where the Lamas and the Göksu rivers flow. Similar to other seasons, the temperature tended to decrease in the east-west direction and increase in coastal and open zones. Spatial changes observed in surface temperature are due to the influence of the flow regime of the region and high flow rate of the Göksu River in the Göksu-Taşucu coastal area. It was evident from the surface distributions of summer physical properties (temperature and salinity) that the effect of the lower flow rate of the Lamas River remains within the limited (nearshore) area (Lane *et al*., 2007). Surface water nutrient salts and TP range were narrower than

the rainy winter-spring period. Although the effect of river waters remained weak compared to other periods, there were small spatial changes in biochemical properties as well as in the physical properties of seawater. The highest values were detected in shallow coastal waters under the influence of local rivers, while open sea features reflected that of the oligotrophic eastern Mediterranean water (Akçay &Tuğrul, 2018). Seawater dissolved oxygen (DO) values are controlled by physical (temperature, salinity) and biological (primary production, decomposition of organic matter) properties and are closely related to the residence time of the water. DO values in the summer period ranged from 6.49 to 6.92 mg/L regionally and the change interval was lower than in other periods. This was because of high-temperature measurements, although surface waters were saturated with oxygen (a known feature of the eastern Mediterranean) (Kress & Herut, 2001).

When stoichiometry ratios are considered, the nitrate: phosphate ratios in the surface waters showed decreasing values in their seasonally arithmetic means in the order winter > spring = fall > summer. Excess NOx load reached in coastal waters of the northeastern Mediterranean directly influenced by Göksu River and Lamas creek runoffs, especially during the rainy winter-spring period, results in limited primary production in terms of phosphorus. As demonstrated by the studies, this has been caused by river and atmospheric nutrient inputs with higher N: P ratios than the Redfield's ratio (Koçak *et al.*, 2010; Ludwig *et al.*, 2009) and thus support the non-Redfield ratio of nitrogen to phosphorus for these seasons. In summer, although the lowest average value was detected in the summer season, quite high values were also obtained in the surface waters of offshore stations. Variations of N:P ratios in summer are either due to biological activities and the fast take-up rate of phosphorus by primary producers (Thingstad and Rassoulzadegan, 1999) or atmospheric input of nutrients (Koçak *et al.*, 2010; Krom *et al.*, 2004).

The silicate: nitrate ratios in the surface waters showed decreasing values in their seasonally arithmetic means in the order fall > summer > spring > winter. The excessive NOx input increases silicate consumption in coastal waters and creates negative pressure on the dominant algae (diatoms) species durability in the region during more extended periods (Maddock & Butler, 1977).

4.2 Biological Parameters

There were significant differences in phytoplankton abundance between seasons and stations. The following respective average values of abundances in surface waters were considered during summer 2018 (227333 cells /l), winter (122159 cells / l), spring (109421 cells/l) and fall (26711 cells/l). When examining phytoplankton abundances, the most prominent stations were the shallow coastal stations 1 and 2 in the east and the stations 25, 24, 29, 26, 20 and 30, which were located near the Göksu River and were directly affected by freshwater inputs. Spatharis *et al*. (2007) have also demonstrated the beneficial effects of riverine inputs that promotes phytoplankton development, similar to our results.

In the study area, diatoms were generally most dominant during the year compared to dinoflagellates and other groups (Eker and Kideyş, 2000, Eker-Develi *et al*., 2003, Kıdeyş *et al*., 1989, Uysal *et al*., 2002, Uysal *et al*., 2008). In shallow continental shelf waters directly affected by river inputs, diatoms predominantly dominated the others (Anderson, 1986). Stations 1, 2 and 3 were directly affected from the Lamas River, and the Erdemli sewage discharge in the east and stations 20, 21, 24-26, 29 and 30 were affected by western currents from the Göksu River formed the dominant and dense areas of the diatoms. One of the main factors enriching phytoplankton in these regions was the terrestrial sources that contain a high amount and variety of nutrient salts. In brief, the excess amount of nitrogen, phosphorus and silicate in their contents causes phytoplankton blooms in nearby coastal areas (Cloern, 1996; Spatharis *et al*., 2007). The abundance of phytoplankton was high in the stations nourished by the Göksu River waters with rich nutrient salts (Spatharis *et al*., 2007). Conversely, in open waters devoid of terrestrial inputs, nutrients are present in trace amounts, and certain small groups (coccolithophores) adapted to live under these conditions were persistent, whereas, dinoflagellate and diatom content remained low (Gregg & Casey, 2007). The change in the quantitative and qualitative characteristics of the offshore phytoplankton was observed most prominently at ETS stations 1 through 11. In these stations, neatly arranged from inshore to offshore, diatom and dinoflagellate contents gradually decreased, and other small groups (specific to open waters) began to dominate towards offshore. The features discussed above also applied to species diversity.

Based on mean values, flora observed in spring (37 species) was most species diverse compared to winter (28 species), summer (26 species) and lastly to fall (24 species). Increased freshwater inputs as well as dissolved nutrients during this period could have favoured more species to flourish in the basin. The number of species seems to be suppressed due to the fact that the temperature of surface waters was still at its highest in the fall period and due to the lack of nutrient salts (Vadrucci *et al*., 2008).

Spring season was more prominent in terms of the number of the species compared to other periods (Armi, Trabelsi, Turki, Béjaoui, & Maïz, 2010). Dinoflagellates were found to be greater in the number of species than diatoms during the three sampling periods in surface waters and were found in equal numbers only in winter. The highest difference was observed in fall. Considering all sampling periods, stations with the most species were ETS-1 and ETS-2 in the eastern part of the sampling area, as well as, station 24 in the impact area of the Göksu River and, at stations 20, 25 and 29 inside and around the Taşucu Bay (Cloern, 1996). Species diversity was significantly lower at stations which were generally affected by oligotrophic open waters (Azov, 1991). In the study area, phytoplankton species were found to be richer and denser, in quantitative and qualitative aspects, compared to open waters in shallow continental shelf waters fed by Göksu river inputs.

Diatoms and dinoflagellates are phytoplankton groups that are dominant worldwide and are, therefore, the most important food sources for the higher trophic levels (Heiskanen, 1998; Beaugrand *et al*., 2014). They both compete for new foods in the spring and can produce spring blooms. Due to the variations in nutritional value, biochemical composition, and phenology of these two groups of organisms, fluctuations in the diatom/dinoflagellate ratio can cause ecosystem-wide results for transferring energy and matter to higher trophic levels. Diatoms quickly turn into high biomass due to the intensive intake of new nutrients (r-strategists), but their flowering quickly decreases, and organisms lose their dominance. Dinoflagellates grow slower than diatoms (Spilling & Markager, 2008; Spilling *et al*., 2014) and can use foods from deeper water layers due to their vertical migration capabilities (K-strategists). They prefer to increase in water temperature (Smayda and Reynolds, 2001). Therefore,

spring blooms have a succession from diatoms to dinoflagellates (Bralewska, 1992; Heiskanen, 1998) and the differences in the timing of this transition have implications for food availability for consumers. In previous studies, the Dia / Dino index obtained by biomass calculation was able to detect the regime shift that occurred in the Baltic Proper in the late 1980s. Diatom dominance and therefore, a high Dia / Dino index is representative in historical data and therefore assumed to reflect functional environmental status (GES) (Wasmund *et al*., 2017). In order to better understand the state of the ecosystem, the abundance data were used in this to calculate Dia / Dino index. Although the abundance data not intended to calculate the standard Dia / Dino index, they provide valuable quantitative information about phytoplankton dominance during spring bloom and therefore can be used to calculate the Dia / Dino index if biomass data are missing (Wasmund, 2017). The Dia/ Dino indices in the surface waters showed decreasing values in the order winter = summer > spring > fall. Except for the fall season, diatoms were dominant group. In fall, co-dominance detected between these two groups of organisms.

The formation of various physical and chemical changes in the marine environment exerts pressure on algae populations, allowing the growth of harmful toxin-producing species that can cause problems in the structure of the ecosystem and public health. These blooms are collectively called Harmful Algae Blooms (HABs). The most significant number of toxic species are found among the dinoflagellates, but evidence has also been provided for some species of diatoms, suggesting those cause HAB formations (Vila & Maso, 2015). The mean abundance of HAB species in the surface waters showed decreasing values in the order spring > summer > winter > fall. As a result of analysis for the whole year, four diatom (mainly *Pseudo-nitzschia* species) and eight dinoflagellate species were identified as HAB species in the study area. From fall to summer, an increase was observed in the frequency of occurrence of HAB species in stations.

Shannon (diversity H') and Pielou (regularity J') values were calculated for each period. The Shannon diversity index considers the number of species as well as their frequency within the total number of species (Pielou, 1966). The Pielou regularity (J') index represents the ratio of observed diversity to maximum diversity. If the

distribution of species within the total frequency was homogeneous, it reaches the highest value of one, and if there are species that dominates to individuals, the values begin to decrease (Bandeira, Jamet, Jamet, & Ginoux, 2013). Shannon index values were generally observed at their highest levels in spring, where the number of species were greatest, followed by fall, winter and summer, respectively. The same applied to Pielou regularity (J') index values. In the case, if there are dominant species present within the community, the values tend to become smaller.

4.3 Statistical Analysis

4.3.1 Spearman Rank-Order Correlation

In fall, a high positive correlation was found between phytoplankton abundance and surface water temperature, and a strong negative correlation with salinity and density. However, no relationship was observed regarding different concentrations of nutrient salts. In winter, there was no relationship observed between abundance and surface temperature and salinity. There was a negative correlation with density and Si: N-ratio, while a positive correlation between nutrient salts as nitrate and silicate and N: P-ratio were present. In spring, a notable negative relationship with salinity and Si: N-ratio, and positive relationship with phosphate and nitrate were found. In summer, a significant negative correlation was found between surface phytoplankton abundance and salinity and temperature. Additionally, a positive correlation was found with phosphate.

4.3.2 MDS

Phytoplankton patchiness based on affinities between sites (stations) varied in time and space in the study area. For example, in fall, and winter, spring, summer periods, 10, 8, 2 and 3 different patches were observed respectively. Despite the very complex affinities observed within various minor patches observed in fall and winter, surface flora have split into two major, namely coastal & offshore, and east & west subpopulations in spring and summer. The presence of different characteristics (near

shore, continental shelf, open waters, Gulf, river impact areas, domestic inputs) within the area covered by stations naturally led to the quantitative and qualitative differentiation of populations. Most of the ETS stations in the east affected from the nearby Lamas creek and Erdemli wastewater outlet have displayed very diverse and rich flora. Open waters generally contained least number of diatoms and dinoflagellates where prymnesiofit *Emiliania huxleyi* and cryptofit *Hillea fusiformis* were generally abundant.

In general, the area affected by the Göksu River separated markedly from the surrounding areas in terms of population abundance and species variety, especially the inner Tasucu Bay waters. For instance, in fall, stations 16 and 20 directly affected by Göksu River waters conveyed by western fluxes constituted a different group than the others. Station 24 in the Taşucu Bay, also under the influence of the Göksu River, formed a separate group by itself. Similarly, with the increase in Göksu flow rate in winter, the freshwater distribution area expanded from the surface to the west and separated stations 16, 20,24,25,29 and 33 as a different group from the others. It is plausible that dilution of freshwaters originating from the Göksu River to the west with the prevailing currents in the region is a major factor in patchiness. The size of the patch in the Göksu River area is controlled mainly by the residence time and flow rate of freshwater coming from Göksu River. This situation occurs most clearly in Taşucu Bay. Freshwaters from the Göksu River input reaching the surface waters of the Gulf are capable of staying there for a long enough time to provide sufficient acclimatisation period for the development of phytoplankton.

5. CONCLUSION

In conclusion, the following are the major outputs reached throughout the study;

- Göksu River and Lamas creek are the two major land-based sources that control the success of phytoplankton in the study area,
- The study area contained contrasting water masses including Göksu River estuary, productive coastal, mesotrophic shelf and oligotrophic offshore waters,
- Nutrient-rich freshwater inputs from both sources encouraged phytoplankton growth significantly in their surrounding areas,
- Having optimal freshwater residence times Taşucu Bay waters always displayed the maximal population densities,
- Freshwater inputs have displayed long-lasting impacts (from winter till summer) over phytoplankton growth in the study area,
- A sharp contrast did exist between the coastal sector enhanced by river inputs and the offshore waters devoid of essential nutrients for algal development,
- Shelf waters of the study area were partly subjected to enhanced flora inputs from the Mersin Bay via the westward flowing Asia Minor Current regime,
- Total number of 246 phytoplankton species belonging to Bacillariophyceae (79), Pyrrophyceae (146), Prymnesiophycea (16), Cryptophyceae, Chrysophycea, Euglenophycea, Ebriophyceae, Chlorophyceae (with single species each) were identified,
- The community was found most diverse during spring followed by winter, summer and fall,
- Based on seasonal surface mean cell abundances, summer population abundances exceeded much the winter, spring and lastly fall population densities,
- Diatoms were the dominating group over dinoflagellates and remaining other groups throughout the study period,
- Flora was found most species diverse and abundant in shallow coastal areas fed by nutrient-rich Göksu river and Lamas creek waters,

- The Dia/ Dino index values in the surface waters was the highest in winter and summer followed by spring and fall. Except for the fall season, diatoms were dominating group.
- The HAB species in the surface waters were most abundant in spring followed by summer, winter and fall. For the whole year, four diatom (mainly *Pseudo-nitzschia* species) and eight dinoflagellate species were identified as HAB species. From fall to summer, the frequency of occurrence of HAB species in stations increased.
- Similar to Pielous' index values Shannon diversity index values were found maximal during spring followed in decreasing order by fall, winter and summer,
- Based on the Spearman Rank Correlation analysis, highly significant positive correlation between surface phytoplankton abundance and ambient temperature and negative correlation with surface salinity whereas almost no correlation with any of nutrient species were observed in fall,
- In contrast, highly significant positive correlations were only present with nutrients (nitrate, nitrite, silicate) and N:P -ratio in winter, also, negative correlation was found with Si: N-ratio in this season,
- Despite a highly significant negative correlation with salinity and Si: N-ratio, highly significant positive correlations with phosphate, nitrate, nitrite were observed in spring,
- In summer, a highly significant negative correlation between phytoplankton abundance and salinity & temperature and a significant positive relationship with phosphate were observed,
- The number of patches observed in fall (10) and in winter (8) have exceeded greatly those observed in spring (2) and summer (3),
- Despite the very complex affinities observed within various minor patches observed in fall and winter, surface flora have split into two major, namely coastal & offshore, and east & west subpopulations in spring and summer.

REFERENCES

Adger, W. N., Hughes, T. P., Folke, C., Carpenter, S. R., & Rockström, J. (2005, August 12). Social-ecological resilience to coastal disasters. *Science*, Vol. 309, pp. 1036–1039. https://doi.org/10.1126/science.1112122.

Akçay, İ., & Tuğrul, S. (2018, October). Riverine nutrient inputs to the Mersin Bay, northeastern Mediterranean. In *International Marine & Freshwater Sciences Symposium Proceedings (MARFRESH2018)*. *Project*, (104Y277).

Anderson, G. F. (1986). Silica, diatoms and a freshwater productivity maximum in Atlantic Coastal Plain estuaries, Chesapeake Bay. *Estuarine, Coastal and Shelf Science*, *22*(2),183–197. https://doi.org/10.1016/0272-7714(86)90112-5.

Armi, Z., Trabelsi, E., Turki, S., Béjaoui, B., & Maïz, N. Ben. (2010). Seasonal phytoplankton responses to environmental factors in a shallow Mediterranean lagoon. *Journal of Marine Science and Technology*, *15*(4), 417–426. https://doi.org/10.1007/s00773-010-0093-y.

Avşar D., Polat S., Işık O., 1998. Phytoplankton species of the Yumurtalık bay, (Adana), (in Turkish). XIV National Biology Congress, 7-10 September 1998 Samsun. Organised by Ondokuz Mayıs University, Art & Sciences faculty, Biology Department, Volume II, pp: 227-239.

Azov, Y. (1991). Eastern Mediterranean—A marine desert? *Marine Pollution Bulletin - MAR POLLUT BULL*, *23*, 225–232. https://doi.org/10.1016/0025-326X(91)90679-M.

Bandeira, B., Jamet, J. L., Jamet, D., & Ginoux, J. M. (2013). Mathematical convergences of biodiversity indices. *Ecological Indicators*. https://doi.org/10.1016/j.ecolind.2013.01.028.

Beaugrand, G., Harlay, X., & Edwards, M. (2014). Detecting plankton shifts in the North Sea: a new abrupt ecosystem shift between 1996 and 2003. Marine Ecology Progress Series, 502, 85-104.

Bergamasco, A., & Malanotte-Rizzoli, P. (2010). The circulation of the Mediterranean Sea: a historical review of experimental investigations. *Advances in Oceanography and Limnology*, *1*(1), 11–28. https://doi.org/10.1080/19475721.2010.491656.

Béthoux, J.P., P. Morin, C. Chaumery, O. Connan, B. Gentili, D. Ruiz-Pino, (1998). Nutrients in the Mediterranean Sea, mass balance and statistical analysis of concentrations with respect to environmental change. Marine Chemistry 63: 155-169

Bralewska, J. M. (1992). "Cyclic seasonal fluctuations of the phytoplankton biomass and composition in the Gdansk Basin in 1987-1988," in ICES Council Meeting/L:15 (Rostock-Warnemünde), 1–40. Available online at: http://www.ices.dk/sites/pub/CM%20Doccuments/1992/L/1992_L15.pdf

Cloern, J. E. (1996). Phytoplankton bloom dynamics in coastal ecosystems: A review with some general lessons from sustained investigation of San Francisco Bay, California. *Reviews of Geophysics*, *34*(2), 127–168. https://doi.org/10.1029/96RG00986.

Çoban-Yıldız, Y., Tuğrul, S., Ediger, D., Yılmaz, A., Polat, S.Ç., 2000. A comparative study on the abundance and elemental composition of POM in three interconnected basins: The Black, the Marmara and the Mediterranean Seas. Mediterranean Marine Science, 1/1, 51-63.

Corcoran, A. A., & Boeing, W. J. (2012). Biodiversity Increases the Productivity and Stability of Phytoplankton Communities. *PLoS ONE*, *7*(11), e49397. https://doi.org/10.1371/journal.pone.0049397.

Demirel, Z. (2010). The Influence of Seawater on a Coastal Aquifer in an International Protected Area, Göksu Delta Turkey. *Journal of Water Resource and Protection*. https://doi.org/10.4236/jwarp.2010.27075.

Drebes, G. (1974). *Marines Phytoplankton: eine Auswahl der Helgoländer Planktonalgen (Diatomeen, Peridineen)* Stuttgard., 186 p.

Dugdale, R. C., & Wilkerson, F. P. (1988). Nutrient sources and primary production in the Eastern Mediterranean. *Oceanol. Acta*, *9*, 179-184.

Eker, E., Kideyş A.E., (2000). Weekly variations in phytoplankton community structure of a harbour in Mersin Bay (north-eastern Mediterranean), Turkish Journal of Botany, 24, 13-24.

Eker-Develi, E., Kideyş, A.E., Tuğrul, S., Yılmaz, D., Ediger, D., (2003). Phytoplankton dynamics in the Northeastern Mediterranean with respect to relative dust deposition A. Yılmaz (Ed.), Proceedings of the Second International Conference on "Oceanography of the Eastern Mediterranean and Black Sea: Similarities and Differences of Two Interconnected Basins", 14–18 October 2002, METU Cultural and Convention Center, Tubitak Publ., Ankara, Turkey, pp. 686-694.

Fernández, V., Dietrich, D. E., Haney, R. L., & Tintoré, J. (2005). Mesoscale, seasonal and interannual variability in the Mediterranean Sea using a numerical ocean model. *Progress in Oceanography*, *66*(2–4), 321–340. https://doi.org/10.1016/j.pocean.2004.07.010.

Field, J., Clarke, K., & Warwick, R. (1982). A Practical Strategy for Analysing Multispecies Distribution Patterns. *Marine Ecology Progress Series*. https://doi.org/10.3354/meps008037.

Grasshoff, K., Ehrhardt, M., Kremling, K., (1983). Determination of nutrients. In: Methods of Seawater Analysis (2nd ed.), Verlag Chemie Gmbh, Weiheim, Germany, pp. 125-188.

Gregg, W. W., & Casey, N. W. (2007). Modeling coccolithophores in the global oceans. *Deep-Sea Research Part II: Topical Studies in Oceanography*, *54*(5–7), 447–477. https://doi.org/10.1016/j.dsr2.2006.12.007.

Harris, G. P. (1988). Phytoplankton ecology: Structure, function and fluctuation. *ICES Journal of Marine Science*. https://doi.org/10.1093/icesjms/44.2.210.

Heiskanen, A. S. (1998). Factors governing sedimentation and pelagic nutrient cycles in the northern Baltic Sea: Finnish environment institute.Monogr. Boreal Environ. Res. 8, 1–80.

Hillmer, I., van Reenen, P., Imberger, J., & Zohary, T. (2008). Phytoplankton patchiness and their role in the modelled productivity of a large, seasonally stratified lake. *Ecological Modelling*, *218*(1–2), 49–59. https://doi.org/10.1016/J.ECOLMODEL.2008.06.017.

Justić, D., Rabalais, N. N., Turner, R. E., & Dortch, Q. (1995). Changes in nutrient structure of river-dominated coastal waters: Stoichiometric nutrient balance and its consequences. *Estuarine, Coastal and Shelf Science*. https://doi.org/10.1016/S0272-7714(05)80014-9.

Kamel, M. S. (1999). *Seasonal Variability of Surface Current in the Eastern Mediterranean Sea*. Bulletin of National Institute of Oceanography and Fisheries, Alexandria, Egypt. Vol (25): 51-67.

Kideyş A E., Ünsal M., and F. Bingel, (1989). Seasonal changes in net phytoplankton off Erdemli, norteastern Mediterranean, DOĞA, Turkish Journal of Botany, 13(1), 45-54.

Koçak, M., Kunilay, N., Tuğrul, S., Mihalopoulos, N.,(2010). Atmospheric nutrient inputs to the northern levantine basin from a long-term observation: sources and comparison with riverine inputs. Biogeosciences 7: 4037-4050

Koçak, M. (2016). Atmospheric Input of Inorganic Macro-Nutrients in the Eastern Mediterranean: Ramifications Regarding Marine Productivity. *The Turkish Part of the Mediterranean Sea*, 612, pp 30-37.

Kress, N., & Herut, B. (2001). Spatial and seasonal evolution of dissolved oxygen and nutrients in the Southern Levantine Basin (Eastern Mediterranean Sea): Chemical characterization of the water masses and inferences on the N : P ratios. *Deep-Sea Research Part I: Oceanographic Research Papers*, *48*(11), 2347–2372. https://doi.org/10.1016/S0967-0637(01)00022-X.

Kress, N., Thingstad, T. F., Pitta, P., Psarra, S., Tanaka, T., Zohary, T., ... & Rassoulzadegan, F. (2005). Effect of P and N addition to oligotrophic Eastern Mediterranean waters influenced by near-shore waters: a microcosm experiment. *Deep Sea Research Part II: Topical Studies in Oceanography*, *52*(22-23), 3054-3073.

Krom, M. D., Kress, N., Brenner, S., & Gordon, L. I. (1991). Phosphorus limitation of primary productivity in the eastern Mediterranean Sea. *Limnology and Oceanography*. https://doi.org/10.4319/lo.1991.36.3.0424.

Krom, M. D., Herut, B., & Mantoura, R. F. C. (2004). Nutrient budget for the Eastern Mediterranean: Implications for phosphorus limitation. *Limnology and Oceanography*, *49*(5), 1582-1592.

Krom, M. D., Emeis, K.-C., & Van Cappellen, P. (2010). Why is the Eastern Mediterranean phosphorus limited? *Progress in Oceanography*, *85*(3–4), 236–244. https://doi.org/10.1016/J.POCEAN.2010.03.003.

Lacombe H Gascard Jc, G. J. B. J. (1981). Response of the mediterranean to the water and energy fluxes across its surface, on seasonal and interannual scales (Gauthier-Villars, Ed.). *Oceanologica Acta*, Vol. 4, pp. 247–255. Retrieved from https://archimer.ifremer.fr/doc/00121/23209/.

Lane, R. R., Day, J. W., Marx, B. D., Reyes, E., Hyfield, E., & Day, J. N. (2007). The effects of riverine discharge on temperature, salinity, suspended sediment and chlorophyll a in a Mississippi delta estuary measured using a flow-through system. *Estuarine, Coastal and Shelf Science*, *74*(1–2), 145–154. https://doi.org/10.1016/j.ecss.2007.04.008.

Lawton, J. H. (1998). Daily, G. C. (Ed.). 1997. Nature's services. Societal dependence on natural ecosystems. Island Press, Washington, DC. 392 pp. ISBN 1-55963-475-8 (hbk), 1 55963 476 6 (soft cover). *Animal Conservation*. https://doi.org/10.1017/s1367943098221123.

Ludwig, W., Dumont, E., Meybeck, M., & Heussner, S. (2009, March). River discharges of water and nutrients to the Mediterranean and Black Sea: Major drivers for ecosystem changes during past and future decades? *Progress in Oceanography*, Vol. 80, pp. 199–217. https://doi.org/10.1016/j.pocean.2009.02.001.

Maddock, L., & Butler, E. I. (1977). The influence of biological activity and physical stability in determining the chemical distributions of inorganic phosphate, silicate and nitrate. *Journal of the Marine Biological Association of the United Kingdom*, *57*(4), 1065–1073. https://doi.org/10.1017/S0025315400026138.

Malanotte-Rizzoli, P. (2001). Current Systems in the Mediterranean Sea. In *Encyclopedia of Ocean Sciences: Second Edition* (pp. 744–751). https://doi.org/10.1016/B978-012374473-9.00375-1.

Malanotte-Rizzoli, P., Artale, V., Borzelli-Eusebi, G. L., Brenner, S., Crise, A., Gacic, M., … Triantafyllou, G. (2014). Physical forcing and physical/biochemical variability of the Mediterranean Sea: A review of unresolved issues and directions for future research. *Ocean Science*, *10*(3), 281–322. https://doi.org/10.5194/os-10-281-2014.

Margat, J., & Treyer, S. (2004). L'eau des méditerranéens: situation et perspectives, Ministère de l'écologie et du développement durable, Agence de l'eau Rhône-Méditerranée-Corse. *PNUE/PAM, Sophia-Antipolis, 347p*.

Martin, J. M., Elbaz-Poulichet, F., Guieu, C., Loÿe-Pilot, M. D., & Han, G. (1989). River versus atmospheric input of material to the mediterranean sea: an overview. *Marine Chemistry*, *28*(1–3), 159–182. https://doi.org/10.1016/0304-4203(89)90193-X.

McGill, D. A. (1965). The relative supplies of phosphate, nitrate and silicate in the Mediterranean Sea. In *Rapport des Procès Verbaux des Réunions de la CIESM*.

Millot, C., Candela, J., Fuda, J. L., & Tber, Y. (2006). Large warming and salinification of the Mediterranean outflow due to changes in its composition. *Deep Sea Research Part I: Oceanographic Research Papers*, *53*(4), 656-666.

Murphy, L. S. and Haugen, E. M., (1985). The distribution and abundance of phototrophic ultraplankton in the north Atlantic. Limnology and oceanography. 30, 47-58.

Özsoy, E., Hecht, A., & Ünlüata, Ü. (1989). Circulation and hydrography of the Levantine Basin. Results of POEM coordinated experiments 1985-1986. *Progress in Oceanography*, *22*(2), 125–170. https://doi.org/10.1016/0079-6611(89)90004-9.

Parsons, E. C. M., Favaro, B., Aguirre, A. A., Bauer, A. L., Blight, L. K., Cigliano, J. A., … Sutherland, W. J. (2014). Seventy-One Important Questions for the Conservation of Marine Biodiversity. *Conservation Biology*, *28*(5), 1206–1214. https://doi.org/10.1111/cobi.12303.

Pavillard, J. (1925). *Bacillariales*: Report on the Danish Oceanographical Expeditions 1908-1910 to the Mediterranean and Adjacent seas. *Biology,* 2, 72 p.

Pielou, E. C. (1966). Shannon's Formula as a Measure of Specific Diversity: Its Use and Misuse. *The American Naturalist*, *100*(914), 463–465. https://doi.org/10.1086/282439.

Polat S, Sarıhan E., (2000). Seasonal changes in the phytoplankton of the northeastern Mediterranean (bay of İskenderun), Turkish Journal of Botany, 24, 1-12.

Polat, S.Ç., Tuğrul, S., (1995). Nutrient and organic carbon exchanges between the Black and Marmara Seas through the Bosporus Strait. Continental Shelf Research, 15, 1115-1132.

Pomati, F., Jokela, J., Simona, M., Veronesi, M., & Ibelings, B. W. (2011). An Automated Platform for Phytoplankton Ecology and Aquatic Ecosystem Monitoring. *Environmental Science & Technology*, *45*(22), 9658–9665. https://doi.org/10.1021/es201934n.

Poulos, S. E., Drakopoulos, P. G., & Collins, M. B. (1997). Seasonal variability in sea surface oceanographic conditions in the Aegean Sea (Eastern Mediterranean): An overview. *Journal of Marine Systems*, *13*(1–4), 225–244. https://doi.org/10.1016/S0924-7963(96)00113-3.

Rampi, L., & Bernhard, M. (1978). *Key for the determination of Mediterranean pelagic diatoms*, (Comitato Nazionale Energia Nucleare, Dipartimento Radiazioni e Richerche di Scurezza e Protezione, Fiascherio) RT/BIO (78)1, 71p.

REDFIELD, A. C. (1960). The biological control of chemical factors in the environment. *Science Progress*.

Robinson, A. R., Malanotte-Rizzoli, P., Hecht, A., Michelato, A., Roether, W., Theocharis, A., Ünlüata, …, Osman, M. (1992). General circulation of the Eastern Mediterranean. *Earth Science Reviews*, *32*(4), 285–309. https://doi.org/10.1016/0012-8252(92)90002-B.

Sakalli, A., & Başusta, N. (2018). Sea surface temperature change in the Mediterranean Sea under climate change: A simulation of the sea surface temperature up to 2100. *International Journal of Climatology*, *38*(13), 4687–4698. https://doi.org/10.1002/joc.5688.

Salihoğlu, I., Saydam, C., Baştürk, Ö., Yilmaz, K., Göçmen, D., Hatipoğlu, E., & Yilmaz, A. (1990). Transport and distribution of nutrients and chlorophyll-a by mesoscale eddies in the northeastern Mediterranean. *Marine Chemistry*. https://doi.org/10.1016/0304-4203(90)90024-7.

Smayda, T. J., & Reynolds, C. S. (2001). Community assembly in marine phytoplankton: application of recent models to harmful dinoflagellate blooms. *Journal of plankton research*, *23*(5), 447-461.

Soukissian, T., Denaxa, D., Flora, K., Prospathopoulos, A., Sarantakos, K., Iona, A., Georgantas, K., Mavrakos, S. (2017). Marine Renewable Energy in the Mediterranean Sea: Status and Perspectives. *Energies*, *10*. https://doi.org/10.3390/en10101512.

Spatharis, S., Tsirtsis, G., Danielidis, D. B., Chi, T. Do, & Mouillot, D. (2007). Effects of pulsed nutrient inputs on phytoplankton assemblage structure and blooms in an enclosed coastal area. *Estuarine, Coastal and Shelf Science*, *73*(3–4), 807–815. https://doi.org/10.1016/j.ecss.2007.03.016.

Spilling, K., and Lindström, M. (2008). Phytoplankton life cycle transformations lead to species-specific effects on sediment processes in the Baltic Sea. Cont. Shelf Res. 17, 2488–2495. doi: 10.1016/j.csr.2008.07.004

Spilling, K., Kremp, A., Klais, R., Olli, K., and Tamminen, T. (2014). Spring bloom community change modifies carbon pathways and C: N: P: Chl a stoichiometry of coastal material fluxes. Biogeosci. Discuss. 11, 7275–7289. doi: 10.5194/bg-11-7275-2014

Strickland, J.D.H., Parsons, T.R., (1972). A Practical Handbook of Seawater Analysis, 2nd edition. Bulletin of the Fisheries Research Board of Canada, No.167, 310 p.

Sykes, J. (1981). *An illustrated guide to the diatoms of British coastal plankton*. Field studies 5, 425-468.

T.C.Orman ve Su İşleri Bakanlığı. (2013). *Yukari havza sel kontrolü eylem planı 2013-2017*. 117. Retrieved from: https://www.ogm.gov.tr/ekutuphane/Yayinlar/Yukar%C4%B1%20Havza%20Sel%20Kontrol%C3%BC%20Eylem%20Plan%C4%B1.pdf (Last Accessed 05/01/2020).

Thingstad, T. F., & Rassoulzadegan, F. (1999). Conceptual models for the biogeochemical role of the photic zone microbial food web, with particular reference to the Mediterranean Sea. *Progress in Oceanography*, *44*(1-3), 271-286

Tornés, E., Pérez, M. C., Durán, C., & Sabater, S. (2014). Reservoirs override seasonal variability of phytoplankton communities in a regulated Mediterranean river. *Science of the Total Environment*, *475*, 225–233. https://doi.org/10.1016/j.scitotenv.2013.04.086.

Trégouboff, G., & Rose, M. (1957). *Manuel de planctonologie méditerranéennetexto*. Retrieved from http://www.sidalc.net/cgi-bin/wxis.exe/?IsisScript=sibe01.xis&method=post&formato=2&cantidad=1&expresion=mfn=009591.

Turner, R. E., Rabalais, N. N., Justic', D., & Dortch, Q. (2003). Future aquatic nutrient limitations. *Marine Pollution Bulletin*, *46*(8), 1032–1034. https://doi.org/10.1016/S0025-326X(03)00049-3.

UNEP/MAP, 2005. Sampling and analysis techniques for the eutrophication monitoring strategy of MED POL, MAP Technical Reports Series No. 163, Athens.

Uysal, Z. (2016). A Bacterioplankton, Cyanobacteria, Phytoplankton. *The Turkish Part of the Mediterranean Sea*, 612, pp. 79-93.

Uysal Z., Iwataki M., T., Koray. 2003. On the presence of *Heterocapsa pygmaea* Loeblich III, Schmidt & Sherley 1981 (Peridiniales Haeckel 1894b, Dinophyceae Pascher 1914) in the northern Levantine basin (eastern Mediterranean), Doğa, Turkish Journal of Botany, 27, 149-152.

Uysal, Z., Latif, M.A., Özsoy, E., Tuğrul, S., Kubilay, N., Beşiktepe, Ş.T., Yemenicioğlu, S., Mutlu, E., Ediger, D., Beşiktepe, Ş., Ediger, V., Ak Örek, Y., Örek, H., Demirel, M., Tunç, Ş.Ç., Terbıyık, T., (2008). Circulation, transport and eutrophication investigations in the Cilician basin coastal ecosystem, (in Turkish), TÜBİTAK project no: 104Y277 Mersin, Turkey, Pp. 520.

Uysal, Z., Senichkina, L., Kuzmenko, L., Georgieva, L., and Altukhov, D., 2003. Weekly changes in phytoplankton species composition, diversity, abundance, and biomass across the northern Levantine basin shelf waters. In Proceedings of the Second International Conference on "Oceanography of the Eastern Mediterranean and Black Sea: Similarities and Differences of Two Interconnected Basins". Yılmaz, A. (ed.) 14–18 October 2002. METU Cultural and Convention Center, Tubitak Publishers, Ankara, Turkey. 680-686.

Vadrucci, M. R., Sabetta, L., Fiocca, A., Mazziotti, C., Silvestri, C., Cabrini, M., … Basset, A. (2008). Statistical evaluation of differences in phytoplankton richness and abundance as constrained by environmental drivers in transitional waters of the Mediterranean basin. *Aquatic Conservation: Marine and Freshwater Ecosystems*, *18*(S1), S88–S104. https://doi.org/10.1002/aqc.951.

Vila, M., & Masó, M. (2005). Phytoplankton functional groups and harmful algae species in anthropogenically impacted waters of the NW Mediterranean Sea. Scientia Marina, 69(1), 31-45.

Wasmund, N., Topp, I., Schories, D., 2006. Optimizing the storage and extraction of chlorophyll samples, OCEANOLOGIA, 48 (1), pp. 125–144.

Wasmund, N., Kownacka, J., Göbel, J., Jaanus, A., Johansen, M., Jurgensone, I., ... & Powilleit, M. (2017). The Diatom/Dinoflagellate Index as an indicator of ecosystem Changes in the Baltic Sea 1. Principle and handling instruction. Frontiers in Marine Science, 4, 22.

Wasmund, N. (2017). The Diatom/Dinoflagellate Index as an indicator of ecosystem changes in the Baltic Sea. 2. Historical data for use in determination of good environmental status. Frontiers in Marine Science, 4, 153.

Yılmaz D., Ediger, D., Eker Develi E., A.E., Kideyş. 2003. Taxonomic composition and pigments of phytoplankton in the Northern Levantine Basin, p. 715-719. In Yılmaz A., (ed.), Oceanography of the Eastern Mediterranean and Black Sea. TÜBİTAK Publisher. Ankara, Turkey.

Yılmaz, A., & Tuğrul, S. (1998). The effect of cold- and warm-core eddies on the distribution and stoichiometry of dissolved nutrients in the northeastern Mediterranean. *Journal of Marine Systems*, *16*(3–4), 253–268. https://doi.org/10.1016/S0924-7963(97)00022-5.

Yücel, N.,(2013). Monthly changes in primary and bacterial productivity in the north-eastern Mediterranean shelf waters. PhD-Thesis in the department of marine biology and fisheries at METU-IMS, Erdemli

APPENDIX

Table 22 Identified species list for all season.

Bacillariophyceae	
Amphiprora gigantea Grunow	*Gyrosigma balticum* (Ehrenberg) Rabenhorst
Amphiprora sp. Ehrenberg	*Gyrosigma* sp. Hassall
Asterionella japonica Cleve	*Haslea wawrikae* (Hustedt) Simonsen
Asterolampra marylandica Ehrenberg	*Hemiaulus hauckii* Grunow in Van Heurck
Asteromphalus flabellatus (Brebisson) Greville	*Lauderia* sp. Cleve
Asteromphalus sp. Ehrenberg	*Leptocylindrus danicus* Cleve
Bacteriastrum delicatulum Cleve	*Leptocylindrus mediterraneus* (H. Peragallo) Hasle
Bacteriastrum hyalinum Lauder	*Leptocylindrus minimus* Gran
Biddulphia sp. Gray	*Licmophora* sp. Agardh
Cerataulina pelagica (Cleve) Hendey	*Lioloma pacificum* (Cupp) Hasle
Chaetoceros affinis Lauder	*Lithodesmium undulatum* Ehrenberg
Chaetoceros anastomosans Grunow	*Meuniera membranacea* (Cleve) P. C. Silva
Chaetoceros curvisetus Cleve	*Navicula* sp. Bory
Chaetoceros dadayi Pavillard	*Nitzschia longissima* (Bréb.) Ralfs
Chaetoceros danicus Cleve	*Nitzschia sigmoidea* (Nitzsch) W. Smith
Chaetoceros decipiens Cleve	*Nitzschia* sp. Hassall
Chaetoceros didymus var *protuberans* (Lauder) Gran & Yendo	*Nitzschia tenuirostris* Mer.
Chaetoceros diversus Cleve	*Phaeodactylum tricornutum* Bohlin
Chaetoceros gracilis Schütt	*Pleurosigma normanii* Ralfs *in* Pritchcard
Chaetoceros lauderi Ralfs in Lauder	*Pleurosigma* sp. W. Smith
Chaetoceros peruvianus Brightwell	*Proboscia alata* (Brightwell) Sundström
Chaetoceros rostratus Lauder	*Proboscia alata* forma *gracillima* (Brightwell) Sundström
Chaetoceros similis Cleve	*Proboscia alata* forma *indica* (H. Peragallo) Licea & Moreno in Moreno
Chaetoceros simplex Meunier	*Pseudo-nitzschia delicatissima* (Cleve) Heiden in Heiden and Kolbe
Chaetoceros socialis Lauder	*Pseudo-nitzschia multistriata* (H.Takano) H.Takano
Chaetoceros sp. Ehrenberg	*Pseudosolenia calcar-avis* (Schultze) B.G.Sundström
Chaetoceros teres Cleve	*Pseudo-nitzschia seriata* (Cleve) H. Perag. in H. Perag. and Perag.
Chaetoceros tetrastichon Cleve	*Rhizosolenia robusta* G.Norman ex Ralfs
Chaetoceros tortissimus Gran	*Rhizosolenia stolterfothii* H.Peragallo
Coscinodiscus sp. Ehrenberg	*Rhizosolenia styliformis* Brightwell
Cylindrotheca closterium (Ehrenberg) Reimann & Lewin	*Skeletonema costatum* (Grev.) Cleve
Cymbella sp. Agardh	*Synedra ulna* (Nitzsch) Ehrenberg

Table 22 *(Continued)*	
Dactyliosolen blavyanus Hasle	*Thalassionema nitzschioides* (Grunow) Van Heurck
Dactyliosolen fragilissimus (Bergon) Hasle	*Thalassiosira decipiens* (Grunow ex Van Heurck) E.G.Jørgensen
Dactyliosolen sp Castracane	*Thalassiosira* sp. Cleve
Diploneis sp. Ehrenberg ex Cleve	*Thalassiothrix frauenfeldii* Grunow
Eucampia cornuta (Cleve) Grunow	*Thalassiothrix longissima* Cleve and Grunow
Fragilaria sp. Lyngbye	*Thalassiothrix* sp. Cleve and Grunow
Guinardia flaccida (Castracane) H. Perag.	*Tropidoneis* sp. Cleve
Guinardia striata (Stolterfoth) Hasle	
Pyrrophyceae	
Amphidinium sp. Claparède and Lachmann	*Kofoidinium velleloides* Pavillard
Asterodinium gracile Sournia	*Micracanthodinium bacilliferum* (Schiller) Deflandre
Azadinium sp. Elbrächter & Tillmann	*Micracanthodinium setiferum* (Lohmann) Deflandre
Brachydinium capitatum F. J. R. Taylor	*Minuscula bipes* (Paulsen) Lebour
Ceratium arcuatum (Gourret) Cleve	*Nematodinium* sp. Kofoid and Swezy
Ceratium candelabrum f. *depressum* (Pouchet) J.Schiller	*Ornithocercus heteroporus* Kofoid
Ceratium candelabrum var. *candelabrum* (Ehrenberg) Stein	*Oxyphysis oxytoxoides* Kofoid
Ceratium contortum var. *karsteni* (Pavill) Sournia	*Oxytoxum adriaticum* Schiller
Ceratium contrarium (Gourret) Pavillard	*Oxytoxum brunellii* Rampi
Ceratium declinatum f. *normale* Jörgensen	*Oxytoxum caudatum* Schiller
Ceratium euarcatum Jörg	*Oxytoxum constrictum* (F.Stein) Bütschli
Ceratium extensum (Gourret) Cleve	*Oxytoxum coronatum* Schiller
Ceratium falcatum (Kofoid) Jörgensen	*Oxytoxum crassum* Schiller
Ceratium fusus var. *seta* (Ehrenberg) E.J.F.Wood	*Oxytoxum curvatum* (Kofoid) Kofoid
Ceratium gibberum var. *dispar* (Pouchet) Sournia	*Oxytoxum depressum* J.Schiller
Ceratium hexacanthum aestuarium (Schroder) J.Schiller	*Oxytoxum globosum* Schiller
Ceratium horridum horridum (Cleve) Gran	*Oxytoxum gracile* Schiller
Ceratium horridum var. *buceros* (Zacharias) Sournia	*Oxytoxum longiceps* Schiller
Ceratium macroceros var. *gallicum* (Kofoid) Peters	*Oxytoxum longum* Schiller
Ceratium macroceros var. *macroceros* (Ehrenberg) Vanhöffen	*Oxytoxum mediterraneum* Schiller
Ceratium pentagonum var. *tenerum* Jörgensen	*Oxytoxum milneri* G.Murray & Whitting
Ceratium symmetricum coarctatum (Pavillard) Graham & Bronikovsky	*Oxytoxum minutum* Rampi
Ceratium teres Kofoid	*Oxytoxum mitra* (Stein) Schiller
Ceratium trichoceros (Ehrenberg) Kofoid	*Oxytoxum ovale* Schiller
Ceratium tripos (O. F. Müller) Nitzsch	*Oxytoxum rampii* Sournia
Ceratium tripos var. *atlanticum* Ostenfeld	*Oxytoxum sceptrum* (Stein) Schröder
Ceratium tripos var. *pulchellum* (Schröder) López	*Oxytoxum scolopax* Stein

Table 22 *(Continued))*	
Ceratoperidinium falcatum (Kofoid & Swezy) Reñé & Salas	*Oxytoxum* sp. Stein
Ceratoperidinium margalefii A.R.Loeblich III	*Oxytoxum sphaeroideum* Stein
Cladopyxis brachiolata F.Stein	*Oxytoxum spinosum* Rampi
Cladopyxis caryophyllum (Kofoid) Pavillard	*Oxytoxum tesselatum* (Stein) Schütt
Cochlodinium polykrikoides Margalef	*Oxytoxum variabilis* Schiller
Cochlodinium pulchellum Lebour	*Oxytoxum viride* Schiller
Cochlodinium sp. Schütt	*Peridinium bipes* Stein
Dinophysis fortii Pavillard	*Peridinium breve* (Paulsen) Paulsen
Dinophysis hastata F.Stein	*Peridinium diabolus* Cleve
Dinophysis ovata Claparéde & Lachmann	*Peridinium heterocanthum* (Dangeard) Balech
Dinophysis ovum F.Schütt	*Peridinium minusculum* Pavillard
Dinophysis parva J.Schiller	*Peridinium* sp. Ehrenberg
Dinophysis parvula (F.Schütt) Balech	*Peridinium steinii* Jörgensen
Dinophysis pusilla Jörgensen	*Phalacroma mitra* Schütt
Dinophysis sp. Ehrenberg	*Phalacroma rapa* Jorgensen
Gonyaulax monocantha Pavillard	*Phalacroma rotundatum* (Claparède and Lachmann) Kofoid
Gonyaulax monospina Rampi	*Podolampas bipes* Stein
Gonyaulax polygramma Stein	*Podolampas palmipes* Stein
Gonyaulax scrippsae Kofoid	*Podolampas spinifer* Okamura
Gonyaulax sp. Diesing	*Polykrikos kofoidi* Chatton
Gonyaulax spinifera (Clap. and J. Lachm.) Diesing	*Polykrikos* sp. Chatton
Gonyaulax verior Sournia	*Pronoctiluca pelagica* Fabre-Domergue
Gymnodinium abbreviatum Kofoid & Swezy	*Prorocentrum aporum* (Schiller) Dodge
Gymnodinium fuscum (Ehrenberg) F. Stein	*Prorocentrum compressum* (Bailey) Abé ex Dodge
Gymnodinium fusiforme Kofoid & Swezy	*Prorocentrum dactylus* (Stein) Dodge
Gymnodinium heterostriatum Kofoid & Swezy	*Prorocentrum dentatum* Stein
Gymnodinium mikimotoi Miyake and Kominami ex Oda	*Prorocentrum gracile* Schütt
Gymnodinium placidum E.C.Herdman	*Prorocentrum lima* (Ehrenberg) Dodge
Gymnodinium sanguineum Hirasaka	*Prorocentrum micans* Ehrenberg
Gymnodinium sp. Stein	*Prorocentrum minimum* (Pavillard) Schiller
Gyrodinium corallinum Kofoid & Swezy	*Prorocentrum ovum* (Schiller) Dodge
Gyrodinium estuariale E.M.Hulbert	*Prorocentrum rotundatum* Schiller
Gyrodinium fusiforme Kofoid & Swezy	*Prorocentrum* sp. Ehrenberg
Gyrodinium fusus (Meunier) Akselman	*Prorocentrum vaginulum* (Ehrenberg) Dodge
Gyrodinium lachryma (Meunier) Kofoid & Swezy	*Protoperidinium crassipes* (Kofoid) Balech
Gyrodinium sp. Kofoid and Swezy	*Protoperidinium divergens* (Ehrenberg) Balech
Gyrodinium spirale (Bergh) Kofoid & Swezy	*Pyrophacus horologium* Stein
Heterocapsa sp. Stein	*Pyrophacus steinii* (Schiller) Wall and Dale
Heterocapsa triquetra (Ehrenberg) Stein	*Scrippsiella trochoidea* (Stein) Balech ex Loeblich III

Table 22 *(Continued)*	
Karenia mikimotoi (Miyake & Kominami ex Oda) Gert Hansen & Moestrup	*Spatulodinium pseudonoctiluca* (Pouchet) J.Cachon & M.Cachon
Karenia papilionacea A.J.Haywood & K.A.Steidinger	*Torodinium robustum* Kofoid and Swezy
Karenia sp. Gert Hansen & Moestrup	*Torodinium teredo* (Pouchet) Kofoid & Swezy
Katodinium glaucum (Lebour) A.R.Loeblich III	*Warnovia* sp. Lindemann
Katodinium sp. Fott	*Warnowia polyphemus* (Pouchet) Schiller
Kofoidinium sp. F. J. R. Taylor	*Warnowia pulchra* (J.Schiller) J.Schiller
Kofoidinium splendens J.Cachon & M.Cachon	
Prymnesiophyceae	
Calciosolenia brasiliensis (Lohmann) J.R.Young	*Michaelsarsia* sp. Gran
Calciosolenia murrayi Gran	*Michaelsarsia splendens* Lohmann
Distephanus crux (Ehrenberg) Haeckel	*Rhabdosphaera stylifer* Lohmann
Dictyocha speculum Ehrenberg	*Rhabdosphaera* sp. Haeckel
Emiliania huxleyi (Lohmann) Hay & Mohler III	*Rhabdosphaera tignifer* Schiller
Halopappus vahselii Lohmann	*Scyphosphaera apsteinii* Lohmann
Hermesinum adriaticum Zacharias	*Syracosphaera pulchra* Lohmann
Michaelsarsia elegans Gran	*Syracosphaera* sp. Lohmann
Cryptophyceae	**Ebriophyceae**
Hillea fusiformis (J.Schiller) J.Schiller	*Ebria tripartita* (J.Schumann) Lemmermann
Chrysophyceae	**Chlorophyceae**
Dinobryon sp. Ehrenberg	*Pterosperma polygonum* Ostenfeld
Euglenophyceae	
Eutreptiella sp. A.M.da Cunha	